5-2010

A Study on Stainless Steel 316L Annealed Ultrasonic Consolidation and Linear Welding Density Estimation

Raelvim Gonzalez
Utah State University

A STUDY ON STAINLESS STEEL 316L ANNEALED ULTRASONIC CONSOLIDATION AND LINEAR WELDING DENSITY ESTIMATION

by

Raelvim Gonzalez

A thesis submitted in partial fulfillment
of the requirements for the degree

of

MASTER OF SCIENCE

in

Mechanical Engineering

Approved:

Dr. Brent Stucker Major Professor	Dr. Leila Ladani Committee Member
Dr. David Geller Committee Member	Dr. Byron Burnham Dean of Graduate Studies

UTAH STATE UNIVERSITY
Logan, Utah

2010

Abstract

A Study on Stainless Steel 316L Annealed Ultrasonic
Consolidation and Linear Welding
Density Estimation

by

Raelvim Gonzalez, Master of Science
Utah State University, 2010

Major Professor: Dr. Brent Stucker
Department: Mechanical and Aerospace Engineering

Ultrasonic Consolidation of stainless steel structures is being investigated for potential applications. This study investigates the suitability of Stainless Steel 316L annealed (SS316L annealed) as a building material for Ultrasonic Consolidation (UC), including research on Linear Welding Density (LWD) estimation on micrographs of samples. Experiment results are presented that include the effect of UC process parameters on SS316L annealed UC, optimum levels of these parameters, and bond quality of ultrasonically consolidated SS316L annealed structures in terms of LWD. In support to these efforts, a Measurement System Analysis for LWD assessment has been performed, and a new instrument for LWD measurement was developed. This work will determine local maximum LWD UC process parameters for SS316L annealed structures based upon systematic evaluation of sample micrographs.

(116 pages)

Acknowledgments

I would like to thank Utah State University PhD student Pedro J. Tejada, Utah State University Professor Richard Cutler, and Indian Institute of Technology Professor G. D. Janaki Ram for their valuable feedback and observations regarding the material outlined in Chapter 2. In addition, the financial support received from the Office of Naval Research (under Grant No. N000140710633) and financial and technical support from Solidica Inc. is acknowledged and made the investigation presented in the Chapter 3 possible.

Contents

List of Tables

List of Figures

Chapter 1

Introduction and Background

Previous research has shown that an additive manufacturing technique known as Ultrasonic Consolidation (UC), which produces three-dimensional structures from metal layers, has been successfully utilized to consolidate Stainless Steel 316L layers [1]. However, from a manufacturing process point of view, the understanding and knowledge needed for fabricating SS316L annealed structures using UC requires information about the level of bond quality expected in SS316L annealed consolidated specimens, and the ability to control the effects of process parameters on SS316L annealed UC. This study addresses the critical issue of optimizing process parameters for SS316L annealed UC based upon a maximum Linear Welding Density criteria (minimum porosity), which is crucial knowledge for manufacturing SS316L annealed parts, and for any application of SS316L annealed structures.

From an application standpoint, there are many reason for using SS 316L annealed in combination with UC. By itself, Stainless Steel 316L is a common austenitic stainless steel alloy, a general purpose marine grade material, and an attractive metal for structural applications in a range of atmospheric environments [2, 3]. On the other hand, as a fabrication method, UC has the advantages of being a low-temperature, metal based, computer-controlled additive manufacturing process. These characteristics make UC a suitable technique to fabricate high tolerances/complex geometry parts, and to integrate components into material structures in a single process; all while avoiding high temperature gradients in metal parts. Since SS316L annealed is corrosion and pitting resistant, has better mechanical strength than Aluminum (Al) — the typical material used in UC machines, and is widely available in foil form (which makes it suitable for the UC process) it could be used in tandem with UC to produce application-tailored structures with superior mechanical and corrosion resistance.

Although the UC process of welding metal foils layer by layer is inherently aimed at obtaining a continuum interface between layers, there is no standard procedure (conventions in terms of magnification level, specimen preparation, measurement system, etc.) used for Linear Welding Density (LWD) measurements, as of the time of this publication. For this reason, this dissertation includes a first attempt at helping to create a standard LWD measurement procedure, and evaluates a newly developed automatic routine for LWD assessment that allows rapid, repeatable measurements, as a basis for a future standard methodology.

1.1 Ultrasonic Consolidation

Additive Manufacturing is a family of technologies for fabricating three-dimensional (3D) structures directly from computer-aided design (CAD) data by means of systematic addition of material. Some of the potential benefits of the Additive Manufacturing approach includes the capability to build multi-material, functionally-graded, and component-embedded structures [4]. Ultrasonic Consolidation (UC) is an additive manufacturing process whereby layers of metal foils can be joined with a metallurgical bond by means of acoustic energy and shaped using CNC machining.

As for the UC procedure, a computer program processes a three-dimensional CAD model of the part to be built, and slices up this model into a number of horizontal layers, each layer with a thickness equal to the thickness of the metal foil used. Ultrasonically deposited foil strips are placed adjacently to each other to create a layer. After a layer is completed (or several layers are completed), a computer controlled milling head shapes the layer to its slice contour. Following this, milling chips are removed and foil deposition for the next layer starts [5]. As a result of continuous addition of layers, a three-dimensional part is produced from bottom to top.

A UC foil deposition schematic is shown in Figure 1.1. First, a thin metal foil is placed over the substrate. Following this, a rotating ultrasonic sonotrode travels along the length of the metal foil, keeping the foil in intimate contact with the substrate while a Normal Force is applied to the metal foil through the sonotrode. The consolidation of the foil and the substrate is accomplished by sonotrode oscillations at an ultrasonic frequency and at

user-set amplitude. The direction of the sonotrode's oscillations (direction of excitation) is along the sonotrode's rotation axis.

As a consequence of sonotrode dynamics, localized shear forces are generated from the combination of sonotrode pressure and oscillation, inducing interfacial stresses between the two mating surfaces and elastic-plastic deformation of surface asperities [6]. Furthermore, asperities deformations break up the oxide film, establishing a metallurgical bond between the foil and the substrate due to relatively clean metal-to-metal surface contact [5]. On a lower scale, atomic diffusion may also aid in the bonding process because local temperatures at the interface and the surrounding affected region (about 20 µm) can reach up to 50% of the melting point of the material being deposited [6], but only for a very brief time. Although still being researched, there is evidence that ultrasonic welding mechanisms for bond formation involve: i) removal of surface oxide layers, ii) plastic deformation at the interface, and iii) to a lesser extent diffusion of metal atoms across the interface. The degree of plastic deformation is considered the most important characteristic leading to metallurgical bonding across the interface [7].

Although localized frictional heating is present in the UC process, the mechanism for UC is not melting [6], and thus negligible shrinkage and thermal stresses result during part building. In turn, ultrasonically consolidated parts have virtually no thermal degradation in material properties. Indeed, parts may be built including complex geometric features (e.g. internal channels) and integrating sensors/actuators for application-tailored structures, on

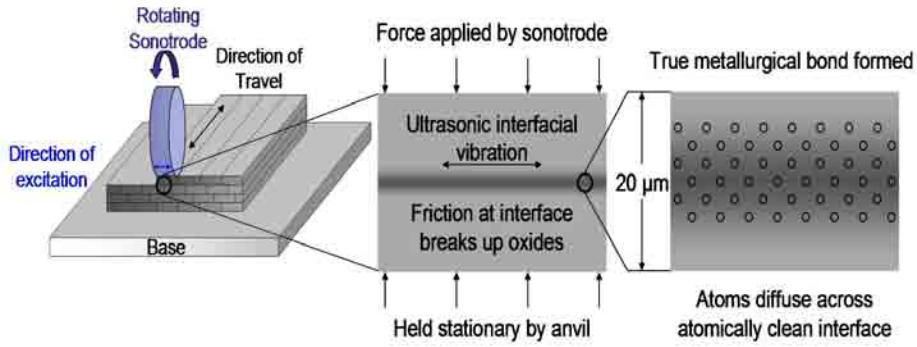

Fig. 1.1: Schematic of the Ultrasonic Consolidation process [8]

account of UC being an additive manufacturing process. Through ultrasonic welding and CNC machining combined in an additive/subtractive manufacturing scheme, the UC process can be used to create multi-material structures utilizing cold-working while avoiding thermal processes that pose properties degradation [5]. In addition to this, UC does not require a controlled atmosphere for layer deposition.

There are four general control parameters for welding within a UC system: Oscillation Amplitude, Contact Pressure Distribution (Normal Force between the horn and foil), Welding Speed along the direction of travel, and Temperature of the substrate. The first three parameters depend on sonotrode interaction with the part being built. In contrast, Temperature depends on the heat applied directly to the substrate from the base plate, with Temperature values from room temperature up to hundreds of kelvin degrees, typically 478 K (400 °F).

Evaluation of the effect UC control parameters have on microstructure and mechanical properties of ultrasonically consolidated parts has been the object of active research [9] [10]. Regarding the object of study of the present thesis project, previous research has demonstrated the feasibility of the UC process using Stainless Steel 316L by exploring the role played by process parameters of Welding Speed, amplitude, Normal Force, and Temperature in Stainless Steel ultrasonic consolidation, and presenting optical microscopy of SS316L ultrasonically consolidated samples [1]. Previous results of an Analysis of Variance (ANOVA) on SS316L UC, with peel strength as the response and amplitude, Normal Force, and Welding Speed as factors, indicated that only amplitude and Welding Speed factors were statistically significant for peel strength (with a 90% confidence interval, p-value < 0.10). In addition, according to this study, the amplitude factor exerted the strongest effect on peel strength [1]. Furthermore, as for the effect of process parameters on peel strength, higher Oscillation Amplitudes and lower Welding Speed increased peel strength. Normal force (up to 1600 N) was not statistically significant, whereas Temperature (up to 422 K (300°F)) was not considered as a factor for SS316L UC [1].

1.2 Linear Welding Density

Linear Welding Density (LWD) is the proportion of bonded area to total area within the weld interface [9]. The selection of LWD as a quality measure is better understood considering that ultrasonically consolidated parts typically show unbonded regions (defects, physical discontinuities) along the layer interfaces. Indeed, the assessment of the proportional bonded region given in a LWD measurement is also important as a quality attribute for porosity in ultrasonically consolidated parts [11]. The relevance of understanding what factors influence LWD has already been observed in a previous study of UC parts [7]. As a matter of fact, LWD strongly affects mechanical properties in the direction normal to the foils for an ultrasonically consolidated part and the mechanical behavior of a UC structure under load-bearing stresses [7]. In consequence, properties like specific weight and Poisson's ratio of ultrasonically consolidated parts are affected by LWD. In the same manner, quality charateristics based on ultrasonically consolidated part porosity (e.g. insulating enclosures) are utterly dependent upon the level of LWD present between metal foils.

For the purposes of this thesis project, LWD will be determined based upon metallography of the weld interface, by sectioning weld samples along the width of the foil. The samples will be mounted, polished to a smooth finish and cleaned in isopropyl alcohol. LWD will be assessed from micrograph images of samples taken from weld cross-sections, according to Equation (1.1).

$$\%LWD = \frac{Bonded\ interface\ length}{Total\ interface\ length} \times 100 \tag{1.1}$$

Regarding methods that have been used for assessing LWD on ultrasonically consolidated samples, manual distance measuring instruments (e.g. rulers, software measuring tools) have been used to estimate both the bonded interface length and the total interface length in Equation 1.1. However, these methods have some inherent limitations and difficulties with LWD measurements, because they are time consuming, prone to human errors, and impractical for accuracy verification.

1.3 Effects of Process Parameters on UC Bond Formation

In a UC system, the controllable variables for a given material are: Amplitude of Oscillation, Contact Pressure distribution (Normal Force between the horn and foil), Welding Speed (along direction of travel) and Temperature of the base. Extensive experimental investigations have been conducted, studying the effects of these factors on the quality of weldment made by UC.

Considering research made on Al 3003/6001, a higher Normal Force and higher Oscillation Amplitude increased LWD up to a certain level, beyond which LWD decreased [9,10]. Additionally, it was observed that lower Welding Speeds (down to 12 mm/s) increase LWD, and higher temperatures produced higher LWD within a range from ambient to 450 K (350 °F) [7]. Based on these studies, Al 3003 UC seems to be sensitive to changes in Oscillation Amplitude values and substrate temperature.

Selection of appropriate process parameters plays a key role in UC bond formation of Al 3003/6061 based on LWD microscopic studies and peel-off tests [9,10]. Although it is possible to have a low peel load response and high linear weld density with Aluminum 6061 (due to excessive strain hardening and cyclical stressing of contact points at the interface) [9]; it has been verified that a high peel load response only occurs in the presence of high LWD [10].

Current published literature about SS316L UC only comprises a paper studying the feasibility of the UC process with SS316L, and exploring the effects of Amplitude, Normal Force, and Welding Speed UC process parameters on peel strength by performing an ANOVA study [1]. However, the effect of temperatures higher than 422 K (300 °F) was not part of the study, and the benchmark used to characterize ultrasonically consolidated parts was peel strength, instead of LWD. Considering these research efforts, a study of parameter optimization of SS316L annealed UC based on a maximum LWD criteria does not have any precedent in literature. Moreover, a broader spectrum of UC parameter sets might contribute to a better optimization of the SS316L annealed UC process with respect to a maximum LWD criteria. In sum, an understanding of the effect of UC process parameters on LWD is required if the SS316L UC is to develop its full application potential.

1.4 Ultrasonic Consolidation System Description

The UC system utilized for the experimental part of this thesis research is the Solidica Formation™ machine. The Solidica Formation™ UC machine (Figure 1.2, Figure 1.3, and Figure 1.4) is an integrated UC building system that combines a rotating ultrasonic sonotrode, a heat plate, a foil-feeding spool mechanism, a three-axis milling head, and a software implementation for material deposition and machining [11]. Furthermore, the Solidica Formation™ sonotrode oscillates transversely according to a half-wave rectified sine wave at a frequency of 20 kHz and at user-set Oscillation Amplitude while traveling over the metal foil. The sonotrode itself is incorporated into a welding head and its position is controlled by numerical control. The maximum build size of the Solidica Formation™ machine is 609.6 mm × 914.4 mm × 203.2 mm (24 in × 36 in × 8 in), and the CNC contour milling head has a tolerance of 0.05 mm (0.002 in) [12]. The sonotrode has a 146.75 mm nominal diameter. Regarding process parameter setting limits, the Solidica Formation™ machine is constrained by the manufacturer to a nominal force less than or equal to 1800 N, nominal amplitudes between 6 µm and 27 µm, Welding Speeds up to 84.7 mm/s (200 ipm), and nominal temperatures ranging from ambient to 478 K (400 °F).

1.5 Research Goals

This is a systematic study exploring the suitability of Stainless Steel 316L annealed (SS316L annealed) as a building material for Ultrasonic Consolidation (UC), including research on Linear Welding Density (LWD) estimation on micrographs of samples. The research is devoted to exploring the capabilities of ultrasonic consolidation to fabricate integral SS316L annealed structures with maximum LWD, based upon systematic evaluation of LWD estimation procedures. The objectives of this thesis project are to:

1. Develop a standard measurement system for LWD measurements, and evaluate SS316L annealed UC bonding in specimens using LWD values as the response variable.

2. Determine the optimum LWD process parameter set for SS316L annealed UC experimentally, and determine the effect of UC process parameters on the LWD of ultrasonically consolidated SS316L annealed structures.

As a result of these goals, a set of experimental and analytical studies were conducted to develop a repeatable methodology for LWD measurements, and an Analysis of Variance was performed to determine critical process parameters for Stainless Steel 316L annealed Ultrasonic Consolidation. All these efforts provide information related to the level of Linear Welding Density attainable in SS316L annealed structures.

1.6 Thesis Statement and Outline

This study addresses parameter optimization for ultrasonic consolidation of Stainless Steel 316L annealed, by evaluating experimental factors of Oscillation Amplitude, Welding Speed, Normal Force and Temperature in order to minimize part porosity and therefore, on the basis of a maximum LWD criteria. This thesis project will be presented in a multi-paper format, in accordance with the requirements set by the Graduate School of Utah State University. This study will include an introduction, background, and conclusion in addition to the main chapters. The main body will consist of papers that have already been published or already submitted for publication. In that respect, the outline of thesis project is structured as follows:

- Chapter 1: Introduction and Background.
- Chapter 2: An automatic routine for Linear Welding Density estimation through image processing.
- Chapter 3: Experimental determination of optimum parameters for stainless steel 316L annealed ultrasonic consolidation.
- Chapter 4: Overall Conclusions.
- Appendix.

Chapters 2 and 3 will be stand-alone journal publications submitted to the Journal of Manufacturing Science and Engineering and the Rapid Prototyping Journal, respectively.

Moreover, Chapter 2 unveils a new MATLAB script routine for assessing LWD on weldment cross section interface micrographs. In this respect, the MATLAB script is presented for rapid, repeatable measurements of LWD, as a basis for a future standard methodology for LWD assessment. In addition, a complete reference guide to the MATLAB script is contained in the Appendix.

Chapter 3 includes two experiments with SS316L annealed: a Taguchi experiment with Type 1 standard samples and a Split Plot experiment with Type 2 standard samples. A scale ruler was used to obtain LWD values in Type 1 experiment samples of the Taguchi experiment, whereas the MATLAB script described in Chapter 2 was employed to measure LWD values in Type 2 experimental samples of the Split Plot experiment.

Fig. 1.2: Solidica Formation™ machine at Utah State University (as shown in [12])

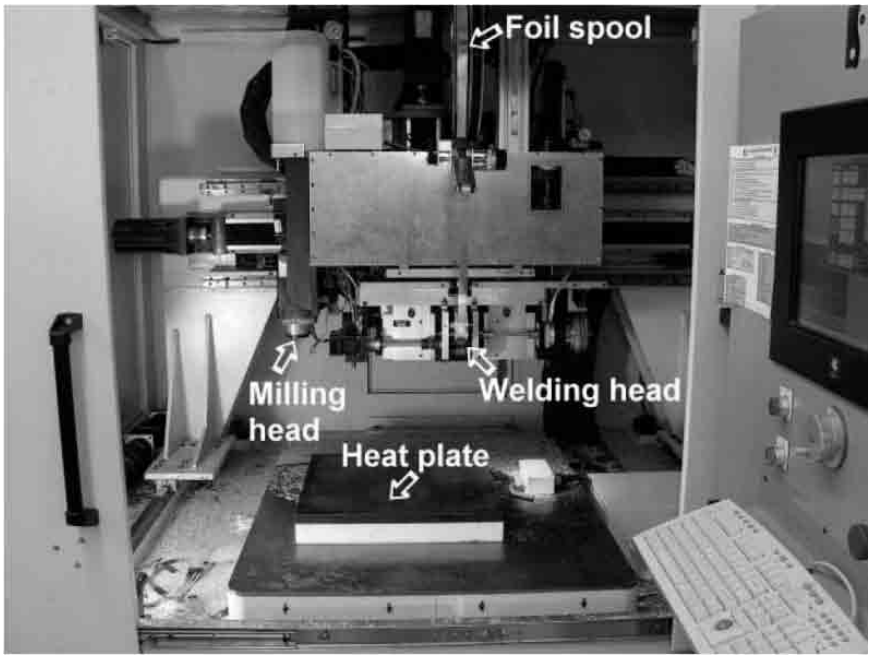

Fig. 1.3: Solidica Formation™ machine main elements (as shown in [11])

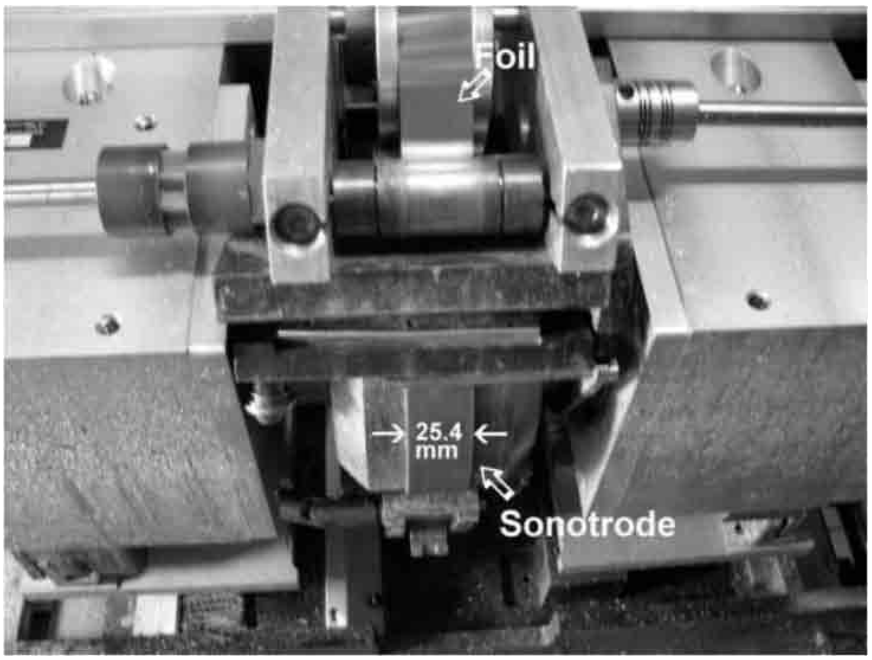

Fig. 1.4: Close-up view of the Welding head, showing the sonotrode from below (as shown in [11])

Chapter 2

An Automatic Routine for Linear Welding Density Estimation through Image Processing[1]

2.1 Abstract

Linear Welding Density (LWD) is a quality benchmark used in ultrasonically consolidated part characterization. In this study, a computer-based method for assessing LWD is presented. A MATLAB script is employed for assessing LWD on weldment cross section interface micrographs. The method presented is based upon the application of image processing techniques on a single metal to metal interface picture for LWD assessment, using a picture brightness criteria. A Measurement System Analysis of Variance was performed in order to evaluate repeatability and reproducibility of the MATLAB script presented in this work against other conventional instruments used for LWD estimation. The experimental results presented show that the MATLAB script can effectively estimate LWD on cross section micrographs.

2.2 Introduction

Ultrasonic Consolidation (UC) is an additive manufacturing process whereby layers of metal foils can be joined with a metallurgical bond by means of acoustic energy and shaped using CNC machining. Some of the UC process advantages are the ability to create metal structures with virtually no thermal degradation in material properties [6] and include some complex geometric features in metal parts (e.g. embedded sensors/actuators), all by taking

[1]Coathored by R. Gonzalez, B. Stucker. This chapter is a paper that has been submitted for publication in the Journal of Manufacturing Science and Engineering.

advantage of the additive manufacturing nature of the process. The process of welding metal foils layer by layer is inherently aimed at obtaining a continuum interface between layers. Although perfect bonding is theoretically possible, ultrasonically consolidated parts typically show unbounded regions in the form of defects, physical discontinuities, and imperfections [11]. In that sense, Linear Welding Density (LWD) is defined by the proportion of bonded area to total area within the weld interface [9]. For instance, LWD measurements have been used to characterize bond quality in Al 3003 ultrasonically consolidated parts [7,13]. In turn, it has been noted that LWD is directly related to porosity in ultrasonically consolidated parts [11], strongly affects mechanical properties in the direction normal to the foils in an ultrasonically consolidated part, and is an important factor to determine the mechanical behavior of ultrasonically consolidated parts under load-bearing stresses [7].

Given a cross section micrograph, the LWD of a given interface is measured using a relation of lengths given by the following equation:

$$\%LWD = \frac{Bonded\ interface\ length}{Total\ interface\ length} \times 100 \tag{2.1}$$

As of the time of this publication, there is no standard procedure (conventions in terms of magnification level, specimen preparation, measurement system, etc.) used for LWD measurements. This paper is a first attempt at helping to create a standard LWD measurement procedure. Indeed, this study presents a MATLAB script capable of assessing LWD given an image containing the interface between two layers and compares results with other LWD assessment methods on the basis of an Analysis of Variance (ANOVA).

2.3 Overview

A MATLAB script, 'lwd.m', was developed to assess LWD in cross section micrographs of weldments. The method is based upon the use of a set of image processing techniques that, when combined, provide a single metal to metal interface LWD assessment. The MATLAB script takes for an input a rectangular region of the cross section micrograph, and provided this region contains the interface of interest and meets standard metallography

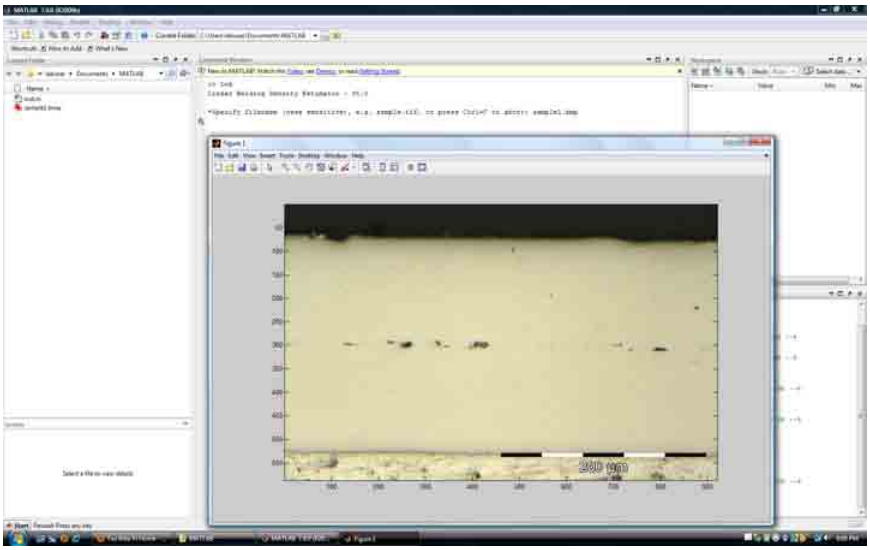

Fig. 2.1: File input example in MATLAB script

quality criterias, the tool can provide an automatic estimation of the LWD present at the interface. Either grayscale or color images can be processed, in both Bitmap (bmp) and Tagged Image File (tif) formats. The most fundamental assumption of the MATLAB script program is that darker areas in the micrograghs represent unbonded areas, and thus, it is dependent upon the brightness of the visual target. On the other hand, in order to use the MATLAB script for LWD assessment, the interface shown in the cross section micrograph must be horizontally oriented, in focus, and the sample must be in not-etched, scratchless, and as-polished conditions. An examination of these and other conditions that affect LWD assessment using the MATLAB script are given in the Discussion section of this work.

The MATLAB script works in MATLAB version 7.0 (R14) or newer, with the Image Processing Toolbox installed. The routine is executed inside the MATLAB command window, and prompts for an image filename first. Figure 2.1 shows an example of how an image file that has already been placed in the MATLAB working directory, namely 'sample1.bmp', is entered as input. Upon specifying this image file (by entering the filename including the file extension), the actual image is shown on screen as a figure and the program waits for the user's confirmation on the image. In this regard, *Ctrl+c* will abort the operation and any other standard keystroke will proceed with analysis.

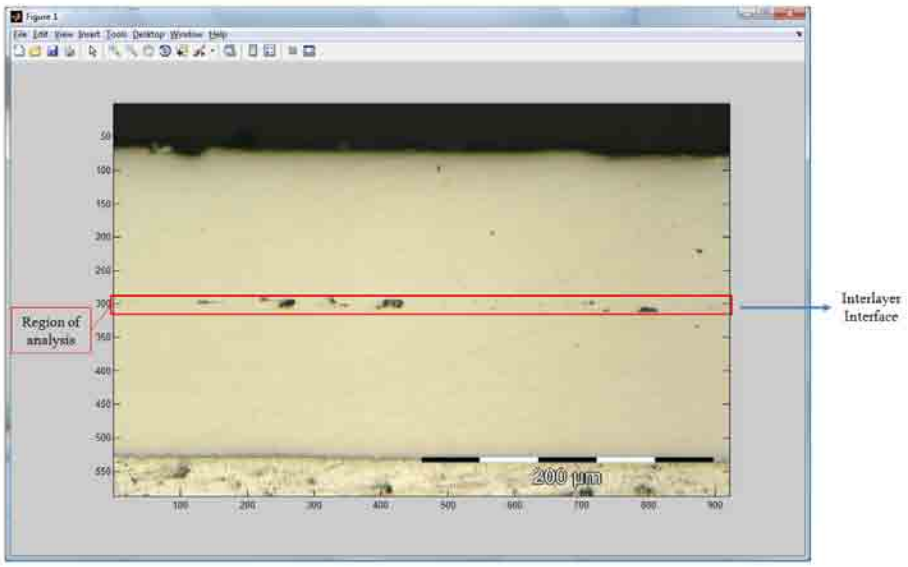

Fig. 2.2: Image, Interlayer Interface, and Region of Interest illustrations

Following this, the rectangular Region of Interest (ROI) needs to be defined by the user. The Region of Interest is the smallest rectangular region, or subset of the original image, that contains all relevant pixels depicting the interface of interest. In this manner, the Region of Interest is a graphical representation of the interface in the form of a rectangle and its contents. Furthermore, all image processing operations are performed on the Region of Interest defined by the user. Figure 2.2 illustrates the image, the target interlayer interface, and a selected Region of Interest in the *sample1.bmp* image file.

The Region of Interest is defined by the user, using either Visual Clicks, Matrix Coordinates, or Relative Coordinates.

The Visual Clicks approach comprises two click-points so as to define the Region of Interest with the aid of a pointing device. These separate clicks specify the rectangle containing the Region of Interest, by defining two rectangle corners diagonally opposite. If the interface extends all across the image, then clicks can be performed outside the image's border but inside the MATLAB figure window. In that way, the script program will adjust the selection to meet the border or borders of the image accordingly. The Visual Clicks approach is the default option. Figure 2.3 illustrates the Visual Clicks approach, showing

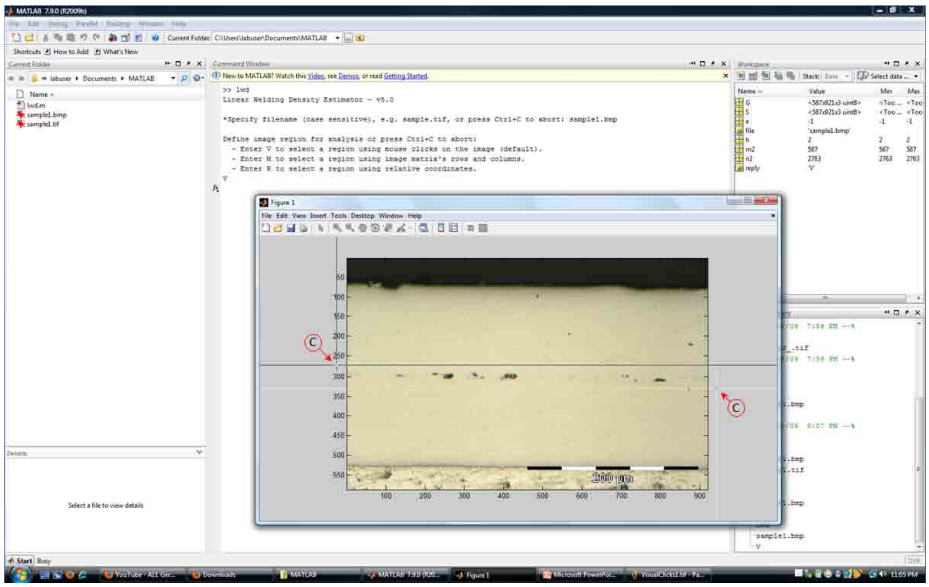

Fig. 2.3: Visual Clicks approach to define the Region of Interest in the MATLAB script

the points where clicks could be performed to select a Region of Interest for the interface shown.

The second option for defining the Region of Interest is Matrix Coordinates. Matrix Coordinates are based upon the matrix representation of an image in MATLAB, called the Image Matrix. Moreover, Matrix Coordinates are given in terms of row number and column number following a standard mathematical matrix scheme. The Region of Interest is defined in Matrix Coordinates by specifying the row and column numbers that bound a rectangular region.

Relative Coordinates is the third option for defining the Region of Interest. Relative Coordinates are Cartesian Coordinates with the origin placed at the lower left corner of the original image, and coordinate's dimensions scaled up so that the height and the width of the original image equals to a unit of distance, respectively. Consequently, coordinated values for both vertical and horizontal axes of the cartesian system are always relative to the size of original image, and lay in between 0 and 1.

Once the Region of Interest is defined by the user using either Visual Clicks, Matrix Coordinates, or Relative Coordinates, an image of the Region of Interest is presented to the

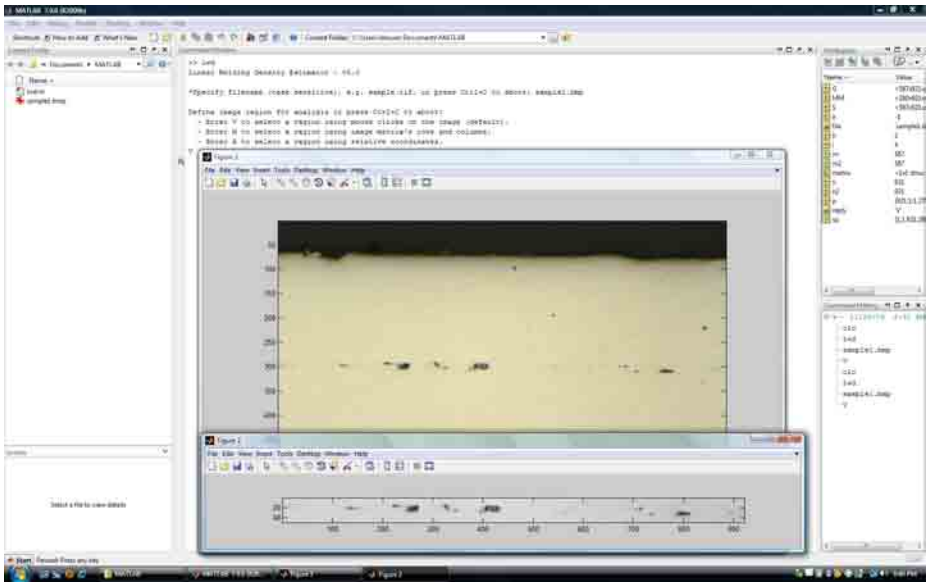

Fig. 2.4: 8-bit grayscale conversion of the Region of Interest example in the MATLAB script

user. The Region of Interest is then converted to grayscale using an 8-bit grayscale conversion. MATLAB supports image processing of grayscale and color images [14], and using this feature, the Region of Interest is converted to an 8-bit grayscale image (an image comprising $2^8 = 256$ different shades of gray) unless the original image is already in this format. Indeed, MATLAB functions *ind2gray* and *rgb2gray* are used to perform 8-bit grayscale conversion for indexed and RGB images, respectively, whenever necessary. Figure 2.4 illustrate the Region of Interest after the 8-bit grayscale conversion.

Once the 8-bit grayscaled Region of Interest has been obtained, black and white binarization is performed. The black and white representation of the Region of Interest is based upon applying the Otsu thresholding algorithm [15] on the 8-bit grayscaled Region of Interest. Otsu's algorithm performs black and white binarization by selecting the threshold shade of gray (intensity of gray) that minimizes the within class variance in the image's grayscale histogram, when the background (pixels with shades of gray darker than the threshold), and foreground (all pixels that are not in the background), are considered as histogram classes [16]. Figure 2.5 shows an image of the previous grayscaled Region of Interest (Figure 2.4) after black and white binarization.

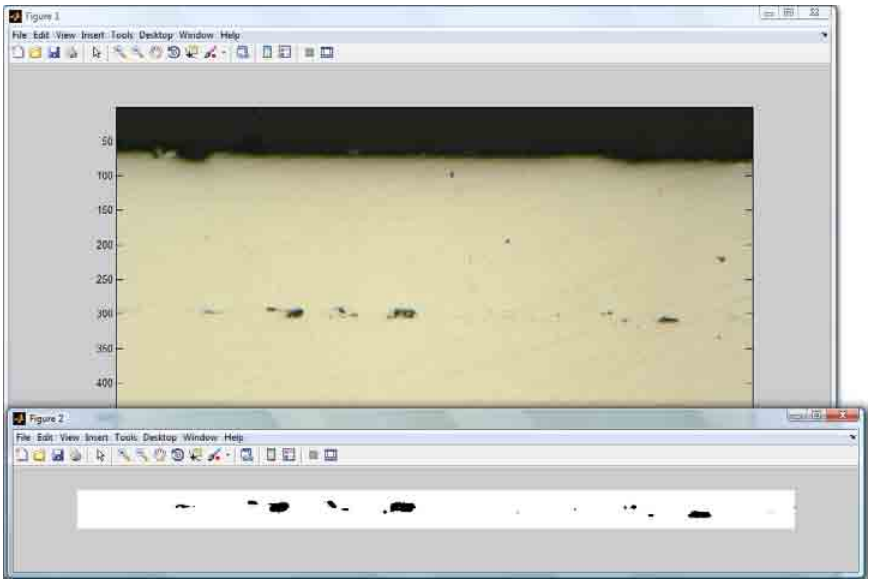

Fig. 2.5: Illustration of black and white binarization using Otsu thresholding algorithm in the MATLAB script

Following black and white binarization, each black pixel in black and white representation of the Region of Interest is projected across the vertical direction, as shown in Figure 2.6. The aim of this image processing task is to consider the worst case scenario of maximum unbonded (black) pixels per row across the Region of Interest. Black pixel projection also simplifies further analysis by making all rows in the resulting image identical.

In MATLAB, color values for black and white colors in an Image Matrix are zeroes and ones respectively, thus providing a means to perform mathematical operations on black and white images. For this particular case, the color values representing black and white colored areas will prove useful as they are associated to unbonded and bonded areas, respectively. For instance, once black pixels are projected vertically, all pixel values in the first row (comprising color values of zeroes and ones) are added up, effectively calculating the number of white pixels in the first row. When the total sum of the first row of pixels is divided by the number of pixels in the first row and multiplied by 100, an estimate of the LWD is obtained, as stated in Equation (2.1).

The output of the MATLAB script is printed after an estimate of the LWD has been

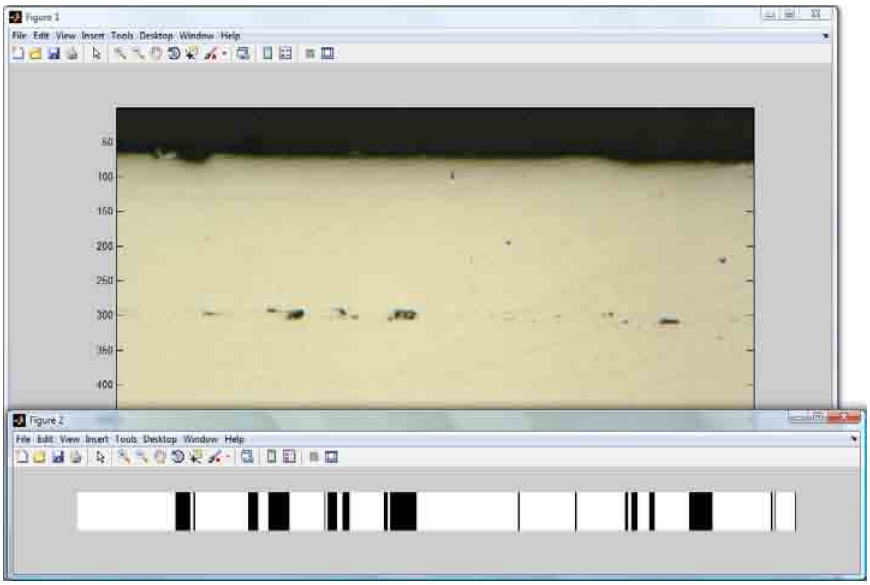

Fig. 2.6: Illustration of black region vertical projection applied on a black and white image in the MATLAB script

calculated. The output of the MATLAB script includes the following information regarding the image file: LWD value, filename, original Image Matrix dimensions, 8-bit grayscale threshold value used, and Matrix Coordinates for the selected Region of Interest. An example of the output is given in Figure 2.7. Since the Region of Interest is given in Matrix Coordinates as part of the output, and because Matrix Coordinates is one option to define the Region of Interest (see Figure 2.7), the output of the script effectively provides a transparent way to refer back to previous results and to repeat estimations, whenever the original file and the associated MATLAB script output are used.

2.4 Measurement System Analysis of Variance

A Measurement System is a formal combination of instruments and auxiliary means to obtain measurements of a defined characteristic [17]. Although the true variability of a measurand can be only determined if there are measurements, in practice, a Measurement System under fixed conditions is limited by the statistical properties of measurements [18]. From a statistical standpoint, each measurement made by an instrument (also known as a gage or measuring device) consists of the true, unknown, value of the characteristic being

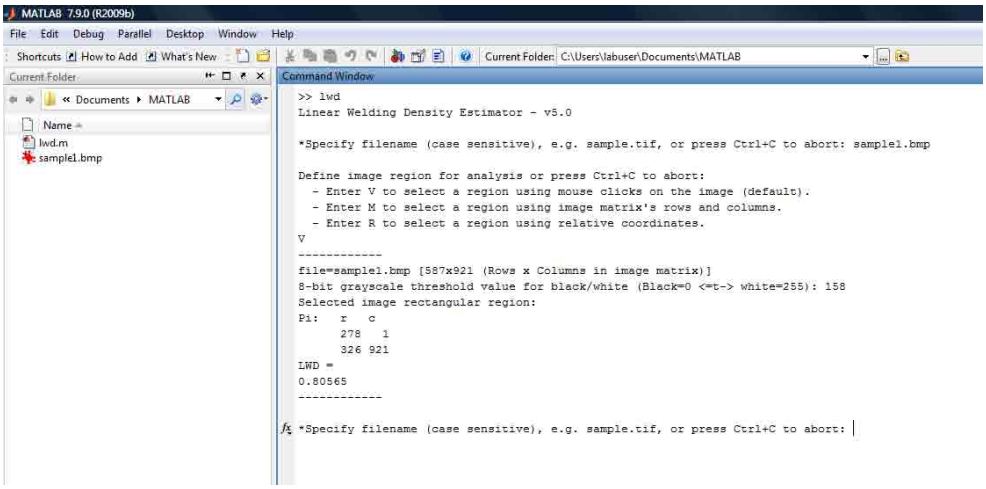

Fig. 2.7: MATLAB script output example

measured plus a measurement error, known also as instrument variation or instrument bias. Moreover, the total variability of the data is also directly related to the dispersion or spread among the experimental units [19]. In consequence, a measurement system is aimed at two main objectives: to minimize measurement errors, and ensure the variability of the instrument is suitably small, as compared to the inherent variability of the experimental units (samples or units from which the characteristic is being measured). In that respect, it is critically important to identify the sources of variation in the measurement, and to ensure the number of measurements provides enough sensitivity, and soundness for variation estimation [20]. In addition, a reliable Measurement System must meet repeatability and reproducibility criterias. *Repeatability* is the variation in repeated measurements made under the same conditions (identical user, part and measuring instrument); whereas *reproducibility* is the variation in measurements observed by different users when all other conditions are fixed (identical part, measuring instrument) [21].

For this study, a comparison of three different methods for LWD measurement were assessed. A set of instructions was prepared to ensure proper use of a scale ruler, GIMP Measure Tool, and the previously described MATLAB script measuring instrument. These instructions provided the methodology framework for the Measurement Systems. The scale ruler instrument was selected because it has already been used as an instrument for LWD

assessment in UC studies, e.g. [7, 11]. Furthermore, the GIMP Measure Tool is a software-based point-to-point distance tool that provides a free and easy-to-use alternative to manual measurements using scale rulers.

Instruction sets serve as a guide for the proper use of the selected LWD instruments, help users to avoid systematic errors, and take into account some particular features of each LWD measuring device. For instance, a fixed scale was required for consistent measurements using the scale ruler, whereas pixel units were employed with the GIMP Measure Tool in order to improve resolution and allow zooming. Complete instruction sets used for scale ruler, GIMP Measure Tool, and MATLAB script instruments are contained in the Addendum of this work.

For the purposes of a Measurement System Analysis of Variance, three different LWD Measurement Systems were evaluated in this study:

- Manual on screen measurements with a scale ruler (herein and after Ruler).
- Measurements using GIMP software's Measure Tool (herein and after GIMP).
- Measurements using the Visual Clicks option of the MATLAB script (herein and after MATLABsc).

Considering populations of cross section single-interface micrographs for all possible combinations of UC parameters, a balanced experiment was performed comparing Ruler, GIMP and MATLABsc measurement systems. Four random single-interface samples, shown in Figure 2.8, were selected and given to ten users for LWD measurements. Each user took three LWD measurements on each sample, as independent trials, using three different gages (measurement systems). Using statistical terminology, each configuration of one factor is called a *factor level*. In this manner, by multiplying the number of all factor levels present, $4 \times 10 \times 3 \times 3 = 360$ observations were recorded. All *treatments* (factor level combinations in the experiment) have the same number of experimental units (items for observations).

The ANOVA model for the data follows a linear combination of mixed effects (model with fixed and random factors) given by:

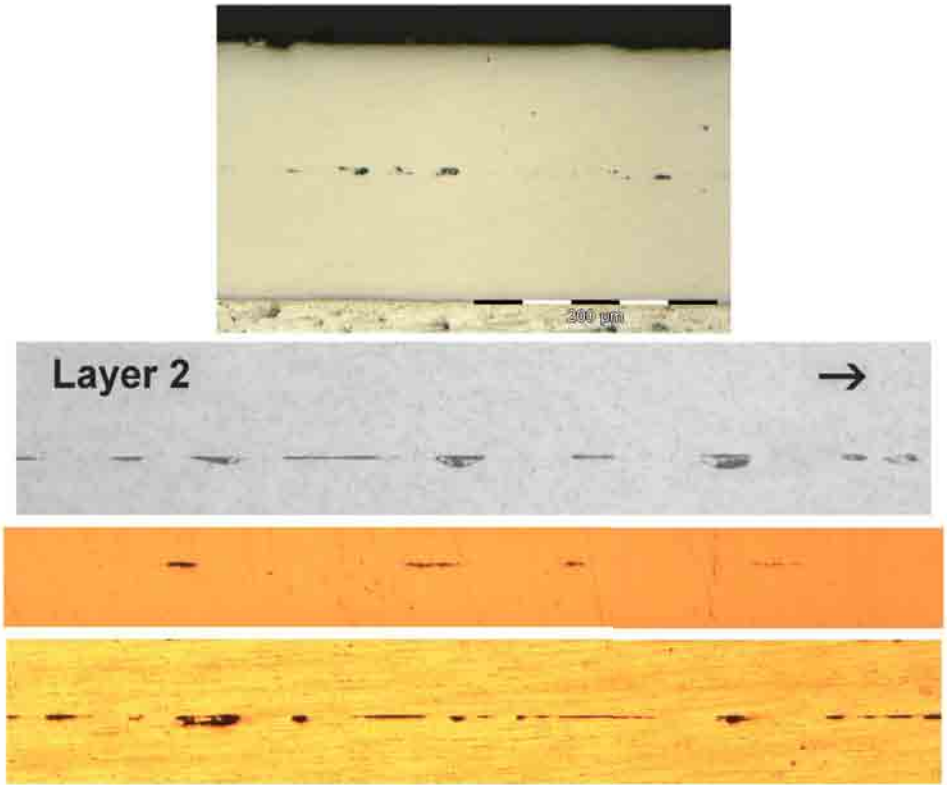

Fig. 2.8: The four randomized single-interface samples used for the Measurement System Analysis (the sample labeled 'Layer 2' was originally published in [7])

$$Y_{ijkl} = \quad + \quad _i + \quad _j + \upsilon_k + (\quad)_{ij} + (\ \upsilon)_{ik} + (\ \upsilon)_{jk} + (\quad \upsilon)_{ijk} + \quad _{l(ijk)} \qquad (2.2)$$

$$\text{for } i = 1 \quad 2 \quad 3; \quad j = 1 \quad 2 \quad 3 \quad 4; \quad k = 1 \quad 2 \qquad 10; \quad l = 1 \quad 2 \quad 3$$

where:

is the expected value or mean value for the *LWD* experimental response,

$_i$ is the effect of the i^{th} level of the *Gage* fixed experimental factor,

$_j$ is the effect of the j^{th} level of the *Sample* random experimental factor,

υ_k is the effect of the k^{th} level of the *User* random experimental factor,

$_{l(ijk)}$ is the random error on the l^{th} trial, and

Y_{ijkl} is the response value, namely *LWD*, for the l^{th} trial, reported by the k^{th} *User*, on the j^{th} *Sample*, and the i^{th}*Gage*.

All other terms denote interactions of respective factor levels. Other ANOVA model assumptions made are:

σ_j are Independent and Identically-Distributed Random Variables, following a normal distribution with mean zero and variance σ_s^2 ,

υ_k are Independent and Identically-Distributed Random Variables, following a normal distribution with mean zero and variance σ_u^2 ,

$(\gamma\sigma)_{ij}$ are Independent and Identically-Distributed Random Variables, following a normal distribution with mean zero and variance σ_a^2 ,

$(\gamma\upsilon)_{ik}$ are Independent and Identically-Distributed Random Variables, following a normal distribution with mean zero and variance σ_b^2 ,

$(\sigma\upsilon)_{jk}$ are Independent and Identically-Distributed Random Variables, following a normal distribution with mean zero and variance σ_c^2 , and

$(\gamma\sigma\upsilon)_{ijk}$ are Independent and Identically-Distributed Random Variables, following a normal distribution with mean zero and variance σ_d^2 .

In that sense, Identically-Distributed Random Variables (also noted as i.i.d) states that each random variable has the same probability distribution, and all random variables are mutually statistically independent (the occurrence of one event does not affect the probability of the other possible outcomes to occur).

The Null Hypothesis (H_0) and Alternative Hypothesis (H_A) are, respectively:

$$H_0 \ : \ \gamma_1 = \ \gamma_2 = \ \gamma_3 = 0 \tag{2.3}$$

$$H_A \ : \ \textit{At least one } \gamma_i \neq 0 \tag{2.4}$$

Table 2.1: Factorial experiment Factors and Levels

Factors	**Levels**				
Gage (Measuring System)	Ruler	GIMP	MATLABsc		
User	User1	User2	User3	...	User10
Sample	Sample1	Sample2	Sample3	Sample4	

Regarding the ANOVA model used, all factors are considered crossed with respect to all the others, and Type 3 tests for fixed effects are performed for the Gage factor. In addition, the following are some important characteristics of the ANOVA model design:

- Univariate (There is only one response or dependent variable).
- Three way factorial (that is, all combinations of User, Gage, and Sample occur in the design).

Table 2.1 shows the experimental factors and levels for the Measuring System ANOVA:

The ANOVA was carried out using SAS™ statistical software. In total, 360 observations were initially considered, comprising three replicates (trials) of each treatment, and a critical probability value of 0.05 was used. However, it was clear in the preliminary results that some assumptions for the analysis were not met, and consequently, a straight ANOVA could not be performed. The main problems encountered were the presence of heteroscedasticity and outliers (points that depart from the overall data trend) in the data. Heteroscedasticity means that the variance of the dependent variable (LWD measurement, in this case) varies across data (between factor levels, in this case). For instance, the graph of Residuals against Explanatory Factors in Figure 2.9 provided first hand evidence of significant difference in spreads (the convention in statistics is that it should not be greater than or equal to five times) between the Gage factor level with the least variability (MATLABsc) and the Gage factor level with the most variability (Ruler), where the spread is illustrated by the vertical chain of symbols shown in the graph. It is worth noting that, in a statistical context, the residual is the deviation of an observation from the estimated true function value, therefore, it is an estimator of the statistical (random) error [22]. In turn, the presence of significant heteroscedasticity poses a problem because the ANOVA model is based upon, among other

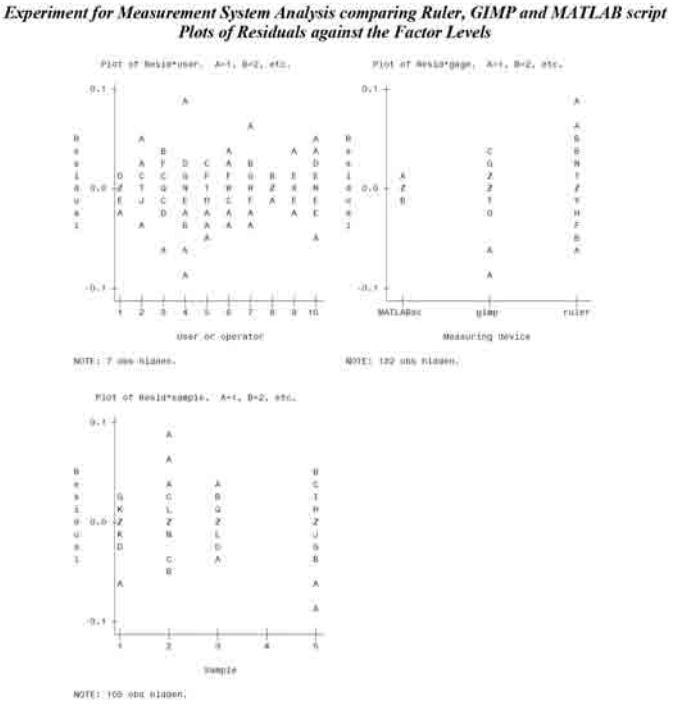

Fig. 2.9: Residuals versus Explanatory Factors before addressing heteroscedasticity

statistical considerations, an assumption of equal variance across the data for the response variable (homoscedasticity). As a consequence, no conclusions could be made from these preliminary results.

It was decided to perform an ANOVA taking into account large differences in Gage factor levels (Ruler, GIMP, and MATLABsc) variability. This decision was based upon clear experimental evidence that there were significant differences in the spread (variability) among the levels of the Gage factor (Figure 2.10). In addition, Figure 2.9 shows that heteroscedasticity is particularly pronounced in the Residuals versus Gage plot, suggesting this factor is the most heteroscedastic of all.

A new ANOVA was performed by including the statement *repeated / group=gage* in the PROC MIXED SAS™ script, so as to include the existence of large differences in Gage levels variances into the analysis. The actual PROC MIXED procedure used to carry out the final ANOVA is shown below:

```
title3 " Using PROC MIXED with the REML Estimation Method";
```

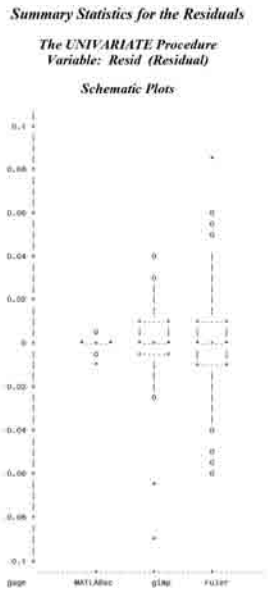

Fig. 2.10: Box plots of the initial data showing high differences in Gage level variances

```
proc mixed data=no_trans covtest cl;
class user gage sample; model _data = gage / ddfm=satterthwaite outp = residuals;
random sample|user gage*sample gage*user gage*sample*user; repeated / group=gage;
lsmeans gage / pdiff=all adjust = Tukey; run;
```

These lines of code instructed SAS™ statistical software to perform an ANOVA considering the significant differences in Gage levels spreads, while maintainig all other previous conditions, and using the residual maximum likelihood (REML) approach to estimate components of variance.

In addition, some data cleaning and outliers removal was performed, resulting in a total of 34 neglected observations. These observations were removed because they comprised extreme outliers in Residuals versus Normal Percentiles plots for each Gage factor level. The presence of these extreme outliers diagnostic hinders the validity of any futher Analysis of Variance, because one of the ANOVA premises is that residuals are normally distributed according to the mathematical theory of errors [22]. As shown in Figure 2.11, the outliers do not reflect the data general line of orientation. After thoughtful considerations, it was decided to withdraw these outliers from the final data set. The final ANOVA included large

variances differences in Gage levels into the analysis and conprises data of only 326 final observations. However, it is worth mention that preliminary straight ANOVA results including outliers (all available data) drew equivalent conclusions to the final ANOVA inferences. Hereinafter, results of the final ANOVA performed are presented.

The Residuals versus Explanatory Factors plots of the final ANOVA are shown in Figure 2.12 and include additional evidence of Gage factor heteroscedasticity. However, this heteroscedastic Gage factor was expected and the final ANOVA has been performed taking into account those significant differences in Gage factor level spreads. Furthermore, the Residuals versus Predicted Values plot for the final data (without outliers) in Figure 3.12 does not show significant evidence of heteroscedasticity since there is not any evident gradient pattern (e.g. a megaphone shape) in the Residuals versus Predicted values plot. In sum, Residuals versus Explanatory Factors plots provide no reason to invalidate final ANOVA results.

Diagnostics confirm that the residuals normality assumption is quite reasonable after performing statistical diagnostics for each level of Gage (Residuals versus Normal Percentiles plots for each level of the Gage factor all show a fairly straight line), as shown in Figure 2.14. In the case of the MATLABsc level of the Gage factor, there is concentration of points near the zero residual value that is of some concern. However, in light of the evidence provided by the MATLABsc histogram (Figure 2.15) and MATLABsc Boxplots and Stem-Leaf plots (Figure 2.16), MATLABsc data was deemed approximately normal, since it resembles a bell-shaped curve with a low standard deviation. Similarly, histograms for the rest of Gage factor levels suggest a reasonable normal distribution fit, as shown in Figure 2.15. Moreover, Boxplots and Stem-Leaf plots for Ruler and GIMP (Figure 2.16) both support reasonable normality based upon graphical correspondence with the bell-shaped distribution of values.

As stated in the ANOVA model, the Null Hypothesis (H_0) postulated in Equation 2.3 that there was no effect due to the Gage factor on the LWD value, meaning that the mean, variance, and shape of all Gage factor level samples' distributions would be identical. In that respect, a p-value is calculated in order to accept or reject the Null Hypothesis.

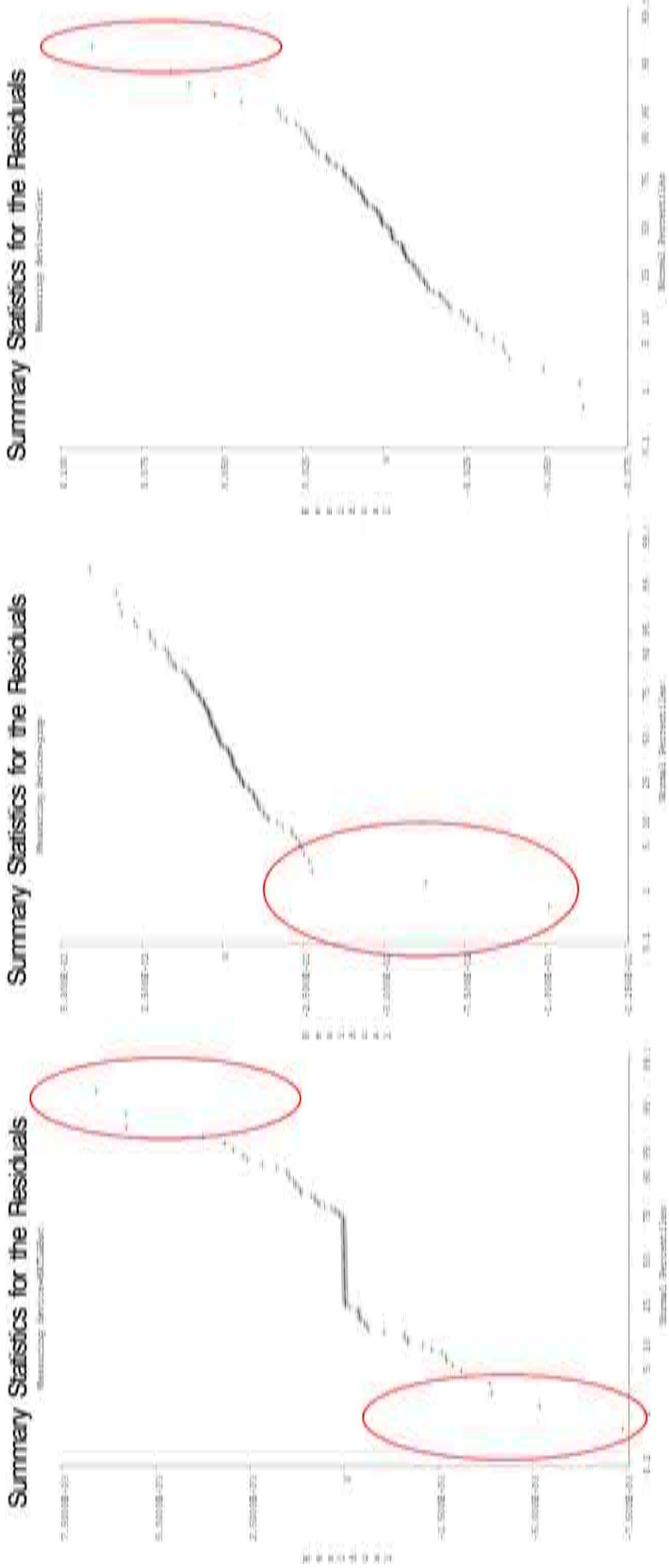

Fig. 2.11: Removed outliers as shown in Residuals vs Normal Percentiles plots for each Gage factor level

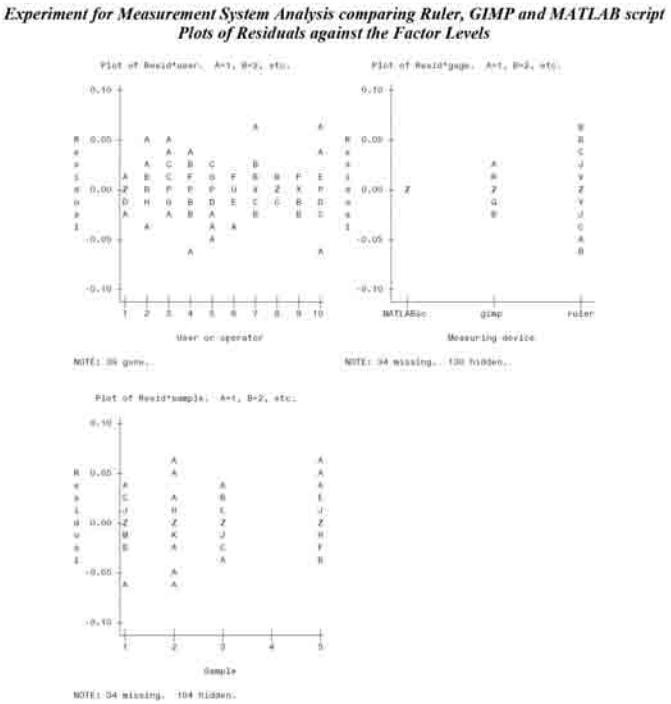

Fig. 2.12: Residuals versus Explanatory Factors plots in final ANOVA

The p-value is the probability of obtaining results at least as extreme as the one that was actually observed, assuming that the Null Hypothesis is true. In our case, since the critical probability value used in this study is 0.05, it means that the Null Hypothesis would be rejected if a p-value equal or less than 0.05 (5% of expected likelihood) is obtained. A Type 3 F-test is performed in the *Type 3 Tests of Fixed Effects* table (Figure 2.17) because the test statistic associated to the p-value has an F-probability distribution [23], and SAS™ utilizes Type 3 F-tests to assess differences between Least Squares Means (LSM) for mixed effects, instead of using differences between the arithmetic treatment means (Type 1 F-test) [24]. In this context, it is worth mentioning that LSM are obtained by performing a regression analysis using the ANOVA model stated in Equation (3.2). As for the ANOVA results, Figure 2.17 shows that a statistically significant p-value of 0.0101 for the Gage factor was obtained as a result of a Type 3 F-test (the p-value obtained is equal or less than the selected critical probability value of 0.05). Consequently, based upon the present statistical study, the condition for the Null Hypothesis to be true is not met, and it is concluded that Gage

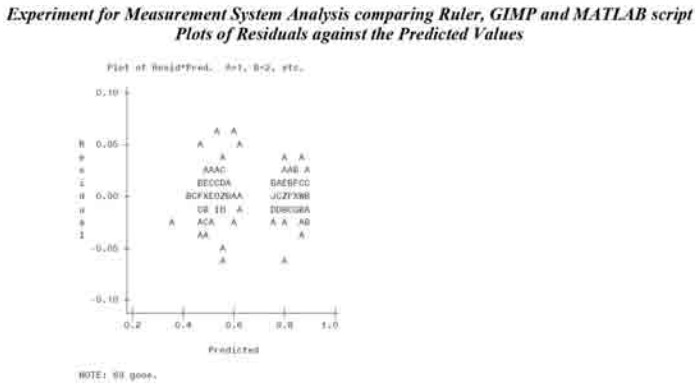

Fig. 2.13: Residuals versus Predicted values plot in final ANOVA

affects LWD measurements. In fact, this Type 3 F-test result provides statistical evidence of the significant effect of the Gage factor on the LWD response, and prompts for a comparison between the three Gage factor level means. The *Least Squares Means* table shown in Figure 2.17 also reveals that all three Gage factor level means are statistically significant for LWD measurements (the p-values shown in the $Pr > |t|$ column of the LSM table are all equal or less than the 0.05 probability critical value). Furthermore, the *Difference of Least Squares Means* table in Figure 2.17 presents statistical evaluations on pairwise combinations of Gage factor levels means. In this context, the difference between Ruler and MATLABsc LWD means were not significant (evidenced by the fact the 1.0000 p-value obtained is greater than the selected critical probability value of 0.05). In conclusion, the *Difference of Least Squares Means* table shows that, based upon the present statistical evidence, measurements taken with MATLABsc and Ruler gages have the same mean, although this does not hold true for any other pair of measuring systems (Ruler-GIMP and GIMP-MATLABsc).

2.5 Discussion

Based upon Measurement System ANOVA results shown in the LSM table (Figure 2.17), the effects of all measurement systems (Gage factor levels) evaluated in this study are significant in affecting LWD measurements on micrographs. Therefore, the selection between Ruler, GIMP, and MATLABsc measurement systems matters in determining LWD values on ultrasonically consolidated samples. Moreover, MATLABsc data exhibits the minimum

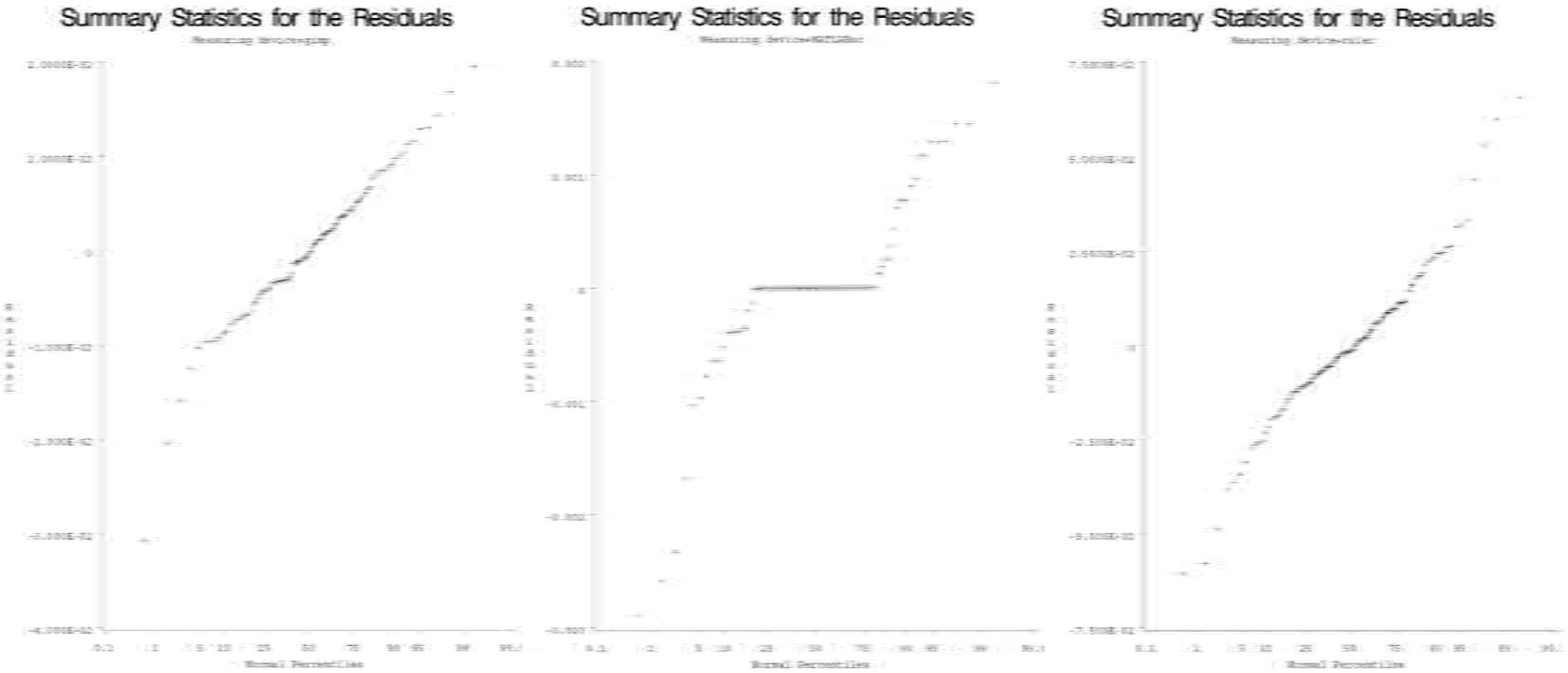

Fig. 2.14: Residuals vs Normal Percentiles plot for each Gage factor level in final ANOVA

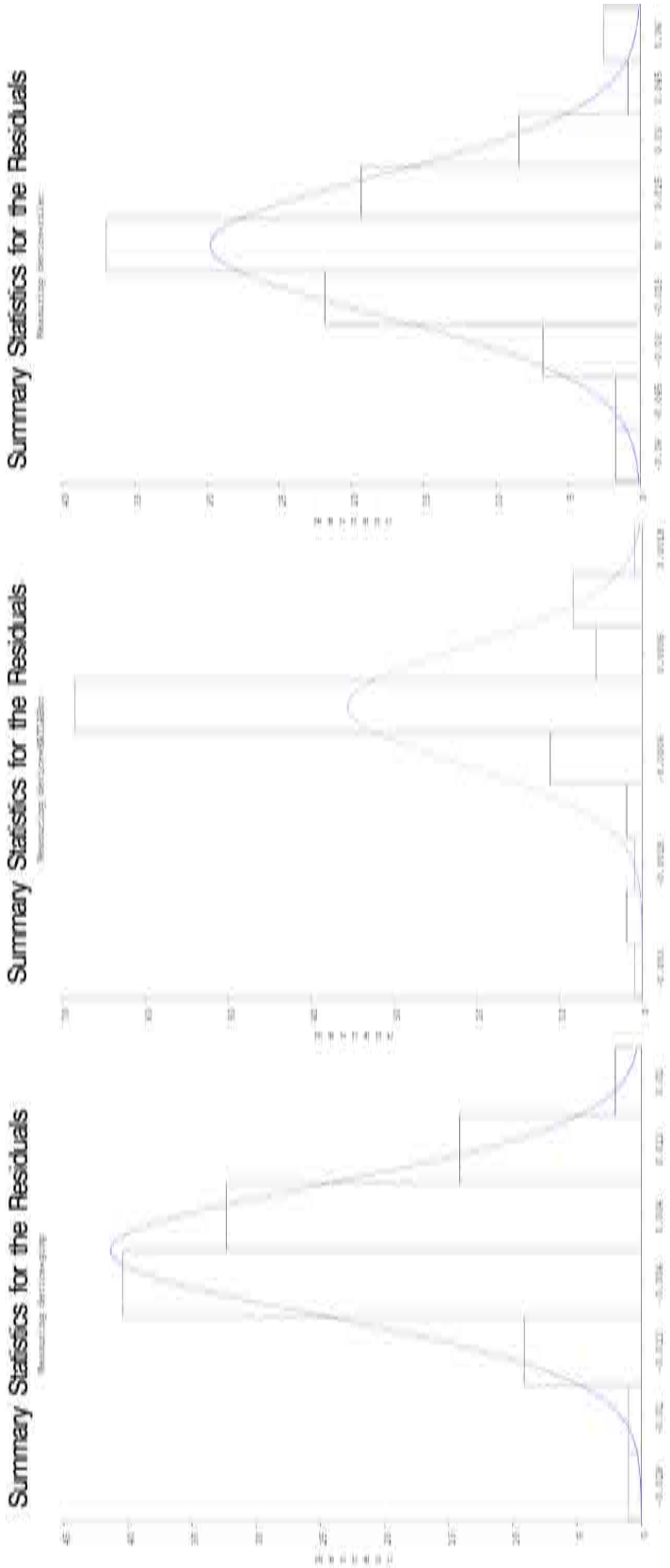

Fig. 2.15: Histogram for each Gage factor level in final ANOVA

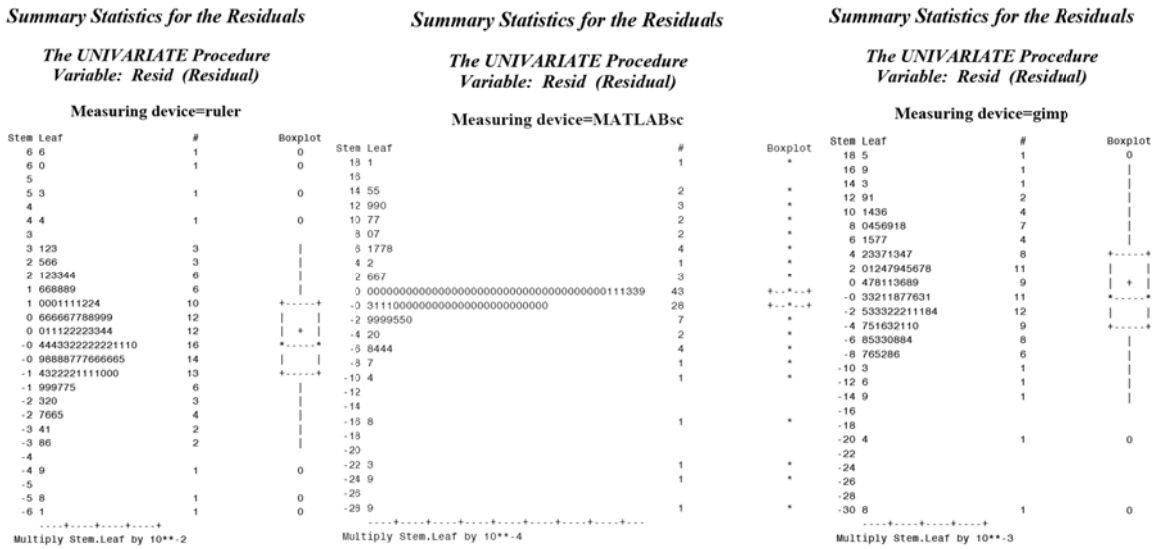

Fig. 2.16: Stem and Leaf plot and Boxplot for each Gage factor level in final ANOVA

spread or variability of all gages, and the latter provides evidence of the suitability of this measurement system in obtaining reproducible LWD measurements.

There are some advantages of using the MATLAB script to perform LWD measurements on ultrasonically consolidated specimens: (1) The MATLAB script provides the highest instrument resolution of all LWD measuring instruments. (2) The MATLAB script can accurately and reliably reproduce traditional Ruler-based methods based upon the image file and Region of Interest information. (3) The spread of LWD measurements using the MATLAB script is minimal (Figure 2.16), making the MATLAB script the most suitable as a standard LWD measurement tool of the three instruments evaluated in this work. Also, ANOVA results show that the measurement means between rulers and MATLAB are statistically the same, and thus the MATLAB approach can be used to compare new data against old, that is ruler-based data, while giving better repeatability for future measurements. However, in order to use the MATLAB script as an application on a general basis, it is important to realize the scope and limitations of this measuring instrument, as it is presented below.

First, one critical step of the script routine is the definition of the Region of Interest, because it is the input on which all further image processing tasks take place. The option of selecting a Region of Interest for assessing LWD in the MATLAB script allows single inter-

Type 3 Tests of Fixed Effects				
Effect	Num DF	Den DF	F Value	Pr > F
gage	2	14.7	6.38	0.0101

Least Squares Means						
Effect	Measuring device	Estimate	Standard Error	DF	t Value	Pr > |t|
gage	MATLABsc	0.6822	0.08994	3.03	7.59	0.0046
gage	gimp	0.6560	0.08995	3.03	7.29	0.0051
gage	ruler	0.6822	0.08997	3.03	7.58	0.0046

Differences of Least Squares Means									
Effect	Measuring device	Measuring device	Estimate	Standard Error	DF	t Value	Pr > |t|	Adjustment	Adj P
gage	MATLABsc	gimp	0.02624	0.008382	13.7	3.13	0.0075	Tukey-Kramer	0.0181
gage	MATLABsc	ruler	9.012E-6	0.008582	15.1	0.00	0.9992	Tukey-Kramer	1.0000
gage	gimp	ruler	-0.02623	0.008640	15.5	-3.04	0.0081	Tukey-Kramer	0.0218

Fig. 2.17: Type 3 fixed effects test and Least Squares Means for Gage factor in final ANOVA

face specification (in sample micrographs with multiple layers) and provides computational simplification for further image processing. However, the interface shown in the Image File input (Figure 2.1) must be horizontally oriented, and it is crucial to define the Region of Interest as close as possible to the interface in order to perform a correct analysis. In this respect, MATLAB has limited dynamic zoom capabilities to facilitate the selection of the Region of Interest using the Visual Clicks option. Specifically, the zoom in/out option can only be used in the MATLAB script routine when the initial image is initially shown on screen (Figure 2.1), and the zoom magnification level cannot be adjusted afterwards. For this reason, it is also important to set an adequate magnification level for sample microscopy. For picture-wide interfaces, the recommended magnification level range for defining the ROI to obtain a LWD estimate using the MATLAB script is 50-100X. Based on several tests performed, some defects could not be clearly seen inside the MATLAB figure window with a microscopy magnification level lower than 50X, without zoom. At the other end, picture-wide interfaces do not have enough interface length for proper analysis when using microscopy magnification levels above 100X. For ROI definitions that are not picture-wide, the zoom option available in the MATLAB script routine can be used with magnification levels above 100X and below 50X, and the practical minimum/maximum magnification for microscopy

will depend upon the specific application. The MATLAB script procedure is designed to work with only one micrograph. Multiple or combined image analysis using the MATLAB script is only indirectly possible at this development point, by stitching together multiple side-by-side micrographs to make a single micrograph of a horizontally oriented contiguous interface, for further analysis. On the other hand, it is worth mention that stitching together micrographs may induce artifacts in the image as opposed to taking individual LWD measurements on each interface, tabulating them in a spreadsheet and averaging.

Second, the Otsu thresholding algorithm used for black and white binarization has several limitations. Among other limiting factors, it has been reported that the Otsu thresholding method does not work well when an uneven lighting disturbance is present on the input image file [25]. Some identified causes for uneven lighting disturbances are non-uniform light distribution on the image and inability to isolate the scene from other object shadows [25]. In addition to avoiding uneven lightning disturbances, input micrographs with good optical characteristics (in-focus image, balanced contrast image, adequate depth of field (image sharpness), absence of blurring or image distortions, etc.) are required in order to ensure accurate LWD assessment by any visual-based method, including the MATLAB script. The Otsu thresholding routine works best in those ROI that include both bonded and unbonded areas with clearly different brightness. Despite this, the micrograph quality necessary for performing accurate black and white binarization using the Otsu method is completely attainable. Based on tests using previous published pictures of ultrasonically consolidated samples ([7]), optically unsuitable micrographs are avoided when good sample preparation (grinding and polishing) and microscopy practices are followed. Experimental results show that grinding and polishing of ultrasonically consolidated samples must be performed down to a grit size equal to or lower than 6.5 microns in average particle size. As for the effect of poor sample preparation on MATLAB script LWD results, Figure 2.18 shows a sample micrograph containing scratches and stains, and one 8-bit grayscale ROI analysis example. Basically, both scratches and stains introduce noise in the Otsu's thresholding (Black and White binarization) routine that derives into black pixels that do not correspond to

unbonded areas, and leads to inaccurate LWD results. The sample must be in not-etched condition because etching creates small cavities that appear as dark areas in micrographs, causing a similar effect to the ROI analysis as the one caused by the stains and scratches. Moreover, good sample preparation (grinding and polishing) is critical due to the brightness criteria used in the MATLAB script procedure to make the distinction between bonded and unbonded regions in the ROI. In general, the MATLAB script does not automatically differentiate between unbonded regions, scratches, stains and etching marks in the Region of Interest. In fact, the MATLAB script gives a conservative LWD estimate for the Region of Interest and any black pixel out of the interlayer interface will result in a LWD assessment bias. For instance, as is shown in Figure 2.18, it only takes one black pixel in a column of the ROI Image Matrix to render the entire column as unbonded area. Thus it is important that users of the MATLAB script look at the Otsu thresholding results to make sure there are no stray black pixels outside the interface region that will affect the LWD measurement, before black pixels are extended vertically across the image.

That being said, it is worth a mention that the MATLAB script can be used to perform LWD measurements on micrographs including multiple interfaces, although in its current implementation, the procedure can only process one interface per run.

The MATLABsc measurement system is also efficient in assessing LWD. For comparative purposes, Table 2.2 shows the average time per user per sample to take LWD measurements (in seconds) using each measuring system of this study. Overall, the amount of time to take measurements using the MATLAB script is 46.36% ($\frac{65.25-35}{65.25}$) less than that of the Ruler and 57.70% ($\frac{82.75-35}{82.75}$) less than that of the GIMP.

2.6 Summary and Conclusion

The experimental results presented show that the MATLAB script can effectively estimate LWD on cross section micrographs. Although there are some limitations for the Image Processing approach used in the MATLAB script routine, this LWD instrument provides the highest resolution of all measuring devices presented in this work.

Moreover, the MATLABsc measuring system shows small spread or variation in the

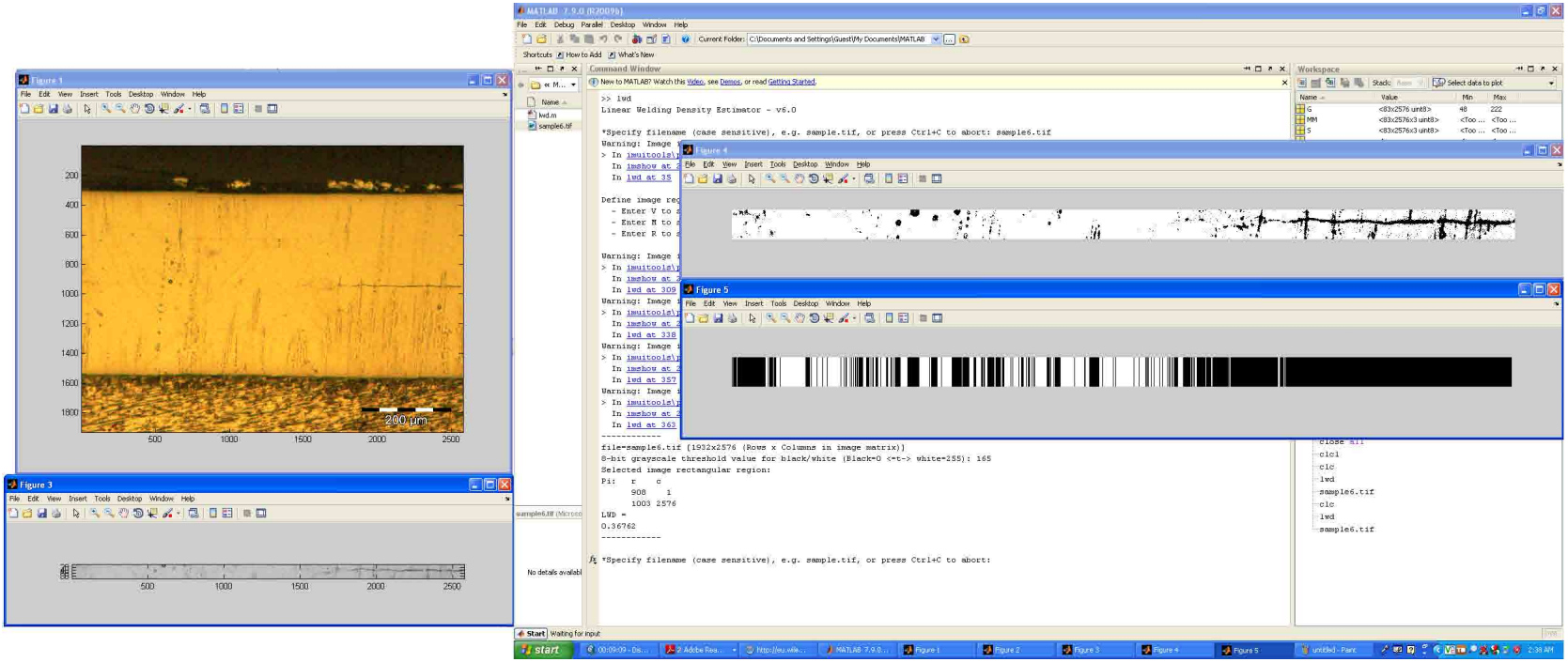

Fig. 2.18: Bad specimen preparation example

Table 2.2: Measuring systems time comparison

	Average time (s)		
Specimen	**Ruler**	**GIMP**	**MATLABsc**
1	57	63	26
2	73	97	31
3	50	55	45
4	81	116	38
Grand average time:	**65.25**	**82.75**	**35**

measurements, and a verifiable methodology to assess LWD in cross section micrographs that is suitable for standardization. In fact, when considering the MATLABsc measuring system spread as a unit, Figure 2.10 shows that the spreads of GIMP and Ruler measuring systems are at least 7.4 and 8.7, respectively.

In addition, experimental results show that Ruler and MATLAB instruments have statistically similar measurement means, and thus the MATLAB script can be used to compare results against past Ruler measurements.

2.7 Future Work

In order to improve upon the usability of the and robustness of the MATLAB script, recommended future work includes the development of a method for efficient identification of sample defects (voids, delamination, inclusions) for better LWD assessment, and the incorporation of an option for processing multiple interfaces in one micrograph in order to provide an average LWD estimate.

The latest version of the MATLAB script is available for free under the terms contained in the *lwd.m* script file and can be downloaded from:

`https://sites.google.com/site/lwdmatlabsc/`

Additional work needs to be done in order to present a complete LWD measurement standard. This includes:

- Specifying the minimum requirements for the optical system used to acquire ultrasonically consolidated sample micrographs.

- Defining a standard for weldment preparation in terms of preparation times, specific preparation materials/equipment, and preparation methods in tandem with the ultrasonically consolidated material used and the level of quality desired.

Addendum

Instructions for Ruler, GIMP and MATLAB script gages for measuring LWD.

- **Ruler Instructions:**

1. Open the GIMP program.
2. On the GIMP Menu bar, select 'File->Open...', select the image file of interest and press 'Open'.
3. Maximize the window containing the image file.
4. Using the 1:200 scale of the metric scale ruler and having the image displayed, measure total horizontal interface length on the screen with the ruler, at current zoom magnification level. Record this measurement.
5. Using the 1:200 scale of the metric scale ruler and having the image displayed, measure the horizontal length of each black pixel region in the interface with the ruler, keeping the same zoom magnification level used in the previous step. Perform all measurements on screen and record each length value.
6. Add up the lenghts of each individual black pixel regions obtained in the previous step to get the Unbonded interface length.
7. Using results from steps 3 and 5, calculate LWD by using the formula:
   $\%LWD = \frac{Total\ interface\ length - Unbonded\ interface\ length}{Total\ interface\ length} \times 100$
8. Repeat steps 2 through 6 with all given sample images and save all LWD results.

- **GIMP Measure Tool Instructions:**

1. Open the GIMP program.
2. On the GIMP Menu bar, select 'File->Open...', select the image file of interest and press 'Open'.
3. Having the image displayed on screen, go to the GIMP program Menu Bar, and select 'Tools->Measure'.
4. Select pixels as length units in the Status Bar of the GIMP window where the image is displayed in.
5. Measure total horizontal interface length in the interface by clicking and dragging the mouse cursor, and record this measurement. You may use Ctrl+Mouse Wheel Scroll to zoom in or out with respect to the original view.
6. Measure the horizontal length of each black pixel region in the interface by clicking and dragging the mouse cursor, and record each length value in pixels. You may use Ctrl+Mouse Wheel Scroll to zoom in or out with respect to the original view.
7. Add up the lenghts of each individual black pixel regions obtained in the previous step to get the Unbonded interface length.
8. Using results from steps 5 and 7, calculate LWD by using the formula:
   $\%LWD = \frac{Total\ interface\ length - Unbonded\ interface\ length}{Total\ interface\ length} \times 100$
9. Repeat steps 2 through 7 for each one of the sample images. Save all LWD results.
10. Close GIMP program.

- **MATLAB Script Visual Clicks Instructions:**

1. Start MATLAB program. Place 'lwd.m' MATLAB script file and all image files of interest in the MATLAB working directory.
2. Enter 'lwd' (without quotes) at MATLAB command window prompt to run the MATLAB script for LWD measurements.

3. Follow on-screen instructions for image file input.

4. When the sample image is shown in a MATLAB Figure window, confirm image file selection by pressing *Enter*, or cancel execution by pressing *Ctrl+c* while the MATLAB window is active. You may use Ctrl+Mouse Wheel Scroll to zoom in or out with respect to the original view at this step. If you cancel the MATLAB script execution, repeat steps 2 and 3.

5. Select a region for the analysis using the mouse clicks option. Two separate clicks specify two diagonally opposite corners of the rectangle that enclose the interface. This click-defined rectangle should be the smallest section of the image that contains the interface to be analyzed. If necessary, you may click outside the image and the selection will be adjusted to match the image borders automatically. Do not select the whole image as your rectangular region.

6. Press enter three times for grayscale images, or four times for color images as it applies. The LWD estimate is given as part of the output in the MATLAB command window, between discontinuous lines (- - -). Record this LWD measurement.

7. Repeat steps 2 through 6 for each one of the sample images. If an error is encountered, re-run the script again (repeat steps 2 through 6). Save all LWD results.

8. Exit the MATLAB script routine by pressing *Ctrl+c* while the MATLAB window is active.

9. Close MATLAB program.

Chapter 3

Experimental Determination of Optimum Parameters for Stainless Steel 316L Annealed Ultrasonic Consolidation[1]

3.1 Abstract

Ultrasonic Consolidation of Stainless Steel foils is being investigated for potential structural applications. In this study, parameter optimization for Ultrasonic Consolidation of Stainless Steel 316L annealed is assessed by evaluating experimental factors of Oscillation Amplitude, Welding Speed, and Normal Force at 478 K (400 °F). A series of experiments were performed to explore the effect of these factors on the Linear Welding Density of utrasonically consolidated samples, determine the statistical significance of these factors, and identify the combination of UC process parameters that maximizes Linear Welding Density.

3.2 Introduction

Ultrasonic Consolidation (UC) is an additive manufacturing process whereby layers of metal foils can be joined with a metallurgical bond by means of acoustic energy and shaped using CNC machining. The UC process has the advantage of creating metal structures without high temperatures [6]. Indeed, although localized frictional heating is involved in the UC process, the mechanism for UC is not melting [6], and thus negligible shrinkage and thermal stresses result during part building [5]. In turn, ultrasonically consolidated parts have virtually no thermal degradation in material properties. Although there are some limitations regarding how high ultrasonically consolidated parts can be made [26],

[1] Coathored by R. Gonzalez, B. Stucker. This chapter is a paper that has been submitted for publication in the Rapid Prototyping Journal.

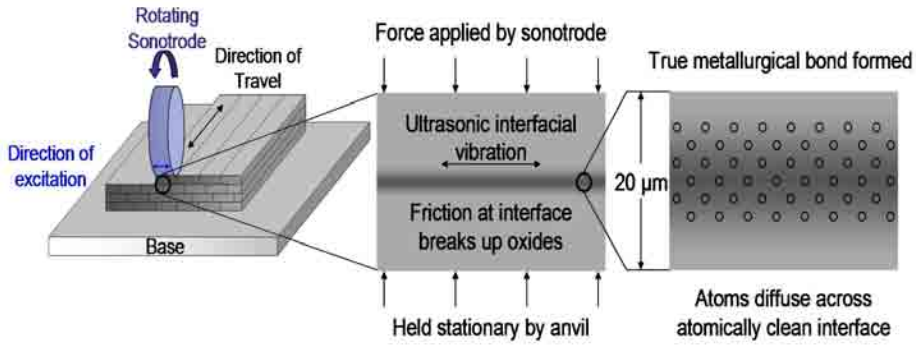

Fig. 3.1: Schematic of the Ultrasonic Consolidation process [8]

these parts may be designed and built to include complex geometric features for specific applications, due to the additive manufacturing nature of the UC process.

Currently, UC manufacturing combines Ultrasonic Welding and CNC milling in a combined additive/subtractive scheme for part building. As for the UC manufacturing procedures, a computer program processes a three-dimensional CAD model of the part to be built, and slices up this model into a number of horizontal layers, each layer with a thickness equal to the thickness of the metal foil used. Ultrasonically deposited foil strips are placed adjacently to each other, to create a layer. After a layer is completed (or after several layers are completed, optionally), a computer controlled milling head shapes the layer to its slice contour. Following this, milling chips are removed and foil deposition for the next layer starts [5]. As a result of a continuous addition of layers, a three-dimensional part is produced from bottom to top.

A UC foil deposition schematic is shown in Figure 3.1. First, a thin metal foil is placed over the substrate. Following this, a rotating ultrasonic sonotrode travels along the length of the metal foil, keeping the foil in intimate contact with the substrate while a Normal Force is applied to the metal foil through the sonotrode. The consolidation of the foil and the substrate is accomplished by sonotrode oscillations at an ultrasonic frequency and at user-set amplitude. The direction of the sonotrode's oscillations (direction of excitation) is along the sonotrode's rotational axis.

As a consequence of sonotrode dynamics, localized shear forces are generated from the

combination of sonotrode pressure and oscillation, inducing interfacial stresses between the two mating surfaces and elastic-plastic deformation of surface asperities [6]. Furthermore, asperities deformations break up the oxide film, establishing a metallurgical bond between the foil and the substrate due to relatively clean metal-to-metal surface contact [5]. On a lower scale, atomic diffusion may also aid in the bonding process because local temperatures at the interface and the surrounding affected region (about 20 µm) can reach up to 50% of the melting point of the material being deposited [6], but only for a very brief time. Although still being researched, there is evidence that ultrasonic welding mechanisms for bond formation involve: (1) removal of surface oxide layers, (2) plastic deformation at the interface, and (3) to a lesser extent, diffusion of metal atoms across the interface. Nonetheless, plastic deformation is considered the most important characteristic in enabling surface oxide layer removal and diffusion mechanisms [7]. All three mechanisms aid in metallurgical bonding across the interface.

There are four general control parameters for welding within a UC system: Amplitude of Oscillation, Contact Pressure Distribution (Normal Force between the horn and foil), Welding Speed along the direction of travel, and Temperature of the substrate. The first three parameters depend upon sonotrode interaction with the part being built. In contrast, Temperature depends on the heat applied directly to the substrate from the base plate, with Temperature values from room temperature up to hundreds of kelvin degrees (e.g. typical platform's limitation is 478 K (400 °F)).

Linear Welding Density (LWD) is the proportion of bonded area to total area within the weld interface [9]. The selection of LWD as a quality measure is better understood considering that ultrasonically consolidated parts typically show unbounded regions (defects, physical discontinuities) along the layer interfaces. Indeed, the assessment of the bonded region proportion given in a LWD measurement is also important as a quality attribute for porosity in ultrasonically consolidated parts [11]. The relevance of understanding what factors influence LWD has already been observed in a previous study of UC parts [7]. As a matter of fact, LWD strongly affects mechanical properties in the direction normal to the foils

for an ultrasonically consolidated part, and the mechanical behavior of a UC made structure under load-bearing stresses [7]. In consequence, properties like specific weight and Poisson's ratio of ultrasonically consolidated parts are affected by LWD. In the same manner, quality charateristics based on ultrasonically consolidated part porosity (e.g. insulating enclosures) are utterly dependent upon the level of LWD present between metal foils.

For the purposes of this study, LWD will be determined based upon metallography of weld interfaces sectioned along the width of the foil. The samples will be mounted, polished to a smooth finish and cleaned in isopropyl alcohol. LWD will be assessed from micrograph images of samples taken from weld cross-sections, based upon the following equation:

$$\%LWD = \frac{Bonded\ interface\ length}{Total\ interface\ length} \times 100 \tag{3.1}$$

Regarding optimum parameters for UC, it is worth mentioning that optimality is not absolute under general conditions. The magnitude of interfacial stresses at the mating surfaces during the UC process depends on current frictional conditions at the sonotrode/foil and substrate/foil interfaces [8,27–29]. Furthermore, sonotrode geometry, material, and surface conditions influence optimum parameter values for UC [11]. Consequently, UC optimum process parameters can vary with sonotrode wear over time, different foil material/thickness and for different UC systems. In general, a significant change in frictional conditions at the sonotrode/foil or substrate/foil interfaces will affect optimum UC parameter values. Therefore, it is necessary to understand that the concept of optimality of UC parameters is restricted to a reasonably consistent range of frictional conditions, whereas new optimum UC process parameters must be established if these frictional conditions change significantly.

Overall, the objectives of the research effort presented here are to (1) Determine the optimum processing parameters for UC of Stainless Steel 316L annealed (SS316L annealed) foils, based on the maximum Linear Welding Density criteria; and (2) Characterize the effect that optimum UC parameters have on SS316L annealed ultrasonically consolidated samples. SS316L annealed was chosen due to its commercial availability in foil form, variety of applications and greater mechanical strength than Aluminum (Al) 3003 — the typical

material used in UC machines. Additionally, research on SS316L UC will allow comparison between previous Al UC studies and this investigation. Even though some researchers have recommended a joint approach for determining optimum UC parameters based on peel testing and LWD measurements [9], the criteria used in this study is minimal part porosity and thus maximum LWD is the benchmark used for determining the optimum UC parameters in this work. Although Peel Strength is another parameter for characterizing ultrasonically consolidated parts, it has been found that peel test results are notoriously scattered compared to LWD, and thus LWD appears to be a more stable parameter [30].

3.3 Literature Review

In previous studies, UC of 3003/6061 Al alloy structures have been investigated using Welding Speed, Oscillation Amplitude, Temperature, and Contact Pressure as the variable process parameters [9, 11, 13]. The evaluation of the effect the aforementioned parameters had on microstructure and mechanical properties of ultrasonically consolidated parts has been the object of active research [9, 10]. In this context, selection of appropriate process parameters plays a key role in UC bond formation of Al 3003/6061 based on LWD microscopic studies and peel-off tests [9, 10]. Although authors have found that it is possible to have a low peel load response and high linear weld density with Aluminum 6061 (due to excessive strain hardening and cycling stressing of contact points at the interface) [9]; it has been verified that a high peel load response only occurs in the presence of high LWD [10]. For instance, higher Oscillation Amplitude values produced higher LWD in Al 3003/6061 and either higher weld strengths (in Al 3003) [10] or no significant effect on weld strength (in Al 6061) [9]. Furthermore, several research efforts included Substrate Temperature as an additional factor for the Al 3003 UC process, and performed a comprehensive study of the effect of Substrate Temperature, Welding Speed, Oscillation Amplitude, Surface Machining and Normal Force on Al 3003 UC [7, 11]. Among other things, it was concluded that higher Normal Force and higher Oscillation Amplitude increase LWD values up to a certain level, beyond which LWD values decrease. Moreover, it was observed that lower Welding Speeds (down to 12 mm/s) increase LWD, and higher temperatures produced higher LWD within

a range from ambient to 450 K (350 °F) [7].

Additionally, previous research has demonstrated the feasibility of the UC process for bonding Stainless Steel 316L. Specifically, one study explored the role played by process parameters of Welding Speed, Amplitude, Normal Force, and Temperature in Stainless Steel 316L Ultrasonic Consolidation, while providing additional insight on UC process parameters effects, and optical microscopy of samples [1]. Results of an analysis of variance (ANOVA) on SS316L UC, with peel strength as the response and Amplitude, Normal Force, and Welding Speed as factors, indicated that only Amplitude and Welding Speed factors were statistically significant for peel strength (with a 90% confidence interval, p-value < 0.10), and Amplitude exerted the strongest effect on peel strength [1]. As for the effect of process parameters on peel strength, higher Oscillation Amplitudes and lower Welding Speed increased peel strength; while Temperature (up to 422 K (300°F)) and Normal Force (up to 1600 N) were not statistically significant.

Considering these research efforts, this study addresses parameter optimization for ultrasonic consolidation of Stainless Steel 316L annealed, by evaluating experimental factors of Oscillation Amplitude, Welding Speed, Normal Force and Temperature in order to minimize part porosity on the basis of a maximum LWD criteria.

3.4 Ultrasonic Consolidation System Description

A series of experiments with SS 316L annealed (composition by weight: 16-18 %Cr, 10-14 %Ni, 2.0-3.0 %Mo, $\leq$ 2 % Mn, $\leq$ 0.75 %Si, $\leq$ 0.010 %N, $\leq$ 0.045 %P, $\leq$ 0.03 %C, $\leq$ 0.03 %S) were performed to assess the effect of various factors in the UC process. A Solidica Formation™ machine was used to create ultrasonic consolidated samples. The Solidica Formation™ UC machine (Figure 3.2 and Figure 3.3) is an integrated UC building system that combines a rotating ultrasonic sonotrode, a heat plate, a foil-feeding spool mechanism, a three-axis milling head, and a software implementation for material deposition and machining [11]. Furthermore, the Solidica Formation™ sonotrode oscillates transversely according to a half-wave rectified sine wave at a frequency of 20 kHz and at user-set Oscillation Amplitude while traveling over the metal foil. The sonotrode itself is incorporated into a welding

head and its position is controlled by numerical control. The maximum build size of the Solidica Formation™ machine is 609.6 mm × 914.4 mm × 203.2 mm (24 in × 36 in × 8 in), and the CNC contour milling head has a tolerance of 0.05 mm (0.002 in) [12]. The sonotrode has a 146.75 mm nominal diameter. Regarding process parameter setting limits, the Solidica Formation™ machine is constrained to a nominal force less than or equal to 1800 N, nominal amplitudes between 6 µm and 27 µm, welding speeds up to 84.7 mm/s (200 ipm), and nominal temperatures ranging from ambient to 478 K (400 °F).

Using the Solidica Formation™ system, part fabrication is performed on a firmly bolted Al 3003 H14 (composition by weight: 0.050-0.20 %Cu, $\leq$ 0.70 %Fe, 1.0-1.50 %Mn, $\leq$ 0.60 %Si, $\leq$ 0.10 %Zn) base plate mounted on a heat plate. Also, the heat plate maintains the substrate at a user-set Temperature, between ambient and 478 K (400°F). A graphical description of the Al 3003 H14 base plate (dimensions: 355 mm × 355 mm × 12 mm) along with the plate/part fixture is presented in Figure 3.4.

A 146.75 mm nominal diameter Titanium sonotrode was employed for UC depositions. Sonotrode roughness was measured using a Mitutoyo Surftest SV-602 stylus profilometer, at three evenly spaced angular locations (0 rad (0°), $\frac{2\pi}{3}$ rad (120°), $\frac{4\pi}{3}$ rad (240°)). The Arithmetic Average of Absolute Values (Ra) was calculated in the sonotrode direction of excitation and around the sonotrode midplane circumference (a one inch long arc centered at each angle location). Results for Ra calculations are presented in Table 3.1.

3.5 Experimental Work

Table 3.1: Sonotrode surface roughmess measurements

	Sonotrode Angular Location		
Measurement Type	**0 rad (0°)**	**$\frac{2\pi}{3}$ rad (120°)**	**$\frac{4\pi}{3}$ rad (240°)**
Ra (µm) in the direction of oscillations	6.06	4.74	4.81
Ra (µm) around the circumference	5.01	3.96	6.59

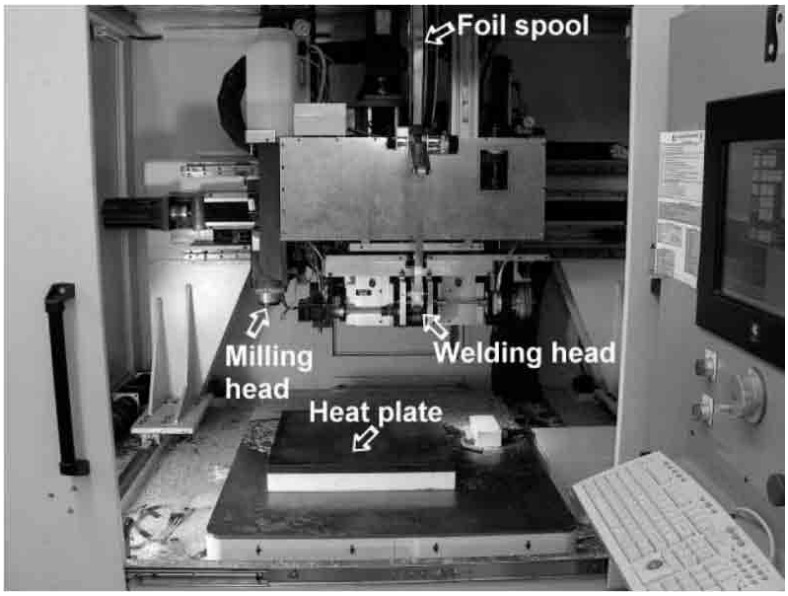

Fig. 3.2: Solidica Formation™ machine (as shown in [11])

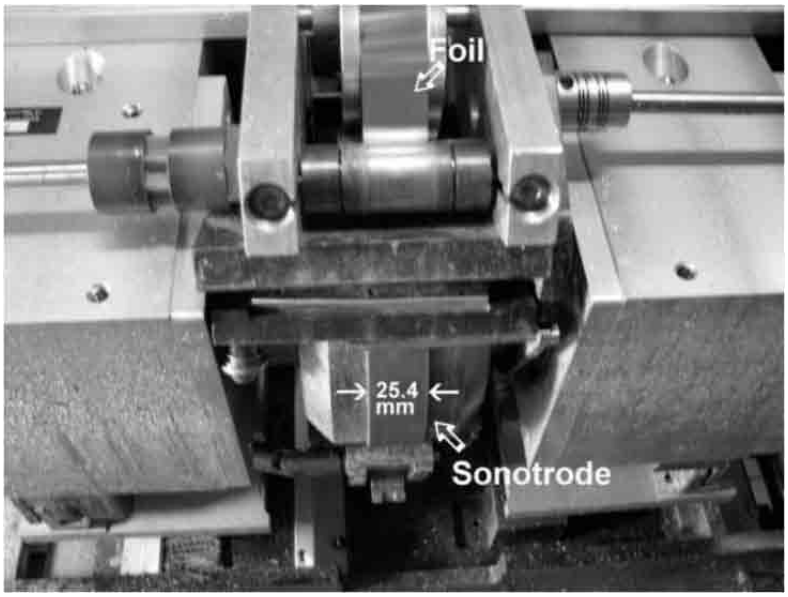

Fig. 3.3: Close-up view of the Welding head, showing the sonotrode from below (as shown in [11])

Fig. 3.4: Base plate and part fixture in the Solidica Formation™ machine (Left), and Geometry of the base plate showing bolt locations (Right)

3.5.1 Experimental Units

The experimental unit (item for observations) used for all experiments in this study, hereinafter called the Standard Sample, consisted of four succesive depositions of 0.1016 mm (0.004 inch) thick SS316L annealed rectangular foils, one on top of the other, made with a constant welding direction and by manual placement of foils. A Standard Sample schematic is shown in Figure 3.5. Each SS316L annealed foil is 26.99 mm (nearly 1.0625 inches) wide with a parametric length L, and each ultrasonically consolidated section of the SS316L annealed foil is 25.4 mm (1 inch) wide with a parametric length λ. Diferent types of standard samples were utilized for each experiment of this study, comprising different values for the L and λ parameters. Specifically, Type 1 standard samples had parametric values of L=76.2 mm (3 inches) and λ=63.5 mm (2.5 inches) and were used for the Taguchi experiment; Type 2 standard samples, with parameter values of L =63.5 mm (2.5 inches) and λ=50.8 mm (2 inches), were used for the Split Plot experiment. Figure 3.5 caption sumarizes the difference between Type 1 and Type 2 standard samples.

Also, each standard sample comprises three SS316L annealed-to-SS316L annealed interfaces, namely Interface 1, Interface 2, and Interface 3 that are illustrated in Figure 3.6. It is worth mentioning that the interface 0 shown in Figure 3.6 (between the first layer and the base plate) was not considered in LWD measurements because it does not constitute a

Stainless Steel to Stainless Steel bond and, in contrast with layer depositions corresponding to Interfaces 1, 2, and 3, there is no initial sonotrode-induced roughness on the substrate.

3.5.2 Taguchi Experiment

An exploratory Taguchi Design was used to look into the effect UC process parameters or Factors (Oscillation Amplitude, Welding Speed, Normal Force and Temperature) have on the LWD of SS316L ultrasonically consolidated samples and pinpoint working combinations of UC parameters for SS316L annealed UC. Using statistical terminology, each evaluated configuration of one factor is called a *factor level*. The Taguchi experiment design comprised four different levels for each parameter, and this is illustrated in Table 3.2. Levels for UC parameters for the Taguchi experiment were selected based upon Solidica Formation™ machine design limits, SS316L annealed UC feasibility tests available in the literature [1], and the combination of UC parameters that produced maximum LWD for Al 3003 UC reported by some researchers [7].

A special Taguchi L-16 orthogonal array, namely the L'16 (4^5 L-16) Taguchi orthogonal array, was utilized to determine the effects of individual process parameters. The L'16 array comprises five different experimental factors, four levels each [31]. Since only four process parameters are being considered for the Taguchi experiment, the fifth factor corresponding to the fifth column of the L'16 orthogonal array was not included and the Taguchi experiment array in Table 3.3 was obtained. Each experimental run produced one Type 1 standard

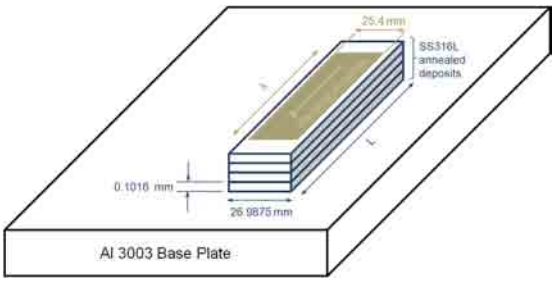

Fig. 3.5: Schematic of a SS316L annealed Standard Sample (In Type 1: L =76.2 mm (3 inches), λ=63.5 mm (2.5 inches); In Type 2: L =63.5 mm (2.5 inches), λ=50.8 mm (2 inches))

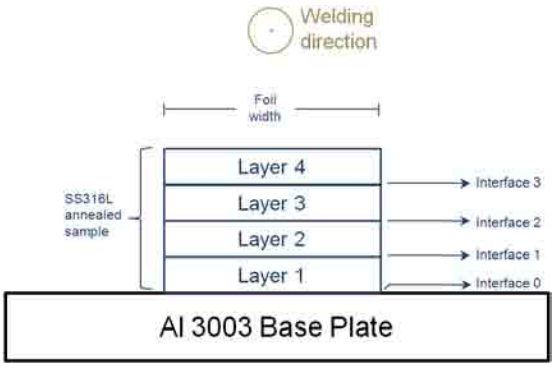

Fig. 3.6: Schematic of the SS316L annealed standard sample interfaces

sample. All 16 experiment runs were performed on a single base plate, and the microscopy of samples was conducted using a Zeiss Axiovert 100A inverted light microscope. The LWD of the interfaces was assessed by applying Equation (3.1) on one 100X magnification interface micrograph taken near the center of the ultrasonically consolidated section of the Type 1 standard samples. The SS316L annealed foils used for the Taguchi experiment were randomized for each of the 16 runs shown in Table 3.3.

Successfully bonded samples from the Taguchi experiment were selected based upon a 50% average LWD minimum criteria for samples. That is, considering standard sample interface schematics shown in Figure 3.6, only samples in which the average LWD for Interfaces 1, 2, and 3 was greater than 50% were deemed bonded. Using this criteria, only three samples were bonded during the Taguchi experiment. LWD measurements of successfully ultrasonically consolidated SS316L annealed samples in the Taguchi experiment are included in Table 3.4, and the micrographs on which these measurements are based are shown in Figures 3.7 through 3.9. From these micrographs it is clear that only one sample, shown in Figure 3.8, did not delaminate at any interface. It is evident, after comparing Table 3.3

Table 3.2: Taguchi experiment Factors (UC process parameters) and Levels

Factors	**Levels**			
Temperature	303 K (85 °F)	361 K (190 °F)	419 K (295 °F)	478 K (400 °F)
Contact Normal Force	500 N	1000 N	1500 N	1800 N
Welding Speed	11 mm/s (26 ipm)	16.1 mm/s (38 ipm)	21.2 mm/s (50 ipm)	26.3 mm/s (62 ipm)
Amplitude	16 µm	20 µm	24 µm	27 µm

Table 3.3: Taguchi L'16 experiment runs matrix

Experiment run	Temperature	Normal Force	Welding Speed	Amplitude
1	303 K (85 °F)	500 N	11 mm/s (26 ipm)	16 µm
2	303 K (85 °F)	1000 N	16.1 mm/s (38 ipm)	20 µm
3	303 K (85 °F)	1500 N	21.2 mm/s (50 ipm)	24 µm
4	303 K (85 °F)	1800 N	26.3 mm/s (62 ipm)	27 µm
5	361 K (190 °F)	500 N	16.1 mm/s (38 ipm)	24 µm
6	361 K (190 °F)	1000 N	11 mm/s (26 ipm)	27 µm
7	361 K (190 °F)	1500 N	26.3 mm/s (62 ipm)	16 µm
8	361 K (190 °F)	1800 N	21.2 mm/s (50 ipm)	20 µm
9	419 K (295 °F)	500 N	21.2 mm/s (50 ipm)	27 µm
10	419 K (295 °F)	1000 N	26.3 mm/s (62 ipm)	24 µm
11	419 K (295 °F)	1500 N	11 mm/s (26 ipm)	20 µm
12	419 K (295 °F)	1800 N	16.1 mm/s (38 ipm)	16 µm
13	478 K (400 °F)	500 N	26.3 mm/s (62 ipm)	20 µm
14	478 K (400 °F)	1000 N	21.2 mm/s (50 ipm)	16 µm
15	478 K (400 °F)	1500 N	16.1 mm/s (38 ipm)	27 µm
16	478 K (400 °F)	1800 N	11 mm/s (26 ipm)	24 µm

and Table 3.4, that most UC parameter combinations of the Taguchi experiment failed. In some cases, delamination occured on substrate foils while sonotrode vibrations were being applied to the current top foil. However, based on Taguchi experiment results in Table 3.4, SS316L UC is possible with nearly 83% LWD by using Oscillation Amplitude=27 µm, Welding Speed=16.1 mm/s (38 ipm), Normal Force=1500 N, and Substrate Temperature=478 K (400 °F) UC parameters. Taking into account succesful Tahuchi experiment runs, a Split Plot experiment was designed to obtain UC process parameters that maximize LWD with SS316L annealed.

3.5.3 Split Plot Experiment and Analysis of Variance

An experiment was conducted using a Split Plot design scheme for randomization. This experiment was performed to evaluate the effect of Oscillation Amplitude, Welding Speed, Normal Force, Position along the Welding Direction, and Interface Level factors on LWD values in Type 2 samples at 478 K (400 °F). Although the initial plot design included two levels of Temperature, namely 303 K (85 °F) and 478 K (400 °F), subsequent experiments showed that SS316L UC was not reliably reproducible at 303 K (85 °F) for any combination

Table 3.4: Successful runs of the Taguchi experiment and corresponding LWD results

Experiment run	Substrate Temperature	Normal Force	Welding Speed	Oscillation Amplitude	LWD Interface 1	LWD Interface 2	LWD Interface 3	Average LWD
6	361 K (190 °F)	1000 N	11 mm/s (26 ipm)	27 µm	90.49%	0.54%	83.62%	58.22%
15	478 K (400 °F)	1500 N	16.1 mm/s (38 ipm)	27 µm	84.47%	87.69%	76.01%	82.73%
16	478 K (400 °F)	1800 N	11 mm/s (26 ipm)	24 µm	95.96%	62.85%	0.00%	52.94%

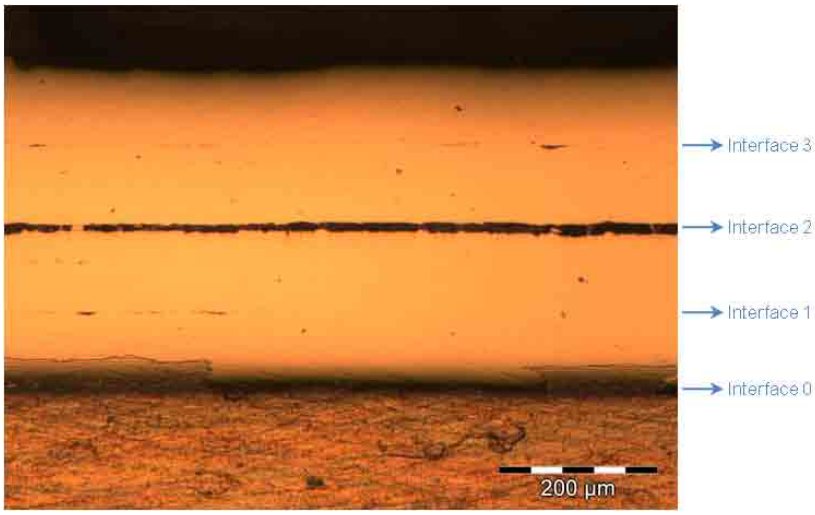

Fig. 3.7: Micrograph of sample of Taguchi experiment run 6

of UC parameters that included welding speeds equal to or greater than 11 mm/s (26 ipm) was used.

Futhermore, an analysis of variance (ANOVA) was conducted to ascertain the variability of LWD values explained by the experiment factors (explanatory variables). In that regard, the Split Plot experiment ANOVA considered populations of Type 2 standard samples ultrasonically consolidated using the described UC system (Section 3.4) and factor level combinations shown in Table 3.5. All treatments (factor level combinations in the experiment) were applied to the same number of experimental units (Type 2 samples).

Twenty seven Type 2 standard samples were built on a single plate using the UC parameter combinations of Normal Force, Welding Speed, and Amplitude factor levels shown in Table 3.5. In this regard, the experiment *plot* in this Split Plot design is the combination

Table 3.5: Split Plot experiment Factors (UC process parameters) and Levels, evaluated at 478 K (400 °F)

Factors	**Levels**		
Normal Force	1500 N	1650 N	1800 N
Welding Speed	11 mm/s (26 ipm)	14 mm/s (33 ipm)	16.9 mm/s (40 ipm)
Amplitude	23 µm	25 µm	27 µm
Position along the welding direction	b (at the begining)	m (in the middle)	e (at the end)
Interface Level	1	2	3

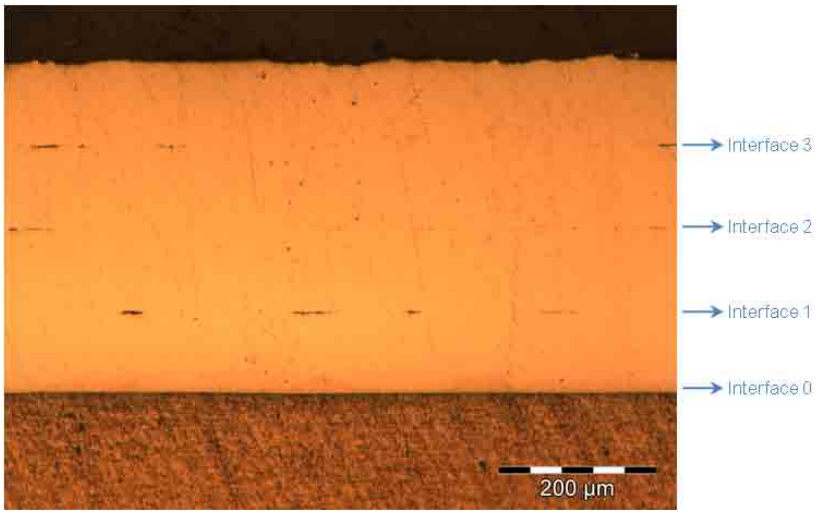

Fig. 3.8: Micrograph of sample of Taguchi experiment run 15

of these three experimental factors. For each Type 2 sample in the plot, three different evenly spaced cross sections were evaluated corresponding to the begining, the middle, and the end positions along the welding direction in the ultrasonically consolidated section (Figure 3.10). Five hundred micron wide cross section micrographs were taken at 100X magnification as shown in Figure 3.10, whenever edge effects ceased towards the center of the ultrasonically consolidated section.

In addition, as illustrated in Figure 3.6, there are three SS316L annealed-to-SS316L annealed interfaces (Interface Level factor levels) at each location, thus resulting in 3 $Positions\times$ 3 $Interfaces = 9$ LWD measurements associated with each Type 2 standard sample. The combination of Position along the Welding Direction and Interface Level factors is the *sub-plot* in this Split Plot design. Similarly, by multiplying the number of all factor levels present in Table 3.5, there are $3 \times 3 \times 3 \times 3 \times 3 = 243$ observations per Plot. There were three replicates per plot or trial run, for a total of $243 \times 3 = 729$ LWD measurements. Experimental runs are shown in Table 3.6.

The ANOVA was carried out using SAS™ statistical software and a critical probability value of 0.05 was used. Preliminary full fifth order interaction ANOVA results showed that only interactions of third order or less were significant, and it was decided to use a modified

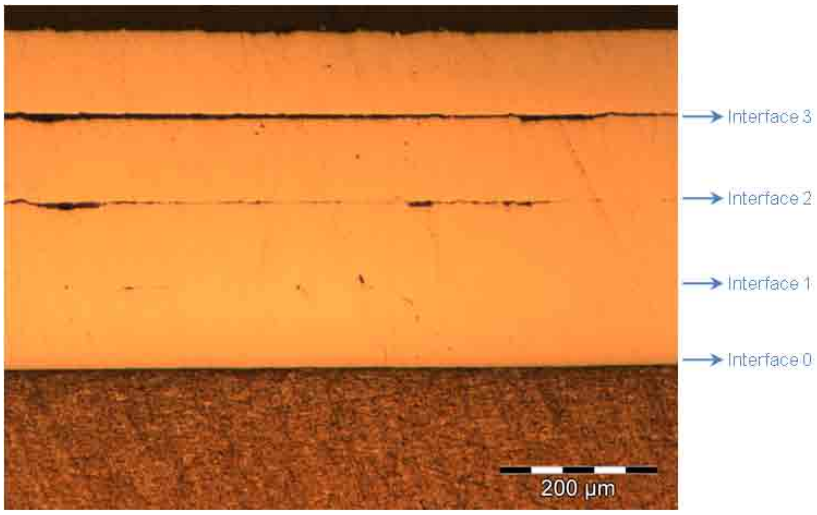

Fig. 3.9: Micrograph of sample of Taguchi experiment run 16

ANOVA model to include up to third order interactions only. The actual ANOVA model used for the data follows:

$$\begin{aligned} Y_{ijklmn} = \quad & \mu + \varphi_i + \sigma_j + \alpha_k + \pi_l + \iota_m + (\varphi\sigma)_{ij} + (\varphi\alpha)_{ik} + \\ & (\varphi\pi)_{il} + (\varphi\iota)_{im} + (\sigma\alpha)_{jk} + (\sigma\pi) + (\sigma\iota)_{jm} + \\ & (\alpha\pi)_{kl} + (\alpha\iota)_{km} + (\pi\iota)_{lm} + (\varphi\sigma\alpha)_{ijk} + (\varphi\sigma\pi)_{ijl} + \\ & (\varphi\sigma\iota)_{ijm} + (\varphi\alpha\pi)_{ikl} + (\varphi\alpha\iota)_{ikm} + (\varphi\pi\iota)_{ilm} + \\ & (\sigma\alpha\pi)_{jkl} + (\sigma\alpha\iota)_{jkm} + (\sigma\pi\iota)_{jlm} + (\alpha\pi\iota)_{klm} + \varepsilon_{n(ijklm)} \end{aligned} \tag{3.2}$$

for $i = 1,\ 2,\ 3;\quad j = 1,\ 2,\ 3;\quad k = 1,\ 2,\ 3;\quad l = 1,\ 2,\ 3;\quad m = 1,\ 2,\ 3;\quad n = 1,\ 2,\ 3$

where:

μ is the expected value or mean value for the *LWD* experimental response,

φ_i is the effect of the i^{th} level of the *Normal Force* fixed experimental factor,

σ_j is the effect of the j^{th} level of the *Welding Speed* fixed experimental factor,

α_k is the effect of the k^{th} level of the *Amplitude* fixed experimental factor,

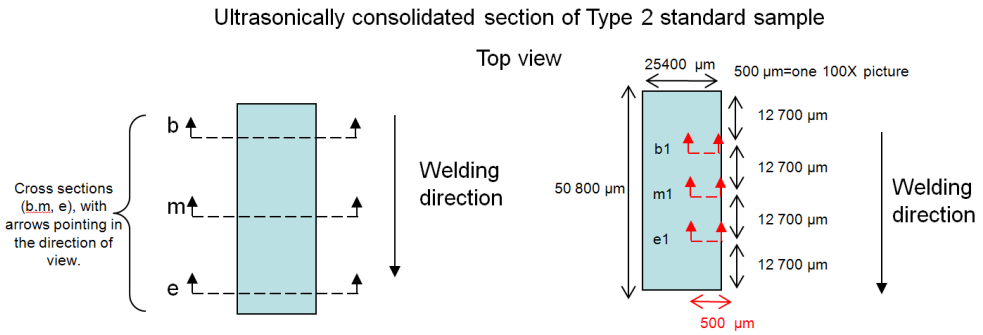

Fig. 3.10: Different locations of the Position along the Welding Direction factor: at the begining (b), in the middle (m), and at the end (e)

π_l is the effect of the l^{th} level of the *Position along the welding direction* fixed experimental factor,

ι_m is the effect of the m^{th} level of the *Interface Level* fixed experimental factor,

$\varepsilon_{n(ijklm)}$ is the random error on the n^{th} trial, and

Y_{ijkl} is the response value, namely *LWD*, for the n^{th} trial, given at the m^{th} level of the *Interface Level* , the l^{th} level of the *Position along the welding direction*, the k^{th} level of the *Amplitude*, the j^{th} level of the *Welding Speed*, and the i^{th} level of the *Normal Force*.

All other terms denote interactions of respective factor levels. The Null Hypothesis (H_0) and Alternative Hypothesis (H_A) are, respectively:

$$\begin{aligned} H_0: \quad & \varphi_1 = \varphi_2 = \varphi_3 = 0 \\ & \sigma_1 = \sigma_2 = \sigma_3 = 0 \\ & \alpha_1 = \alpha_2 = \alpha_3 = 0 \\ & \pi_1 = \pi_2 = \pi_3 = 0 \\ & \iota_1 = \iota_2 = \iota_3 = 0 \end{aligned} \tag{3.3}$$

$$\begin{aligned} H_A: \quad & \textit{At least one } \varphi_i \neq 0 \\ & \textit{At least one } \sigma_j \neq 0 \\ & \textit{At least one } \alpha_k \neq 0 \\ & \textit{At least one } \pi_l \neq 0 \\ & \textit{At least one } \iota_m \neq 0 \end{aligned} \tag{3.4}$$

In addition, the ANOVA model is Univariate, because there is only one response or dependent variable, and all factors are considered crossed with respect to all the others. Type 3 tests for fixed effects are performed for all factors and interactions and the residual

maximum likelihood (REML) method is used to estimate components of variance. As for ANOVA assumptions examination, data residuals are evaluated first. In a statistical context, the residual is the deviation of an observation from the estimated true function value, therefore, it is an estimator of the statistical (random) error [22]. Moreover, Residuals versus Explanatory Factors plots are shown in Figure 3.11, and provide evidence of a highly homoscedastic data. The convention in statistics for homoscedasticity in Residuals versus Explanatory Factors plots is that there should not be a difference in spreads equal to or greater than five times when comparing any pair of factor levels in the same Explanatory factor plot (the spread is illustrated by the vertical chain of symbols corresponding to each factor level). Furthermore, the Residuals versus Predicted Values plot for the data in Figure 3.12 also shows significant evidence of homoscedasticity since there is not any clear gradient pattern (e.g. a megaphone shape) in the plot.

Moreover, all other diagnostics confirm that the residuals normality assumption is quite reasonable. For instance, the Residuals versus Normal Percentiles plot illustrated in Figure 3.13 shows a fairly straight line, while the Histogram shown in Figure 3.14, and the Stem-Leaf plot in Figure 3.15 both support normality based upon graphical correspondence with the bell-shaped distribution of values. In summary, all diagnostics provide no reason to invalidate the ANOVA results, in light of the evidence that residuals are normally distributed according to the mathematical theory of errors [22].

As stated in Equation 3.3, the Null Hypothesis (H_0) postulated that there was no effect due to the any of the factors on the LWD value, meaning that the distributions of the mean, variance, and shape of all factor-level samples would be identical. In that respect, a p-value is calculated in order to accept or reject the Null Hypothesis. The p-value is the probability of obtaining results at least as extreme as the one that was actually observed, assuming that the Null Hypothesis is true. In our case, since the critical probability value used in this study is 0.05, it means that the Null Hypothesis would be rejected if a p-value equal to or less than 0.05 (5% of expected likelihood) is obtained. Moreover, Type 3 F-test are performed to obtain the p-values shown in Figure 3.16 because the test statistic associated to the p-value

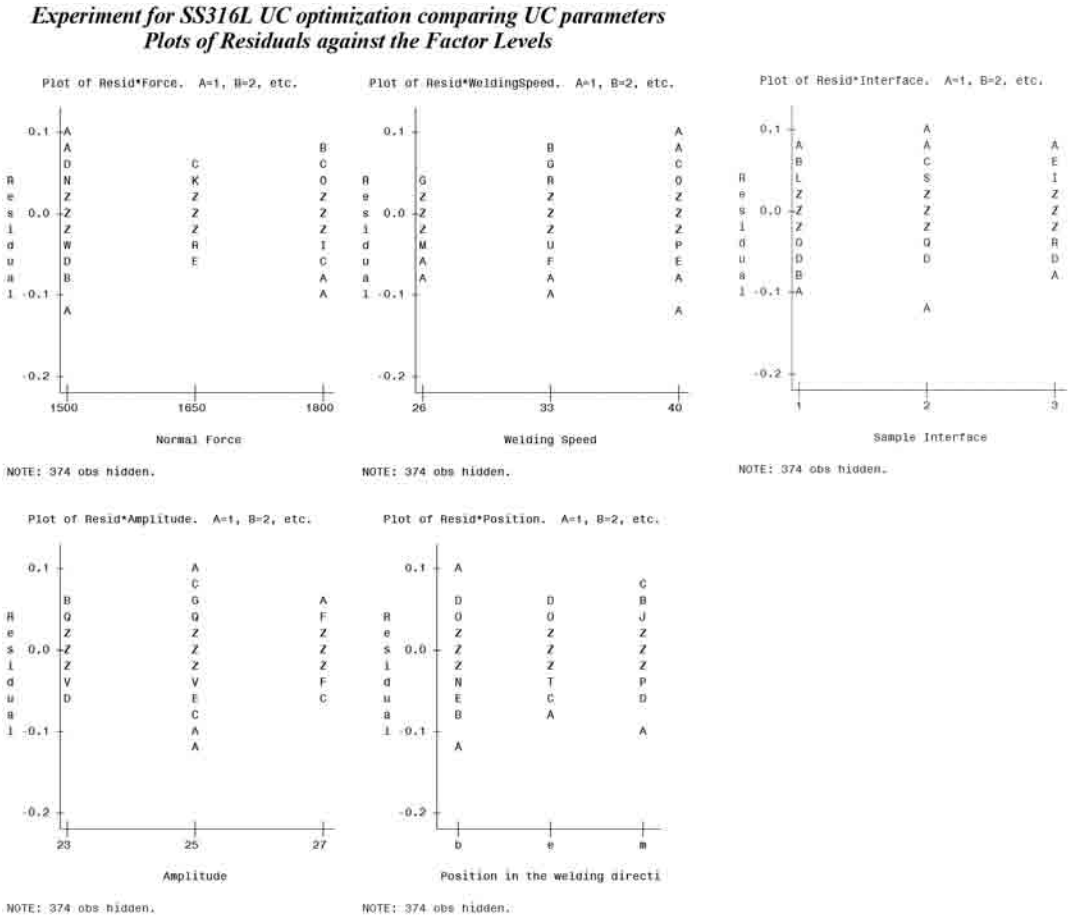

Fig. 3.11: Residuals versus Explanatory Factors plots for Split Plot ANOVA model

has an F-probability distribution [23]. SAS™ utilizes Type 3 F-tests to assess differences between Least Squares Means (LSM) for mixed effects, instead of using differences between the arithmetic treatment means (Type 1 F-test) [24]. In this context, it is worth mentioning that LSM are obtained by performing a regression analysis using the ANOVA model stated in Equation (3.2).

As for the ANOVA results, Figure 3.16 shows that statistically significant p-values, that is, p-values equal to or less than the selected critical probability value of 0.05, were obtained for the following factors/interactions: Force, WeldingSpeed, Amplitude, Force*WeldingSpeed, Force*Amplitude, WeldingSpeed*Amplitude, Force*WeldingSpeed*Amplitude, and Amplitude*Interface. This means that, based upon Type 3 test results of the Split Plot ANOVA

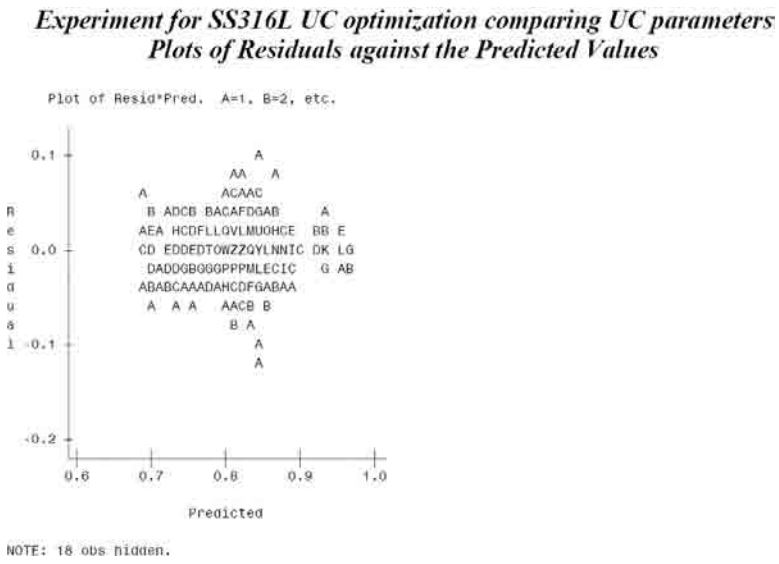

Fig. 3.12: Residuals versus Predicted values plot for Split Plot ANOVA model

(Figure 3.16), the condition for the Null Hypothesis to be true is not met on the aforementioned significant factors/interactions, and further comparison between LWD means associated to the levels of these factors/interactions is required to select the optimum set of parameters for SS316L annealed UC. The following PROC MIXED procedure is run in SAS™ to obtain information about LSM associated to the levels of these factors/interactions:

```
title3 " Using PROC MIXED with the REML Estimation Method";
proc mixed data=SS316LannUC covtest cl;
class Force WeldingSpeed Amplitude Position Interface;
model lwd = Force|WeldingSpeed|Amplitude|Position|Interface @3
/ ddfm=satterthwaite outp = residuals;
random Trial Force*WeldingSpeed*Amplitude*Trial;
lsmeans Force WeldingSpeed Amplitude Position Interface
Force*WeldingSpeed Force*Amplitude WeldingSpeed*Amplitude
Force*WeldingSpeed*Amplitude Amplitude*Interface / pdiff=all adjust = Tukey;
run;
```

Indeed, the LSM table for the significant factors/interactions shown in Figure 3.17 reveals that statistically, the optimum combination of UC parameters obtained is Normal Force=1800 N, Welding Speed=11 mm/s (26 ipm), and Amplitude=27 µm (row 63), because they correspond to the maximum value in the 'Estimate' column of the LSM table in

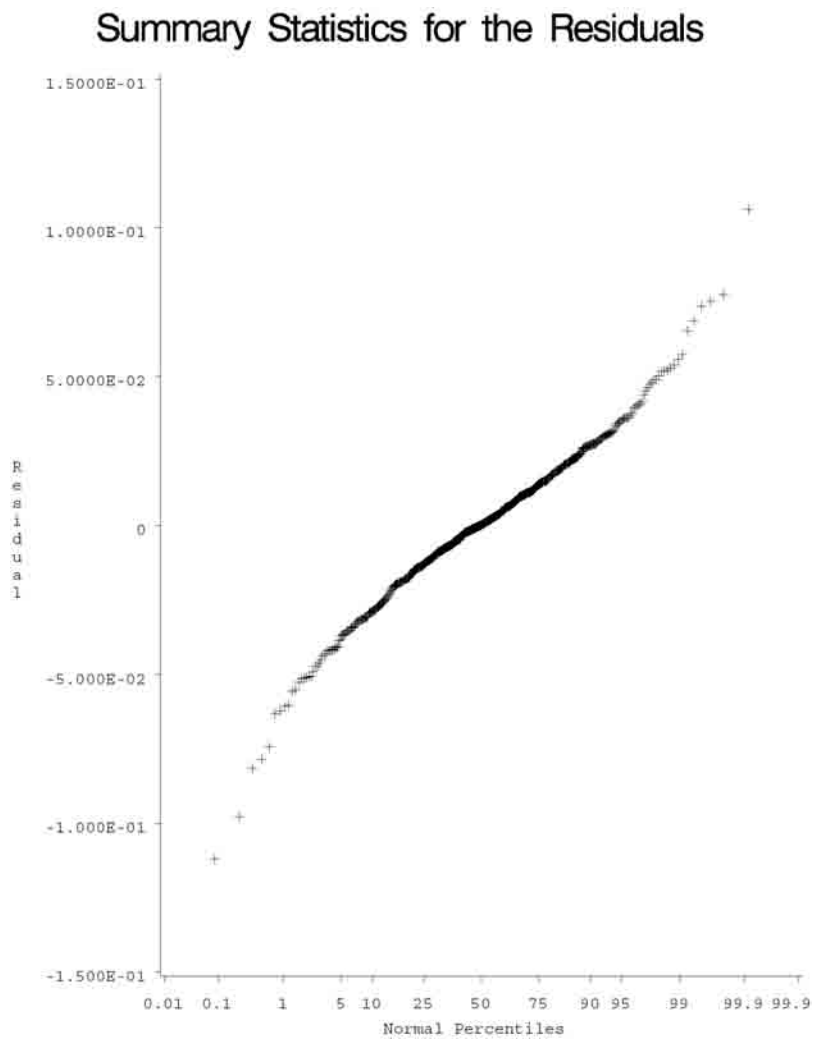

Fig. 3.13: Residuals vs Normal Percentiles plot for Split Plot ANOVA model

Figure 3.17. Furthermore, the Difference of Least Squares Means (DLSM) table in Figure 3.18 presents all evaluations involving the optimum parameter set identified for SS316L annealed UC in this study. In this context, the difference between LWD means are significant for all LSM comparisons (the p-values shown in the $Pr > |t|$ column of the DLSM table are all equal to or less than the 0.05 probability critical value). Therefore, in light of the statistical evidence presented in Figure 3.18, no other combination of UC parameters in Table 3.6 provides similar LWD values to the ones found using the indentified optimum UC parameter set for Type 2 standard samples.

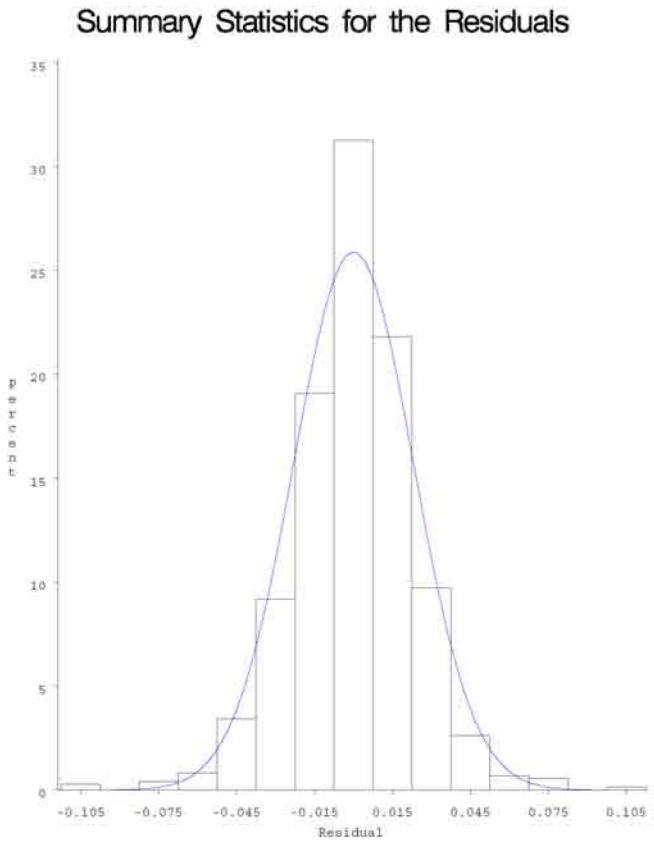

Fig. 3.14: Histogram for each Gage factor level for Split Plot ANOVA model

Table 3.6: Split Plot experiment runs matrix

Experiment run	**Temperature**	**N. Force**	**W. Speed**	**Amplitude**
1	478 K (400 °F)	1500 N	11 mm/s (26 ipm)	23 µm
2	478 K (400 °F)	1500 N	11 mm/s (26 ipm)	25 µm
3	478 K (400 °F)	1500 N	11 mm/s (26 ipm)	27 µm
4	478 K (400 °F)	1500 N	14 mm/s (33 ipm)	23 µm
5	478 K (400 °F)	1500 N	14 mm/s (33 ipm)	25 µm
6	478 K (400 °F)	1500 N	14 mm/s (33 ipm)	27 µm
7	478 K (400 °F)	1500 N	16.9 mm/s (40 ipm)	23 µm
8	478 K (400 °F)	1500 N	16.9 mm/s (40 ipm)	25 µm
9	478 K (400 °F)	1500 N	16.9 mm/s (40 ipm)	27 µm
10	478 K (400 °F)	1650 N	11 mm/s (26 ipm)	23 µm
11	478 K (400 °F)	1650 N	11 mm/s (26 ipm)	25 µm
12	478 K (400 °F)	1650 N	11 mm/s (26 ipm)	27 µm
13	478 K (400 °F)	1650 N	14 mm/s (33 ipm)	23 µm
14	478 K (400 °F)	1650 N	14 mm/s (33 ipm)	25 µm
15	478 K (400 °F)	1650 N	14 mm/s (33 ipm)	27 µm
16	478 K (400 °F)	1650 N	16.9 mm/s (40 ipm)	23 µm
17	478 K (400 °F)	1650 N	16.9 mm/s (40 ipm)	25 µm
18	478 K (400 °F)	1650 N	16.9 mm/s (40 ipm)	27 µm
19	478 K (400 °F)	1800 N	11 mm/s (26 ipm)	23 µm
20	478 K (400 °F)	1800 N	11 mm/s (26 ipm)	25 µm
21	478 K (400 °F)	1800 N	11 mm/s (26 ipm)	27 µm
22	478 K (400 °F)	1800 N	14 mm/s (33 ipm)	23 µm
23	478 K (400 °F)	1800 N	14 mm/s (33 ipm)	25 µm
24	478 K (400 °F)	1800 N	14 mm/s (33 ipm)	27 µm
25	478 K (400 °F)	1800 N	16.9 mm/s (40 ipm)	23 µm
26	478 K (400 °F)	1800 N	16.9 mm/s (40 ipm)	25 µm
27	478 K (400 °F)	1800 N	16.9 mm/s (40 ipm)	27 µm

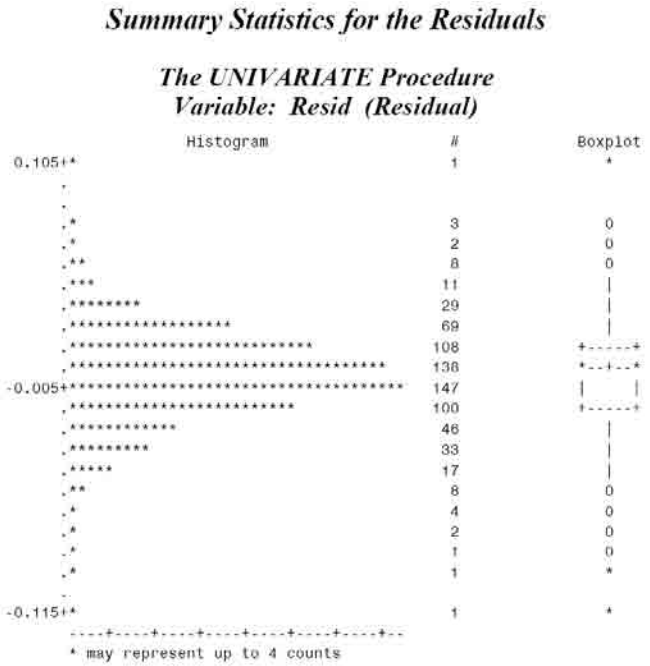

Fig. 3.15: Stem and Leaf plot and Boxplot for each Gage factor level for Split Plot ANOVA model

Type 3 Tests of Fixed Effects				
Effect	**Num DF**	**Den DF**	**F Value**	**Pr > F**
Force	2	598	101.26	<.0001
WeldingSpeed	2	598	420.01	<.0001
Force*WeldingSpeed	4	598	3.69	0.0056
Amplitude	2	598	901.45	<.0001
Force*Amplitude	4	598	63.6	<.0001
WeldingSpe*Amplitude	4	598	19.42	<.0001
Force*Weldin*Amplitu	8	598	24.14	<.0001
Position	2	598	0.24	0.7875
Force*Position	4	598	1.12	0.346
WeldingSpee*Position	4	598	0.4	0.8095
Force*Weldin*Positio	8	598	0.22	0.9867
Amplitude*Position	4	598	0.48	0.7494
Force*Amplit*Positio	8	598	0.72	0.6698
Weldin*Amplit*Positi	8	598	0.59	0.7844
Interface	2	598	0.88	0.4151
Force*Interface	4	598	0.52	0.7181
WeldingSpe*Interface	4	598	1.55	0.1856
Force*Weldin*Interfa	8	598	1.13	0.3441
Amplitude*Interface	4	598	3.49	0.0078
Force*Amplit*Interfa	8	598	0.58	0.7952
Weldin*Amplit*Interf	8	598	1.5	0.1539
Position*Interface	4	598	0.74	0.5669
Force*Positi*Interfa	8	598	1.55	0.1366
Weldin*Positi*Interf	8	598	0.88	0.5334
Amplit*Positi*Interf	8	598	1.11	0.356

Fig. 3.16: Type 3 fixed effects test results of the Split Plot ANOVA

	Least Squares Means									
	Effect	Position in the welding direction axis	Normal Force (N)	Welding Speed (ipm)	Amplitude (µm)	Sample Interface	Estimate	Standard Error	DF	t Value	Pr > |t|
1	Force		1500				0.8049	0.001636	598	491.87	<.0001
2	Force		1650				0.8191	0.001636	598	500.53	<.0001
3	Force		1800				0.8378	0.001636	598	511.94	<.0001
4	WeldingSpeed			26			0.8516	0.001636	598	520.36	<.0001
5	WeldingSpeed			33			0.8253	0.001636	598	504.3	<.0001
6	WeldingSpeed			40			0.785	0.001636	598	479.67	<.0001
7	Amplitude				23		0.7668	0.001636	598	468.58	<.0001
8	Amplitude				25		0.8319	0.001636	598	508.33	<.0001
9	Amplitude				27		0.8631	0.001636	598	527.43	<.0001
10	Position	b					0.8205	0.001636	598	501.38	<.0001
11	Position	e					0.8215	0.001636	598	501.96	<.0001
12	Position	m					0.8199	0.001636	598	500.99	<.0001
13	Interface					1	0.82	0.001636	598	501.06	<.0001
14	Interface					2	0.8224	0.001636	598	502.51	<.0001
15	Interface					3	0.8195	0.001636	598	500.76	<.0001
16	Force*WeldingSpeed		1500	26			0.8374	0.002834	598	295.43	<.0001
17	Force*WeldingSpeed		1500	33			0.8068	0.002834	598	284.65	<.0001
18	Force*WeldingSpeed		1500	40			0.7706	0.002834	598	271.87	<.0001
19	Force*WeldingSpeed		1650	26			0.8482	0.002834	598	299.25	<.0001
20	Force*WeldingSpeed		1650	33			0.8208	0.002834	598	289.57	<.0001
21	Force*WeldingSpeed		1650	40			0.7883	0.002834	598	278.12	<.0001
22	Force*WeldingSpeed		1800	26			0.8691	0.002834	598	306.62	<.0001
23	Force*WeldingSpeed		1800	33			0.8482	0.002834	598	299.25	<.0001
24	Force*WeldingSpeed		1800	40			0.796	0.002834	598	280.83	<.0001
25	Force*Amplitude		1500		23		0.7425	0.002834	598	261.95	<.0001
26	Force*Amplitude		1500		25		0.8327	0.002834	598	293.77	<.0001
27	Force*Amplitude		1500		27		0.8396	0.002834	598	296.23	<.0001
28	Force*Amplitude		1650		23		0.7873	0.002834	598	277.75	<.0001
29	Force*Amplitude		1650		25		0.8245	0.002834	598	290.88	<.0001
30	Force*Amplitude		1650		27		0.8455	0.002834	598	298.31	<.0001
31	Force*Amplitude		1800		23		0.7707	0.002834	598	271.9	<.0001
32	Force*Amplitude		1800		25		0.8384	0.002834	598	295.8	<.0001
33	Force*Amplitude		1800		27		0.9042	0.002834	598	319	<.0001
34	WeldingSpe*Amplitude			26	23		0.7961	0.002834	598	280.86	<.0001
35	WeldingSpe*Amplitude			26	25		0.8529	0.002834	598	300.91	<.0001
36	WeldingSpe*Amplitude			26	27		0.9057	0.002834	598	319.52	<.0001
37	WeldingSpe*Amplitude			33	23		0.7709	0.002834	598	271.98	<.0001
38	WeldingSpe*Amplitude			33	25		0.8341	0.002834	598	294.26	<.0001
39	WeldingSpe*Amplitude			33	27		0.8708	0.002834	598	307.23	<.0001
40	WeldingSpe*Amplitude			40	23		0.7334	0.002834	598	258.76	<.0001
41	WeldingSpe*Amplitude			40	25		0.8086	0.002834	598	285.28	<.0001
42	WeldingSpe*Amplitude			40	27		0.8129	0.002834	598	286.78	<.0001
43	Force*Weldin*Amplitu		1500	26	23		0.7969	0.004909	598	162.32	<.0001
44	Force*Weldin*Amplitu		1500	26	25		0.8409	0.004909	598	171.28	<.0001
45	Force*Weldin*Amplitu		1500	26	27		0.8744	0.004909	598	178.1	<.0001
46	Force*Weldin*Amplitu		1500	33	23		0.7329	0.004909	598	149.29	<.0001
47	Force*Weldin*Amplitu		1500	33	25		0.8423	0.004909	598	171.56	<.0001
48	Force*Weldin*Amplitu		1500	33	27		0.8453	0.004909	598	172.19	<.0001
49	Force*Weldin*Amplitu		1500	40	23		0.6977	0.004909	598	142.1	<.0001
50	Force*Weldin*Amplitu		1500	40	25		0.8149	0.004909	598	165.99	<.0001
51	Force*Weldin*Amplitu		1500	40	27		0.7992	0.004909	598	162.8	<.0001
52	Force*Weldin*Amplitu		1650	26	23		0.8135	0.004909	598	165.7	<.0001
53	Force*Weldin*Amplitu		1650	26	25		0.8473	0.004909	598	172.58	<.0001
54	Force*Weldin*Amplitu		1650	26	27		0.8838	0.004909	598	180.02	<.0001
55	Force*Weldin*Amplitu		1650	33	23		0.8038	0.004909	598	163.72	<.0001
56	Force*Weldin*Amplitu		1650	33	25		0.8223	0.004909	598	167.5	<.0001
57	Force*Weldin*Amplitu		1650	33	27		0.8362	0.004909	598	170.33	<.0001
58	Force*Weldin*Amplitu		1650	40	23		0.7445	0.004909	598	151.65	<.0001
59	Force*Weldin*Amplitu		1650	40	25		0.8039	0.004909	598	163.74	<.0001
60	Force*Weldin*Amplitu		1650	40	27		0.8166	0.004909	598	166.33	<.0001
61	Force*Weldin*Amplitu		1800	26	23		0.7779	0.004909	598	158.44	<.0001
62	Force*Weldin*Amplitu		1800	26	25		0.8706	0.004909	598	177.33	<.0001
63	Force*Weldin*Amplitu		1800	26	27		0.9589	0.004909	598	195.31	<.0001
64	Force*Weldin*Amplitu		1800	33	23		0.776	0.004909	598	158.07	<.0001
65	Force*Weldin*Amplitu		1800	33	25		0.8376	0.004909	598	170.61	<.0001
66	Force*Weldin*Amplitu		1800	33	27		0.931	0.004909	598	189.63	<.0001
67	Force*Weldin*Amplitu		1800	40	23		0.7582	0.004909	598	154.43	<.0001
68	Force*Weldin*Amplitu		1800	40	25		0.8071	0.004909	598	164.4	<.0001
69	Force*Weldin*Amplitu		1800	40	27		0.8227	0.004909	598	167.58	<.0001
70	Amplitude*Interface				23	1	0.7666	0.002834	598	270.45	<.0001
71	Amplitude*Interface				23	2	0.764	0.002834	598	269.54	<.0001
72	Amplitude*Interface				23	3	0.7699	0.002834	598	271.61	<.0001
73	Amplitude*Interface				25	1	0.8302	0.002834	598	292.89	<.0001
74	Amplitude*Interface				25	2	0.84	0.002834	598	296.33	<.0001
75	Amplitude*Interface				25	3	0.8255	0.002834	598	291.23	<.0001
76	Amplitude*Interface				27	1	0.8632	0.002834	598	304.53	<.0001
77	Amplitude*Interface				27	2	0.8631	0.002834	598	304.51	<.0001
78	Amplitude*Interface				27	3	0.8631	0.002834	598	304.49	<.0001

Fig. 3.17: Least Square Means table of the Split Plot ANOVA

	Differences of Least Squares Means																
	Effect	Position in the welding direction axis	Normal Force	Welding Speed	Amplitude	Sample Interface	Position in the welding direction axis	Normal Force	Welding Speed	Amplitude	Sample Interface	Estimate	Standard Error	DF	t Value	Pr > |t|	Adjustment	Adj P
454	Force*Weldin*Amplitu		1800	26	27			1800	33	23		0.1828	0.006943	598	26.33	<.0001	Tukey	<.0001
455	Force*Weldin*Amplitu		1800	26	27			1800	33	25		0.1213	0.006943	598	17.46	<.0001	Tukey	<.0001
456	Force*Weldin*Amplitu		1800	26	27			1800	33	27		0.02788	0.006943	598	4.02	<.0001	Tukey	0.0173
457	Force*Weldin*Amplitu		1800	26	27			1800	40	23		0.2007	0.006943	598	28.91	<.0001	Tukey	<.0001
458	Force*Weldin*Amplitu		1800	26	27			1800	40	25		0.1517	0.006943	598	21.86	<.0001	Tukey	<.0001
459	Force*Weldin*Amplitu		1800	26	27			1800	40	27		0.1361	0.006943	598	19.61	<.0001	Tukey	<.0001

Note: full table has 510 entries.

Fig. 3.18: Difference of Least Square Means involving the optimum parameter set found for SS316L annealed UC in the Split Plot ANOVA

Micrographs of the Type 2 samples made using the optimum parameter set found in the Split Plot experiment are shown in Figures 3.19, 3.20, and 3.21.

3.6 Discussion

In this study, an optimum combination of UC parameters was obtained at Normal Force=1800 N, Welding Speed=11 mm/s (26 ipm), and Amplitude=27 µm, by evaluating factors and levels in Table 3.5 independently from part-geometry induced effects. Even though SS316L UC feasibility studies have been performed in the past [1], LWD has not been the experimental response in any previous study of SS316L UC. Since other frictional-related conditions in the UC process were not researched in this study, the optimum SS316L UC parameter set identified in this work is representative of only the frictional conditions between the SS316L annealed foils and the sonotrode described above. If these frictional conditions change significantly, as it may be the case with a different sonotrode size/material, sonotrode wear over time, different foil material/thickness and different UC system, then new optimum UC process parameters should be established. For this reason, this UC study included specific sonotrode surface roughness data (Table 3.1) for reference.

Nonetheless, the present work independently verified that bond formation during ultrasonic consolidation of SS316L annealed can be obtained consistently. Moreover, the Split Plot ANOVA results provides evidence of the effect the factors/interactions shown in Table 3.5 have on SS316L annealed UC. For instance, both Interface Level and Position along welding direction factors were not signifficant for LWD values on Type 2 standard samples. Additionally, although not part of the Split Plot ANOVA, Temperature is a significant factor in SS316L annealed UC processing because bonding was achieved far more consistently at 478 K (400 °F) than at 303 K (85 °F) over the same number of trials. Successful depositions were obtained at all Welding Speed configurations tested and shown in Table 3.6. In similitude with Al 3003 UC [10], Oscillation Amplitude was proven to be influential in SS316L annealed UC. Indeed, it was observed that the LWD of Type 2 standard samples tends to increase with higher Amplitudes, as reported previously in literature [1].

All in all, the experimental results presented as part of this work reveal some important

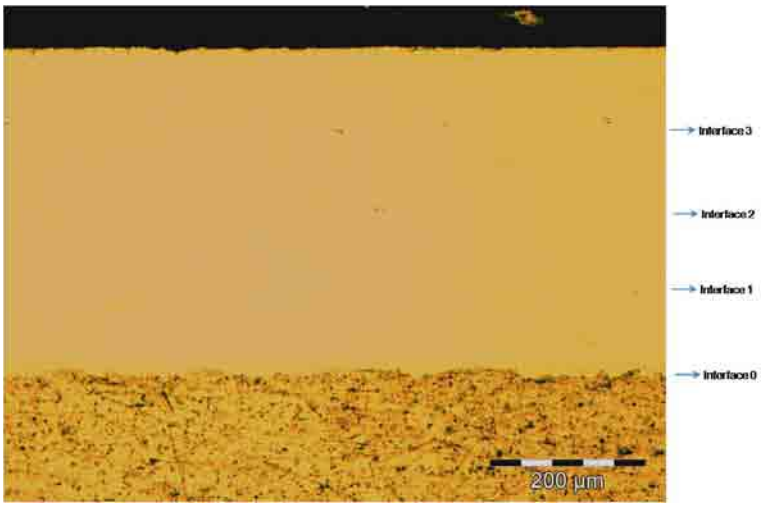

Fig. 3.19: Micrograph of Type 2 standard sample at the begining, made using Split Plot optimum parameters (Normal Force=1800 N, Welding Speed=11 mm/s (26 ipm), and Amplitude=27 µm, at 478 K (400 °F))

trends of the SS316L annealed UC process. Specifically, the optimum parameter set obtained as part of the Split Plot ANOVA includes maximum settings for Normal Force and Amplitude for the UC system utilized. This clearly suggests the acoustic energy necessary for SS316L annealed UC is greater than that needed for Al 3003 UC, and indicates that a more powerful UC system is needed to examine SS316L annealed UC full potential. Even with the available UC system limitations, UC of SS316L annealed was confirmed with LWD values comparable to those found for Al 3003/6061 UC previously [7, 9]. Further machine improvements that enable larger oscillation amplitudes, higher normal forces, and higher temperatures may enable UC of SS316L annealed foils with higher LWD values than the one obtained for the optimum in this study. Nevertheless, the estimated Least Square Mean LWD value for the optimum combination of UC parameters found in Figure 3.17 as 95.89% (row 63) is evidence that high-quality SS316L parts can be made on standard UC machines.

Figure 3.22 shows LSM estimates for Normal Force, Welding Speed, and Amplitude factor levels extracted from the 'Estimate' column in Figure 3.17. Based upon Taguchi and Split Plot experiment results, effects of UC process parameters and other experimental factors on the LWD values in ultrasonically consolidated SS316L annealed parts include:

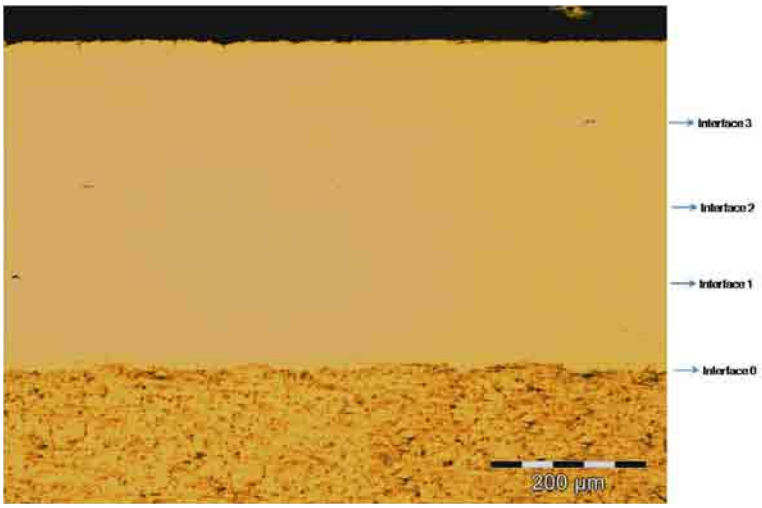

Fig. 3.20: Micrograph of Type 2 standard sample in the middle, made using Split Plot optimum parameters (Normal Force=1800 N, Welding Speed=11 mm/s (26 ipm), and Amplitude=27 µm, at 478 K (400 °F))

- Interface Level and Position along welding direction factors were not significant for LWD values. This means that LWD values in ultrasonically consolidated SS316L annealed parts is only dependent on UC process control parameters (Normal Force, Welding Speed, Temperature, and Amplitude).

- Temperature is a significant factor in SS316L annealed UC processing because bonding was achieved far more consistently at 478 K (400 °F) than at 303 K (85 °F) over the same number of trials. This result is similar to the one observed in Al 3003 UC, where elevated substrate temperatures promote bond formation [11].

- LSM tables showed that LWD tends to increase asymptotically with higher Amplitudes and also tends to increase independently with higher Normal Forces, as it is shown in Figure 3.22. Linear Welding Density values in ultrasonically consolidated SS316L annealed parts made with higher Amplitudes and Normal Forces than the ones shown in Figure 3.22 can only be researched using a higher power UC system. However, previous research with Al 3003 has shown that independently, LWD values reach a maximum with Normal Force and Amplitudes, and then experience a decrease, due to excess shear stresses and/or fatigue breaking bonds at the interface [11].

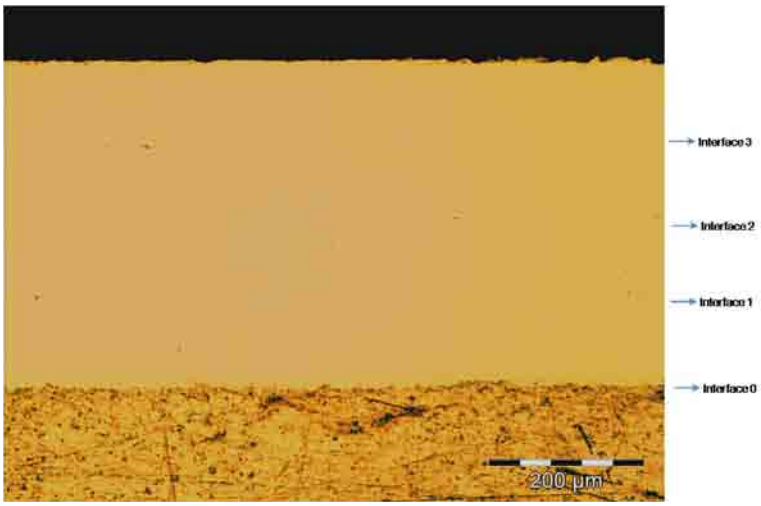

Fig. 3.21: Micrograph of Type 2 standard sample at the end, made using Split Plot optimum parameters (Normal Force=1800 N, Welding Speed=11 mm/s (26 ipm), and Amplitude=27 µm, at 478 K (400 °F))

- LSM tables showed that LWD tends to increase with lower Welding Speeds (Figure 3.22). Indeed, all Welding Speed (11 mm/s (26 ipm), 14 mm/s (33 ipm), 16.9 mm/s (40 ipm)) levels used in the Split Plot experiment proved succesful for SS316L annealed UC bonding. The fact that LWD increased with lower Welding Speeds has also been observed for Al 3003 UC. Indeed, LWD asymptotically approaches 100% in ultrasonically consolidated Al 3003 samples as Welding speed decreases, as long as the other factors are optimum [11]. On the other hand, the main drawbacks with decreasing welding speeds are the increase in build time and possible bond failure due to embrittlement/fatigue of the metal, as it has been reported on Al 3003 UC [11].

3.7 Conclusion

This study confirms the reproducibility of the UC process with SS316L annealed foils based upon a Linear Welding Density benchmark. Optimum LWD UC parameters for SS316L annealed resulting from the present study were identified as: Normal Force=1800 N, Welding Speed=11 mm/s (26 ipm), and Amplitude=27 µm, while Temperature was fixed at 478 K (400 °F). Furthermore, this optimum UC parameter set produced Type 2

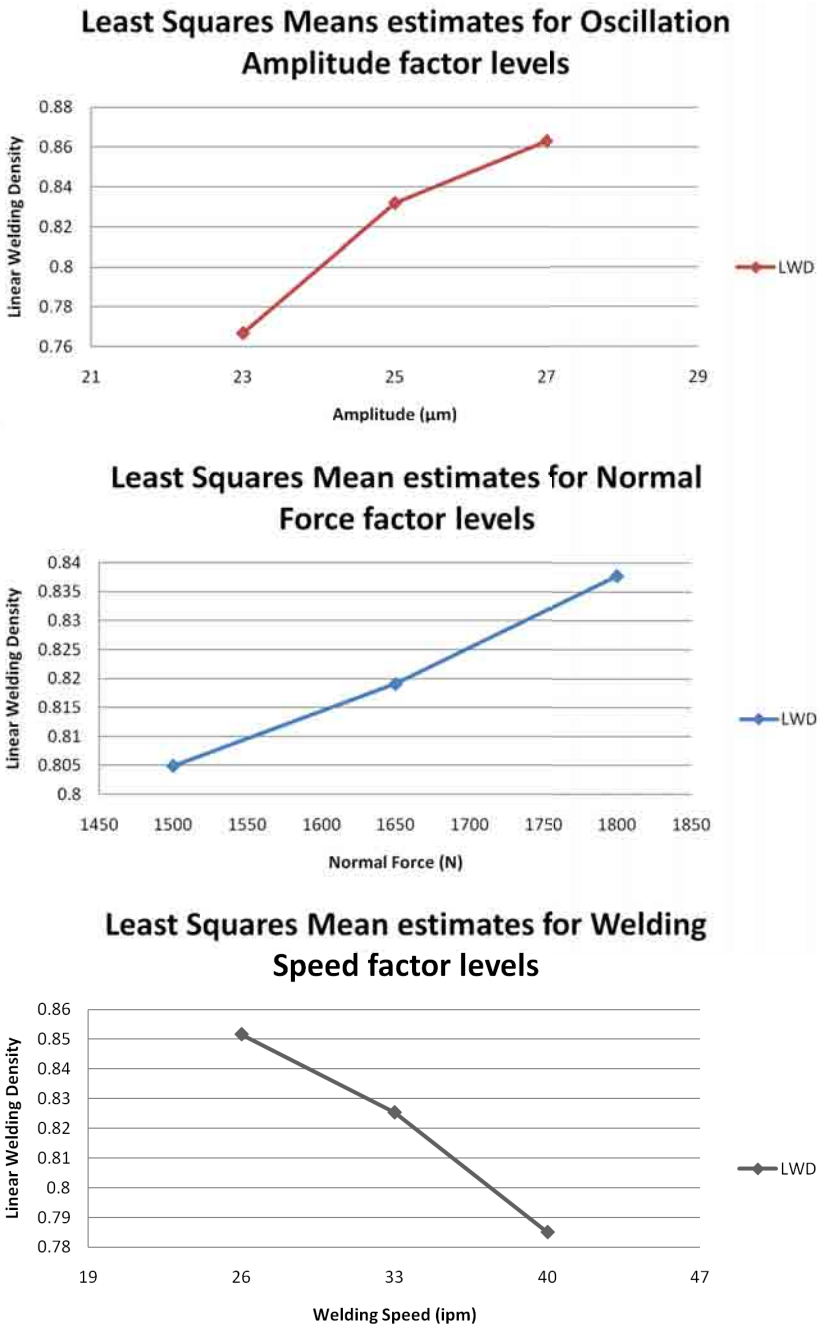

Fig. 3.22: Least Squares Mean estimates for Normal Force, Welding Speed, and Amplitude factor levels

standard samples with an estimated Least Square Mean LWD value of 95.89%. Although the maximum LWD parameter set found may not be the global optimum for SS316L annealed UC due to uninvestigated results with higher power UC machines, the LWD values obtained using the optimum parameter set for SS316L annealed are comparable to the maximum LWD values found for Al 3003 [11], and thus the optimum parameter set is very acceptable for structural part fabrication.

3.8 Future Work

Further experiments at lower welding speeds than 11 mm/s (26 ipm) with other factor levels fixed can provide additional information about the SS316L annealed UC process on the UC system utilized in this study. Although Welding Speed can be set arbitrarily low, this particular factor presents a clear trade-off between LWD and part build time [11]. In addition, studies involving interface microstructural analysis are necessary to explore SS316L annealed crystallography in the interface region of ultrasonically consolidated layers.

Per consideration of the fact that maximum allowable settings for Normal force and Amplitude were employed to obtain the optimum UC parameter set for SS316L annealed in the available UC system, it is deemed that a more powerful UC system may enable further evaluation of UC of SS316L annealed foils beyond the optimum parameter set obtained in this study. Higher power UC systems could be employed to perform a more general optimization experiment for SS316L annealed UC, and explore part-geometry induced effects like overhanging, ribbed, or near-corner configurations, and height-to-width ratio limits.

Chapter 4

Overall Conclusions

Ultrasonically consolidated structures with enhanced strength, rigidity, and stiffness are one significant step towards the practical application of Ultrasonic Consolidation (UC) technology. This dissertation has investigated the effect of UC process parameters on Stainless Steel 316L (SS316L) annealed foils based upon a Linear Welding Density (LWD) benchmark. Along this research effort, a new instrument for LWD estimation on ultrasonically consolidated samples has been developed, and a Measuring System Analysis of LWD assessment has been performed. The knowledge and understanding achieved in the current study provides a clear understanding of the issues involved in the application of UC to the fabrication of SS316L annealed structures.

4.1 MATLAB Script for LWD Estimation through Image Processing

The assessment of LWD is an important benchmark to characterize UC bond quality on SS316L samples. In fact, certain properties of SS316L annealed ultrasonically consolidated parts could only be specified once UC bond quality is known. For instance, properties like specific weight and Poisson's ratio of ultrasonically consolidated parts are affected by LWD. The MATLAB script presented in this study offers a computer-assisted method for assessing LWD. The method presented is based upon the application of image processing techniques on a single metal to metal interface picture for LWD assessment, using a picture brightness criteria. A step-by-step guide to the MATLAB script is included in the Appendix.

The experimental results presented show that the MATLAB script can effectively estimate LWD on cross section micrographs. Results from the Measurement System Analysis of Variance of LWD instruments performed indicate that: (1) The MATLAB script provides the highest instrument resolution of all LWD measuring instruments. (2) The MATLAB

script can accurately and reliably reproduce traditional Ruler-based methods based upon the image file and Region of Interest information. (3) The spread of LWD measurements using the MATLAB script is less than the spread associated with the Ruler and GIMP Measure Tool instruments, making the MATLAB script the most suitable as a standard LWD measurement tool of the three instruments evaluated in this work. Measuring System ANOVA results also show the MATLABsc measurement system is efficient in assessing LWD. The average time per user per sample to take LWD measurements (in seconds) using the MATLAB script is 46.36% less than that of the Ruler and 57.70% less than that of the GIMP.

Although there are some limitations for the Image Processing approach used in the MATLAB script routine, they are mostly related to the single horizontal interface conservative analysis paradigm implemented and micrograph optical requirements. In order to use the MATLAB script properly, high quality micrographs and level of sample preparation (grinding and polishing) are required. In turn, it has been observed that aside poor sample preparation and/or microscopy, the MATLAB script can estimate LWD on high contrast cross section micrographs on a reproducible basis. Tested results show that grinding and polishing of ultrasonically consolidated samples must be performed down to a grit size equal or lower than 6.5 microns in average particle size.

That being said, it is worth mentioning that the MATLAB script can be used to perform LWD measurements on micrographs including multiple interfaces, although at its current stage, the procedure can only process one interface per run. It is important to set an adequate magnification level for sample microscopy. For picture-wide interfaces, the recomended magnification level range for defining the ROI to obtain a LWD estimate using the MATLAB script is 50-100X. Based on several tests performed, some defects could not be clearly seen inside the MATLAB figure window with a microscopy magnification level lower than 50X, without zoom. At the other end, picture-wide interfaces do not have enough interface length for proper analysis when using microscopy magnification levels above 100X. For ROI definitions that are not picture-wide, the zoom option available in the MATLAB script

routine can be used with magnification levels above 100X and below 50X, and the practical minimum/maximum magnification for microscopy will depend upon the specific application. The MATLAB script procedure is designed to work with only one micrograph. Multiple or combined image analysis using the MATLAB script is only indirectly possible at this development point, by stitching together multiple side-by-side micrographs to make a single micrograph of an horizontally oriented contiguous interface, for futher analysis.The latest version of the MATLAB script can be downloaded from:

https://sites.google.com/site/lwdmatlabsc/

4.2 Maximum LWD UC Parameters for SS316L Annealed UC

The quality of an ultrasonically consolidated part is highly dependent on UC processing parameters. From a research standpoint, the relevance of this research effort consists in a systematic study of SS316L annealed UC based on the relation between UC parameters and resulting LWD values on samples, independent from part geometry induced effects. There are four machine-related processing parameters in an UC system: Oscilation Amplitude, Welding Speed, Normal Force and Substrate Temperature. Besides these four machine-related parameters, this research project included two additional factors to be considered, which are the Position along the welding direction and the Interface Level. Specifically, maximum LWD UC parameters for SS316L annealed parts using the available UC system were identified at: Normal Force=1800 N, Welding Speed=11 mm/s (26 ipm), and Amplitude=27 µm, while Temperature was fixed at 478 K (400 °F). Furthermore, SS316L annealed standard samples produced with the identified optimum UC parameter set yielded nearly 96% of LWD.

This study has experimentally investigated the effects of processing parameters on UC bond quality in SS316L annealed structures using a LWD criteria and has identified optimum levels for UC parameters. On the other hand, frictional-related conditions in the UC process were not researched in this study. In consequence, the optimum SS316L UC parameter set identified in this work is representative of a restricted range of frictional conditions between the SS316L annealed foils and the sonotrode. If these frictional conditions change

significantly, as it may be the case with a different sonotrode size/material, sonotrode wear over time, different foil material/thickness and different UC system, then new optimum UC process parameters should be established, and specific sonotrode surface roughness data should be recorded for reference. Nonetheless, the present work independently verified that bond formation during ultrasonic consolidation of SS316L annealed can be obtained consistently. Moreover, the Split Plot ANOVA results provide evidence of the effect the UC parameter factors/interactions have on SS316L annealed UC. For instance, both Interface Level and Position along welding direction factors were not related to LWD values on standard samples. In turn, although it was not part of the Split Plot ANOVA, Temperature is a significant factor in SS316L annealed UC process because bonding was achieved far more consistently at 478 K (400 °F) than at 303 K (85 °F) over the same number of trials. Successful depositions were obtained at Welding Speed of 11 mm/s (26 ipm), 14 mm/s (33 ipm), and 16.9 mm/s (40 ipm), but the complete process parameter window of Welding speeds was not fully explored on the available UC system in this study.

All in all, the experimental results presented as part of this work reveal some important trends for the SS316L annealed UC process. Experiment outcomes on ultrasonically consolidated SS316L annealed parts indicated that only variations in Oscilation Amplitude, Welding Speed, Normal Force and Substrate Temperature produce statistically significant variations in LWD values. Specifically, it was observed that higher values of Oscillation Amplitude, Normal Force, and Substrate Temperature respectively resulted in higher LWD values, whereas Welding Speed was found to affect LWD in the opposite manner: The higher the Welding Speed, the smaller the LWD produced. Specifically, the optimum parameter set obtained as part of the Split Plot ANOVA includes maximum settings for Normal Force and Amplitude for the UC system utilized. This clearly suggests the acoustic energy necessary for SS316L annealed UC is greater than that for Al 3003 UC, and indicates that a more powerful UC system is needed to examine the full potential of SS316L annealed UC. Even with the available UC system limitations, UC of SS316L annealed was confirmed with LWD values comparable to those found for Al 3003/6061 UC previously. Further machine

improvements that enable larger Oscillation Amplitudes, higher Normal Forces, and higher temperatures may enable UC of SS316L annealed foils with higher LWD values than the one obtained for the optimum in this study.

4.3 Future Work

Regarding the MATLAB script, future work includes the need to improve the robustness of the MATLAB script procedure for efficient identification of sample defects (voids, delamination, inclusions) and LWD assessment. Also, an option for processing multiple interfaces in one micrograph will be incorporated in order to provide an average LWD estimate for all interfaces in a micrograph. However, it has been noted that a complete LWD measurement standard would require additional work, including specific information about minimum requirements for the optical system (used to acquire ultrasonically consolidated sample micrographs), and weldment preparation in terms of preparation times, specific preparation materials/equipment, and preparation methods in tandem with the ultrasonically consolidated material used and the level of quality desired.

Future work related to SS316L annealed UC includes mechanical characterization and mechanical properties testing for SS316L annealed ultrasonically consolidated samples. Per consideration of the fact that maximum allowable settings for Normal force and Amplitude were employed to obtain the optimum UC parameter set for SS316L annealed in the available UC system, it is posited that a more powerful UC system may enable further evaluation of UC of SS316L annealed foils beyond the optimum parameter set obtained in this study. In addition to this, further experiments at lower Welding Speeds than 11 mm/s (26 ipm) with other factor levels fixed can provide additional information about the SS316L annealed UC process on the UC system utilized in this study. Higher power UC systems could be employed to perform a more general optimization experiment for SS316L annealed UC, and explore part-geometry induced effects like overhanging, ribbed, or near-corner configurations, and height-to-width ratio limits. Moreover, studies involving interface microstructural analysis are necessary to explore SS316L annealed crystallography in the interface region of ultrasonically consolidated layers.

References

[1] Tuttle, R. B., 2007, "Feasibility study of 316L stainless steel for the ultrasonic consolidation process," Journal of Manufacturing Processes, **9**(2), pp. 87–93.

[2] Weiss, B., and Stickler, R., 1972, "Phase instabilities during high temperature exposure of 316 austenitic stainless steel," Metallurgical and Materials Transactions B, **3**, pp. 851–866.

[3] Davies, D., Adcock, P., Turpin, M., and Rowen, S., 2000, "Stainless steel as a bipolar plate material for solid polymer fuel cells," Journal of Power Sources, **86**, pp. 237–242.

[4] Hernandez, L. A., 2009, "Integration of ultrasonic consolidation and direct-write to fabricate an embedded electrical system within a metallic enclosure," Master's thesis, Utah State University, Logan, UT, USA.

[5] Yang, Y., Ram, G. D. J., and Stucker, B. E., 2007, "An experimental determination of optimum processing parameters for Al/SiC metal matrix composites made using ultrasonic consolidation," Journal of Engineering Materials and Technology, **129**, pp. 538–549.

[6] Daniels, H. P. C., 1965, "Ultrasonic welding," Ultrasonics, **3**(4), pp. 190–196.

[7] Ram, G. J., Y. Yang, C. R., J. George, and Stucker, B., 2006, "Improving linear weld density in ultrasonically consolidated parts," *Proceedings of the 17th Solid Freeform Fabrication Symposium*, pp. 692–708.

[8] Zhang, C., Zhu, X., and Li, L., 2006, "A 3-D coupled-field dynamic model for ultrasonic welding of aluminum foils," *Materials Science & Technology 2006, Symp. on Joining of Advanced and Specialty Materials Including Affordable Joining of Titanium and Joining Technologies for MMCs.*

[9] Kong, C. Y., Soar, R. C., and Dickens, P. M., 2003, "Characterisation of aluminium alloy 6061 for the ultrasonic consolidation process," Materials Science and Engineering A, **363**(1-2), pp. 99–106.

[10] Kong, C. Y., Soar, R. C., and Dickens, P. M., 1991, "Optimum process parameters for ultrasonic consolidation of 3003 aluminum," Journal of Materials Processing Technology, **146**, pp. 181–187.

[11] Ram, G. J., Yang, Y., and Stucker, B., 2007, "Effect of process parameters on bond formation during ultrasonic consolidation of aluminum alloy 3003," Journal of Manufacturing Systems, **25**(3), pp. 221–238.

[12] Robinson, C. J., 2005, "Integration of ultrasonic consolidation and direct-write to fabricate a mini-sar phased array antenna," Master's thesis, Utah State University, Logan, UT, USA.

[13] Kong, C., Soar, R., and Dickens, P., 2002, "An investigation of the control parameters for aluminum 3003 under ultrasonic consolidation," *Proceedings of the 13th Solid Freeform Fabrication Symposium*, pp. 199–210.

[14] Stanley J. Reeves, "MATLAB for digital image processing," http://www.eng.auburn.edu/ sjreeves/Classes/IP/IP.html (Last accessed: November 17th, 2009).

[15] Otsu, N., 1979, "A threshold selection method from gray-level histograms," IEEE Transactions on Systems, Man and Cybernetics, **9**(1), pp. 62–66.

[16] Morse, B. S., 2000, "Lecture 4: Thresholding," http://www.eng.auburn.edu/ sjreeves/Classes/IP/IP.html (Last accessed: December 1st, 2009).

[17] Sydenham, P., and Thorn, R., eds., 2005, *Handbook of Measuring System Design: Common Sources of Errors in Measurement Systems*, Wiley, pp. 1-6.

[18] Senol, S., 2004, "Measurement system analysis using designed experiments with minimum α-β Risks and n," Measurement, **36**(2), pp. 131–141.

[19] Krishnamoorthi, K. S., 2006, *A first course in quality engineering: integrating statistical and management methods of quality*, Prentice-Hall, Upper Saddle River, NJ, pp. 234–246.

[20] Leon, R., and Mee, R., 2000, "Blocking multiple sources of error in small analytic studies," Quality Engineering, **12**, pp. 497–501.

[21] Simion, C., 2005, "The study of a measurement system precision," *13th International Scientific Conference on Achievements in Mechanical and Materials Engineering*, pp. 585–588.

[22] Cook, R. D., and Weisberg, S., 1982, *Residuals and Influence in Regression*, Springer, New York, NY, pp. 10-93.

[23] Oehlert, G. W., 2000, *A first course in design and analysis of experiments*, W. H. Freeman, New York, NY, pp 323-455.

[24] SAS, 2004, *SAS/STAT 9.1 user's guide: The MIXED Procedure*, SAS Publishing, Cary, NC, pp. 2661-2844.

[25] Huang, Q., Gao, W., and Cai, W., 2005, "Thresholding technique with adaptive window selection for uneven lighting image," Pattern Recognition Letters, **26**, pp. 801–808.

[26] Robinson, C., Zhang, C., Ram, G. J., Siggard, E., Stucker, B., and Li, L., 2006, "Maximum height to width ratio of freestanding structures built using ultrasonic consolidation," *Proceedings of 17th Solid Freeform Fabrication Symposium.*

[27] Doumanidis, C., and Gao, Y., 2004, "Mechanical modeling of ultrasonic welding," Welding Journal, **83**, pp. 140–146.

[28] Zhang, C., and Li, L., 2006, "A study of dynamic mechanical behavior of substrate in ultrasonic consolidation," *Proceedings of 17th Solid Freeform Fabrication Symposium.*

[29] Zhang, C., Zhu, X., and Li, L., 2006, "A study of friction behavior in ultrasonic welding (consolidation) of aluminum," *87th FABTECH International and AWS Welding Show Professional Program.*

[30] Yang, Y., Ram, G. J., and Stucker, B., 2010, "Mechanical properties & microestructures of SiC fiber reinforced metal matrix composites made using ultrasonic consolidation," Journal of Composite Materials, **In press**.

[31] Roy, R. K., 2001, *Design of Experiments Using the Taguchi Approach: 16 Steps to Product and Process Improvement*, Wiley, John & Sons, Inc., New York, NY, pp. 95-206.

Appendix

Appendix

A.1 MATLAB Script Supplement

A.1.1 How to Obtain the MATLAB Script

The latest version of the MATLAB script is available for free under the terms contained in the *lwd.m* script file and can be downloaded from:

`https://sites.google.com/site/lwdmatlabsc/`

A.1.2 MATLAB Script User Guide

A MATLAB script, 'lwd.m', was developed to assess LWD in cross section micrographs of weldments. The method is based upon the use of a set of image processing techniques that, when combined, provide a single metal to metal interface LWD assessment. The MATLAB script takes for an input a rectangular region of the cross section micrograph, and provided this region contains the interface of interest and meets standard metallography quality criterias, the tool can provide an automatic estimation of the LWD present at the interface. Either grayscale or color images can be processed, in both Bitmap (bmp) and Tagged Image File (tif) formats. The most fundamental assumption of the MATLAB script program is that darker areas in the micrograghs represent unbonded areas, and thus, it is dependent upon the brightness of the visual target. On the other hand, in order to use the MATLAB script for LWD assessment, the interface shown in the cross section micrograph must be horizontally oriented, in focus, and the sample must be in not-etched, scratchless, and as-polished conditions. An examination of these and other conditions that affect LWD assessment using the MATLAB script are given in the Discussion section of this work.

The MATLAB script works in MATLAB version 7.0 (R14) or newer, with the Image Processing Toolbox installed. The routine is executed inside the MATLAB command window, and prompts for an image filename first. Figure A.1 shows an example of how an image

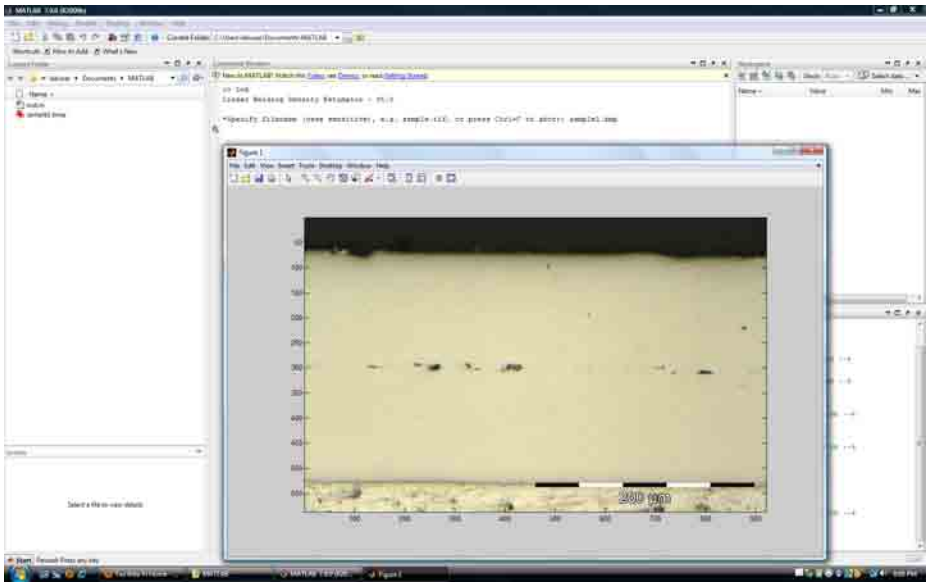

Fig. A.1: File input example in MATLAB script

file that has already been placed in the MATLAB working directory, namely 'sample1.bmp', is entered as input. Upon specifying this image file (by entering the filename including the file extension), the actual image is shown on screen as a figure and the program waits for the user's confirmation on the image. In this regard, *Ctrl+c* will abort the operation and any other standard keystroke will proceed with analysis.

Following this, the rectangular Region of Interest (ROI) needs to be defined by the user. The Region of Interest is the smallest rectangular region, or subset of the original image, that contains all relevant pixels depicting the interface of interest. In this manner, the Region of Interest is a graphical representation of the interface in the form of a rectangle and its contents. Furthermore, all image processing operations are performed on the Region of Interest defined by the user. Figure A.2 illustrates the image, the target interlayer interface, and a selected Region of Interest in the *sample1.bmp* image file.

The Region of Interest is defined by the user, using either Visual Clicks, Matrix Coordinates, or Relative Coordinates.

The Visual Clicks approach comprises two click-points so as to define the Region of Interest with the aid of a pointing device. These separate clicks specify the rectangle con-

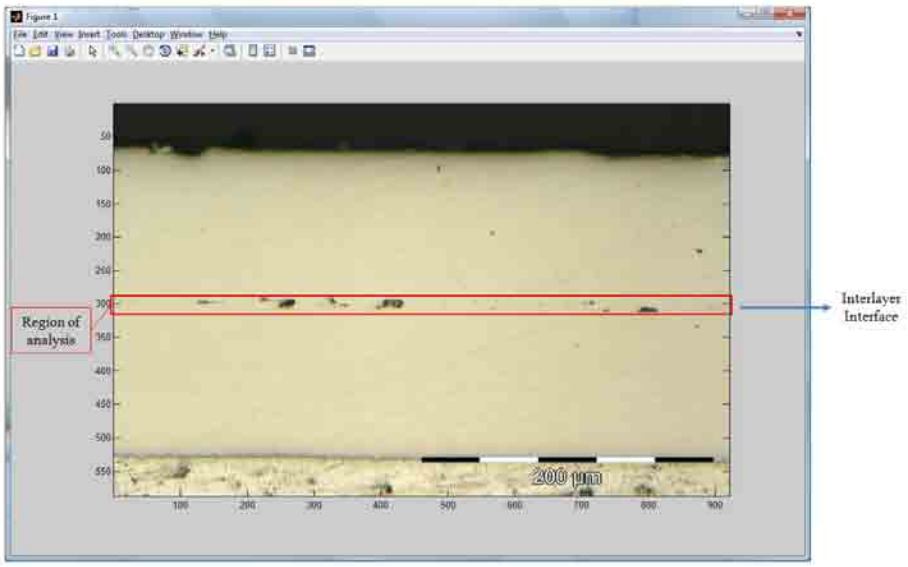

Fig. A.2: Image, Interlayer Interface, and Region of Interest illustrations

taining the Region of Interest, by defining two rectangle corners diagonally opposite. If the interface extends all across the image, then clicks can be performed outside the image's border but inside the MATLAB figure window. In that way, the script program will adjust the selection to meet the border or borders of the image accordingly. The Visual Clicks approach is the default option. Figure A.4 illustrates the Visual Clicks approach, showing the points where clicks could be performed to select a Region of Interest for the interface shown.

The second option for defining the Region of Interest is Matrix Coordinates. Matrix Coordinates are based upon the matrix representation of an image in MATLAB, called the

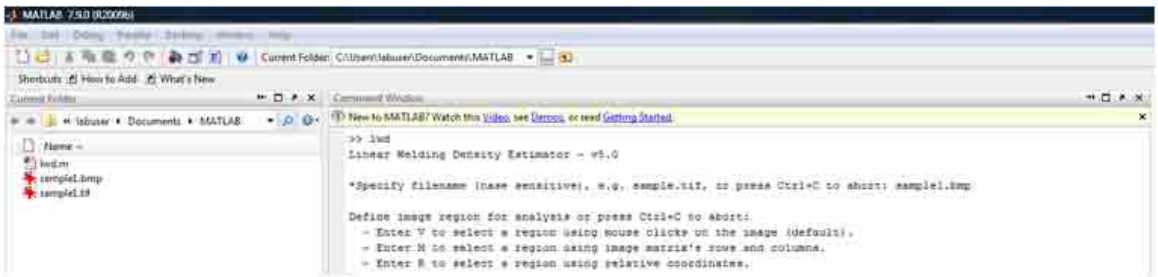

Fig. A.3: Options menu to define the Region of Interest in the MATLAB script

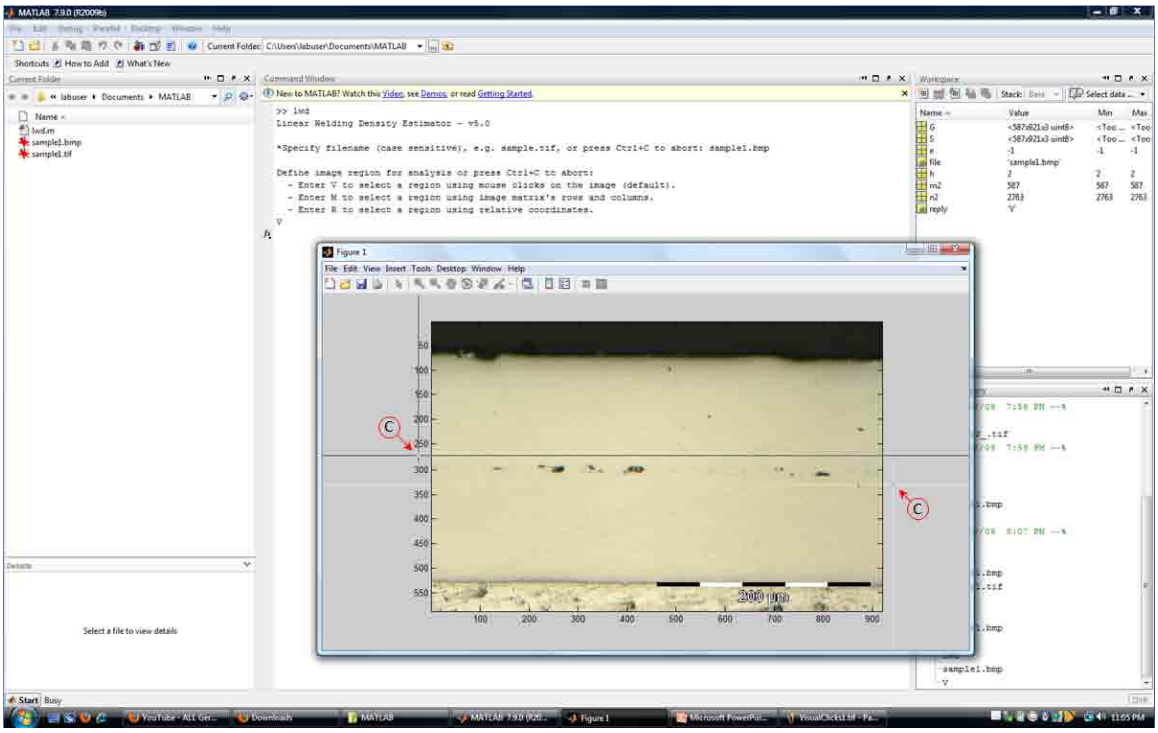

Fig. A.4: Visual Clicks approach to define the Region of Interest in the MATLAB script

Image Matrix. Moreover, Matrix Coordinates are given in terms of row number and column number following a standard mathematical matrix scheme. The element at the upper left corner of the image corresponds to the element at row 1, column 1, in the Image Matrix; with row number increasing downwards, and column number increasing rightwards. The Region of Interest is defined in Matrix Coordinates by specifying the row and column numbers that bound a rectangular region. This is ilustrated in Figure A.5.

Relative Coordinates is the third option for defining the Region of Interest. Relative Coordinates are Cartesian Coordinates with the origin placed at the lower left corner of the original image, and coordinate's dimensions scaled up so that the height and the width of the original image equals to a unit of distance, respectively. Consequently, coordinated values for both vertical and horizontal axes of the cartesian system are always relative to the size of original image, and lay in between 0 and 1. Figure A.6 illustrates the Relative Coordinates approach.

Once the Region of Interest is defined by the user using either Visual Clicks, Matrix

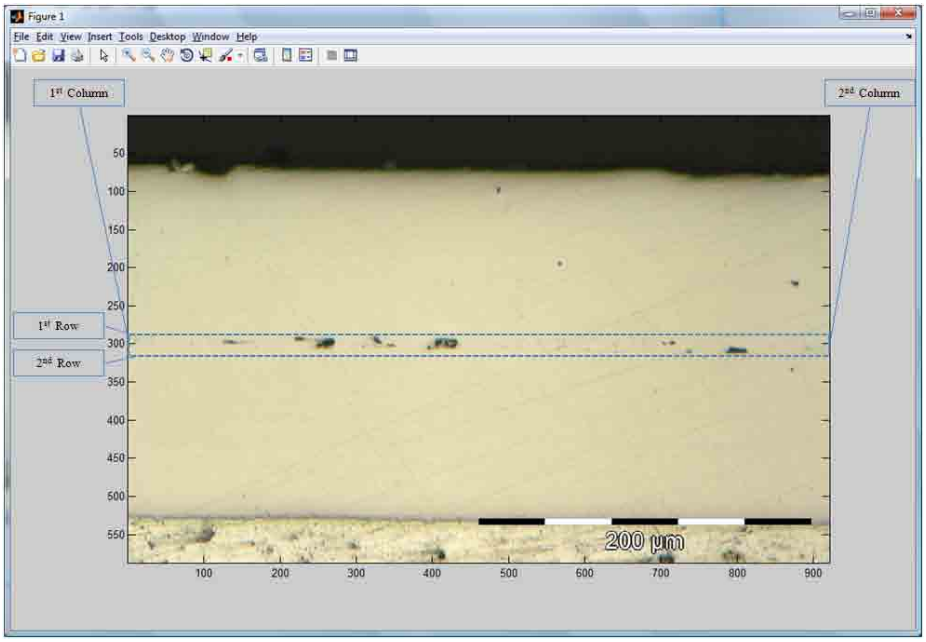

Fig. A.5: Matrix Coordinates approach to define the Region of Interest in the MATLAB script

Coordinates, or Relative Coordinates, an image of the Region of Interest is presented to the user. Figure A.7 shows a Region of Interest selection example.

The Region of Interest is then converted to grayscale using an 8-bit grayscale conversion. MATLAB supports image processing of grayscale and color images [14], and using this feature, the Region of Interest is converted to an 8-bit grayscale image (an image comprising $2^8 = 256$ different shades of gray) unless the original image is already in this format. Indeed, MATLAB functions *ind2gray* and *rgb2gray* are used to perform 8-bit grayscale conversion for indexed and RGB images, respectively, whenever necessary. In order to perform the 8-bit conversion using the MATLAB script, click on the figure that shows the Region of Interest and press *Enter* (it must be the active window). Figure A.8 illustrate the Region of Interest after the 8-bit grayscale conversion.

Once the 8-bit grayscaled Region of Interest has been obtained, black and white binarization is performed. The black and white representation of the Region of Interest is based upon applying the Otsu thresholding algorithm [15] on the 8-bit grayscaled Region of Inter-

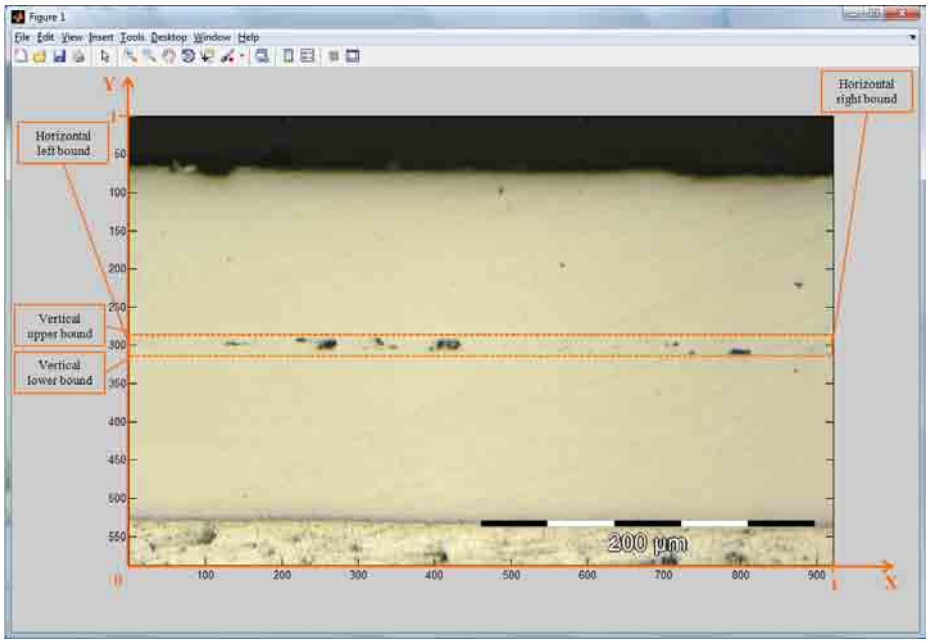

Fig. A.6: Relative Coordinates approach to define the Region of Interest in the MATLAB script

est. Otsu's algorithm performs black and white binarization by selecting the threshold shade of gray (intensity of gray) that minimizes the within class variance in the image's grayscale histogram, when the background (pixels with shades of gray darker than the threshold), and foreground (all pixels that are not in the background), are considered as histogram classes [16]. In order to perform the black and white binarization using the MATLAB script, click on the figure that shows the 8-bit grayscaled Region of Interest (it must be the active window) and press *Enter*. Figure A.9 shows an image of the previous grayscaled Region of Interest (Figure A.8) after black and white binarization.

Following black and white binarization, each black pixel in black and white representation of the Region of Interest is projected across the vertical direction, as shown in Figure A.10. The aim of this image processing task is to consider the worst case scenario of maximum unbonded (black) pixels per row across the Region of Interest. Black pixel projection also simplifies further analysis by making all rows in the resulting image identical.

In MATLAB, color values for black and white colors in an Image Matrix are zeroes and

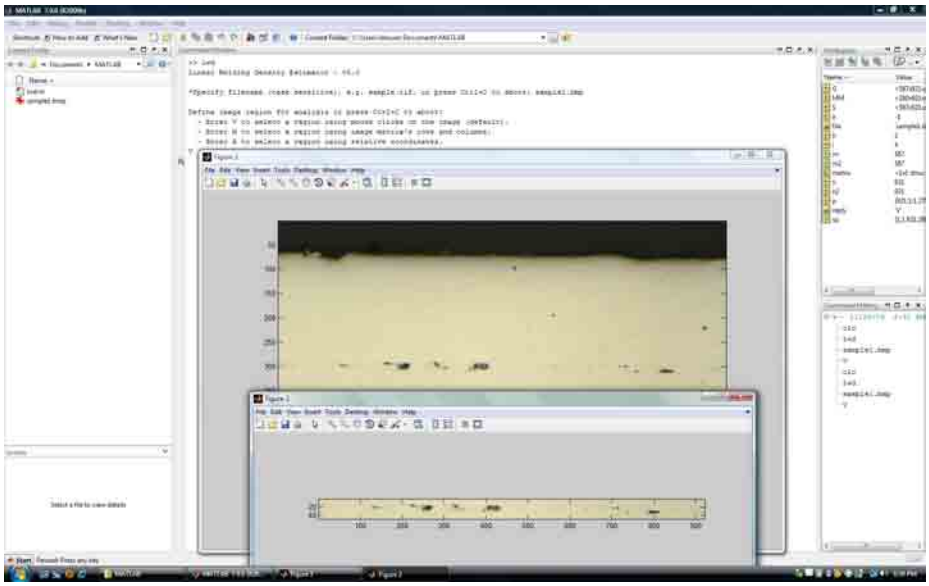

Fig. A.7: Region of Interest example in the MATLAB script

ones respectively, thus providing a means to perform mathematical operations on black and white images. For this particular case, the color values representing black and white colored areas will prove useful as they are associated to unbonded and bonded areas, respectively. For instance, once black pixels are projected vertically, all pixel values in the first row (comprising color values of zeroes and ones) are added up, effectively calculating the number of white pixels in the first row. When the total sum of the first row of pixels is divided by the number of pixels in the first row and multiplied by 100, an estimate of the LWD is obtained, as stated in Equation (A.1), that provides the LWD of a given interface using a relation of lengths:

$$\%LWD = \frac{Bonded\ interface\ length}{Total\ interface\ length} \times 100 \tag{A.1}$$

The output of the MATLAB script is printed after an estimate of the LWD has been calculated. The output of the MATLAB script includes the following information regarding the image file: LWD value, filename, original Image Matrix dimensions, 8-bit grayscale threshold value used, and Matrix Coordinates for the selected Region of Interest. An example of the output is given in Figure A.11. Since the Region of Interest is given in Matrix Coordinates as part of the output, and because Matrix Coordinates is one option to define

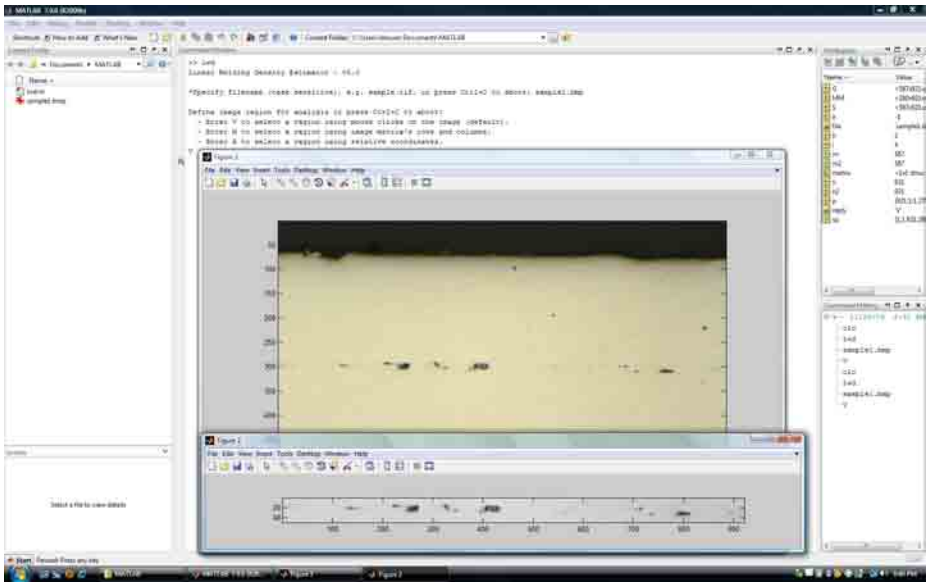

Fig. A.8: 8-bit grayscale conversion of the Region of Interest example in the MATLAB script

the Region of Interest (see Figure A.11), the output of the script effectively provides a transparent way to refer back to previous results and to repeat estimations, whenever the original file and the associated MATLAB script output are used.

After each run, the program resumes and prompts for the next image filename input. In consequence, the MATLAB script routine allows the sequential file execution until a stop signal is entered by pressing *Ctrl+c* keystroke combination in MATLAB's command window.

A.1.3 Known Limitations of the MATLAB Script

In order to use the MATLAB script as an application on a general basis, it is important to realize the scope and limitations of this measuring instrument, as it is presented below.

First, one critical step of the script routine is the definition of the Region of Interest, because it is the input on which all further image processing tasks take place. The option of selecting a Region of Interest for assessing LWD in the MATLAB script allows single interface specification (in sample micrographs with multiple layers) and provides computational simplification for further image processing. However, the interface shown in the Image File input (Figure A.1) must be horizontally oriented, and it is crucial to define

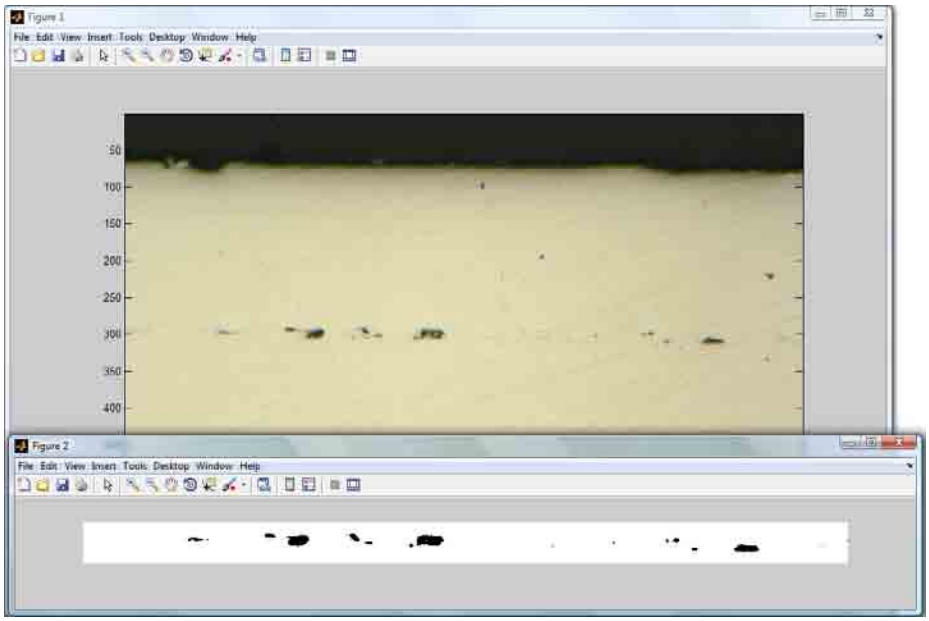

Fig. A.9: Illustration of black and white binarization using Otsu thresholding algorithm in the MATLAB script

the Region of Interest as close as possible to the interface in order to perform a correct analysis. In this respect, MATLAB has limited dynamic zoom capabilities to facilitate the selection of the Region of Interest using the Visual Clicks option. Specifically, the zoom in/out option can only be used in the MATLAB script routine when the initial image is initially shown on screen (Figure A.1), and the zoom magnification level cannot be adjusted afterwards. For this reason, it is also important to set an adequate magnification level for sample microscopy. For picture-wide interfaces, the recommended magnification level range for defining the ROI to obtain a LWD estimate using the MATLAB script is 50-100X. Based on several tests performed, some defects could not be clearly seen inside the MATLAB figure window with a microscopy magnification level lower than 50X, without zoom. At the other end, picture-wide interfaces do not have enough interface length for proper analysis when using microscopy magnification levels above 100X. For ROI definitions that are not picture-wide, the zoom option available in the MATLAB script routine can be used with magnification levels above 100X and below 50X, and the practical minimum/maximum magnification for microscopy will depend upon the specific application.

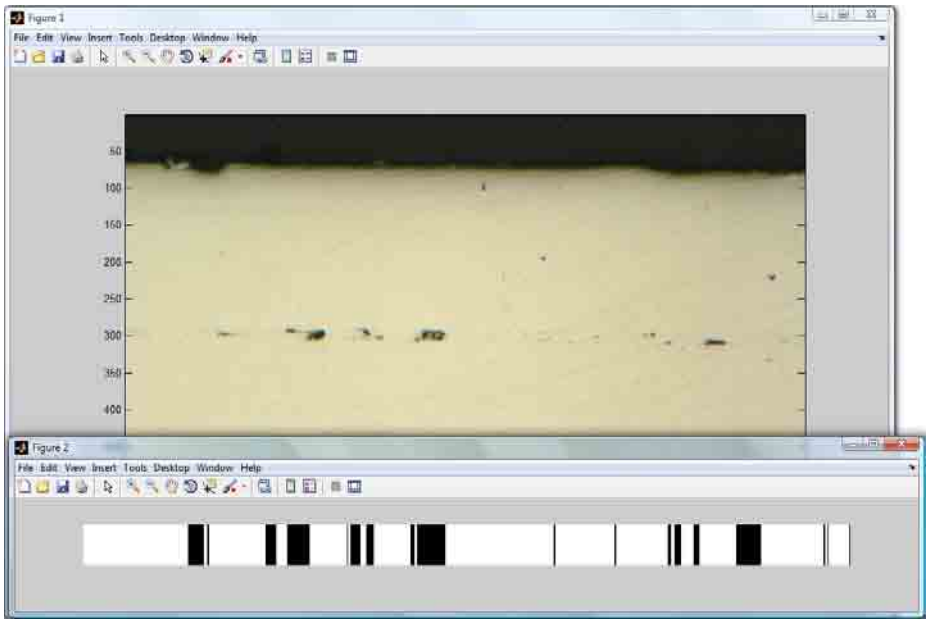

Fig. A.10: Illustration of black region vertical projection applied on a black and white image in the MATLAB script

The MATLAB script procedure is designed to work with only one micrograph. Multiple or combined image analysis using the MATLAB script is only indirectly possible at this development point, by stitching together multiple side-by-side micrographs to make a single micrograph of a horizontally oriented contiguous interface, for further analysis. On the other hand, it is worth mention that stitching together micrographs may induce artifacts in the image as opposed to taking individual LWD measurements on each interface, tabulating them in a spreadsheet and averaging. That being said, it is worth a mention that the MATLAB script can be used to perform LWD measurements on micrographs including multiple interfaces, although in its current implementation, the procedure can only process one interface per run.

Second, the Otsu thresholding algorithm used for black and white binarization has several limitations. Among other limiting factors, it has been reported that the Otsu thresholding method does not work well when an uneven lighting disturbance is present on the input image file [25]. Some identified causes for uneven lighting disturbances are non-uniform light distribution on the image and inability to isolate the scene from other object shadows [25].

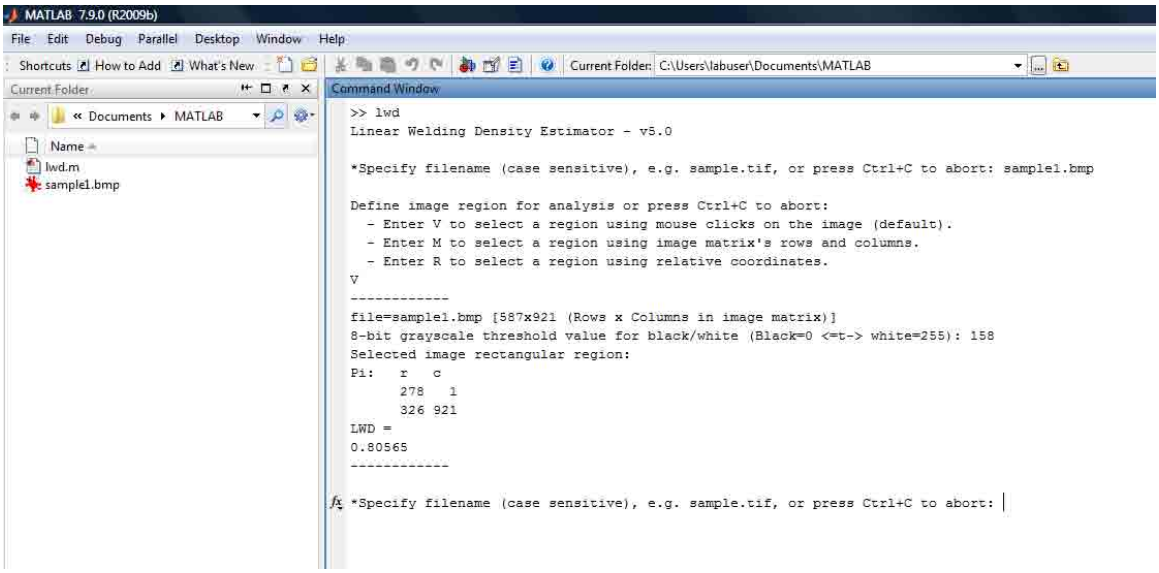

Fig. A.11: MATLAB script output example

In addition to avoiding uneven lightning disturbances, input micrographs with good optical characteristics (in-focus image, balanced contrast image, adequate depth of field (image sharpness), absence of blurring or image distortions, etc.) are required in order to ensure accurate LWD assessment by any visual-based method, including the MATLAB script. The Otsu thresholding routine works best in those ROI that include both bonded and unbonded areas with clearly different brightness. Despite this, the micrograph quality necessary for performing accurate black and white binarization using the Otsu method is completely attainable. Based on tests using previous published pictures of ultrasonically consolidated samples ([7]), optically unsuitable micrographs are avoided when good sample preparation (grinding and polishing) and microscopy practices are followed. Experimental results show that grinding and polishing of ultrasonically consolidated samples must be performed down to a grit size equal to or lower than 6.5 microns in average particle size.

As for the effect of poor sample preparation on MATLAB script LWD results, Figure A.12 shows a sample micrograph containing scratches and stains, and one 8-bit grayscale ROI analysis example. Basically, both scratches and stains introduce noise in the Otsu's thresholding (Black and White binarization) routine that derives into black pixels that do

not correspond to unbonded areas, and leads to inaccurate LWD results. The sample must be in not-etched condition because etching creates small cavities that appear as dark areas in micrographs, causing a similar effect to the ROI analysis as the one caused by the stains and scratches. Moreover, good sample preparation (grinding and polishing) is critical due to the brightness criteria used in the MATLAB script procedure to make the distinction between bonded and unbonded regions in the ROI. In general, the MATLAB script does not automatically differentiate between unbonded regions, scratches, stains and etching marks in the Region of Interest. In fact, the MATLAB script gives a conservative LWD estimate for the Region of Interest and any black pixel out of the interlayer interface will result in a LWD assessment bias. For instance, as is shown in Figure A.12, it only takes one black pixel in a column of the ROI Image Matrix to render the entire column as unbonded area. Thus it is important that users of the MATLAB script look at the Otsu thresholding results to make sure there are no stray black pixels outside the interface region that will affect the LWD measurement, before black pixels are extended vertically across the image.

A.1.4 Step by Step MATLAB Script Visual Clicks Instructions

1. Start MATLAB program. Place 'lwd.m' MATLAB script file and all image files of interest in the MATLAB working directory.

2. Enter 'lwd' (without quotes) at MATLAB command window prompt to run the MATLAB script for LWD measurements.

3. Follow on-screen instructions for image file input.

4. When the sample image is shown in a MATLAB Figure window, confirm image file selection by pressing *Enter*, or cancel execution by pressing *Ctrl+c* while the MATLAB window is active. You may use Ctrl+Mouse Wheel Scroll to zoom in or out with respect to the original view at this step. If you cancel the MATLAB script execution, repeat steps 2 and 3.

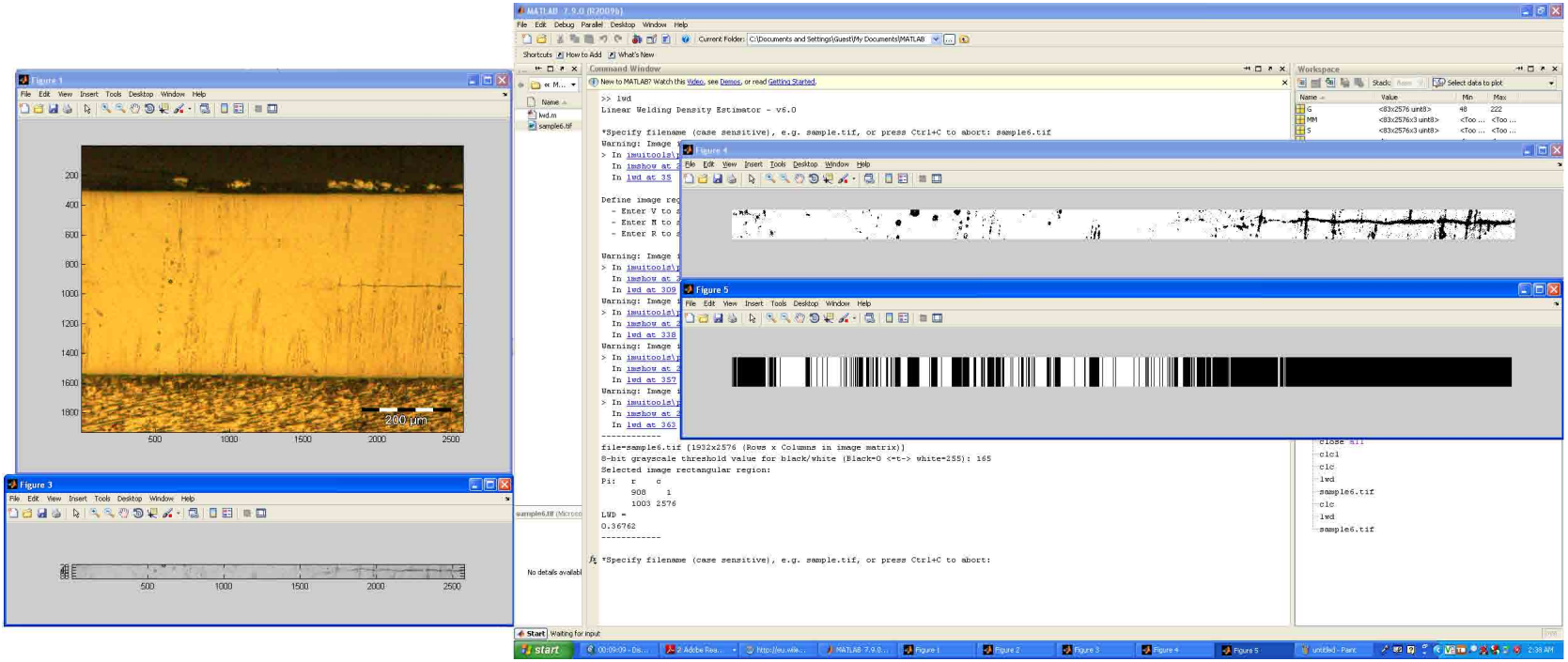

Fig. A.12: Bad specimen preparation example

5. Select a region for the analysis using the mouse clicks option. Two separate clicks specify two diagonally opposite corners of the rectangle that enclose the interface. This click-defined rectangle should be the smallest section of the image that contains the interface to be analyzed. If necessary, you may click outside the image and the selection will be adjusted to match the image borders automatically. Do not select the whole image as your rectangular region.

6. Press enter three times for grayscale images, or four times for color images as it applies. The LWD estimate is given as part of the output in the MATLAB command window, between discontinuous lines (- - -). Record this LWD measurement.

7. Repeat steps 2 through 6 for each one of the sample images. If an error is encountered, re-run the script again (repeat steps 2 through 6). Save all LWD results.

8. Exit the MATLAB script routine by pressing *Ctrl+c* while the MATLAB window is active.

9. Close MATLAB program.

A.1.5 MATLAB Script Original Code

The original version of the MATLAB script follows:

```
% Copyright @ 2009 by Raelvim Gonzalez
% All rights reserved.  This material may be freely copied and distributed under the terms of this copyright notice.
% Redistribution and use in source and binary forms, with or without modification, are permitted provided that the following conditions are met:
% * Redistributions of source code must retain the above copyright notice, this list of conditions and the following disclaimer.
% * Redistributions in binary form must reproduce the above copyright notice, this list of conditions and the following disclaimer in the documentation and/or other materials provided with the distribution.
% * This material or any derivative works may be copied, distributed, displayed and performed only if credits to the author are given in the documentation and/or other materials provided.
% * Written permission from the author is required only if this material or any derivative works is used to make, endorse or promote government or commercial profits.
%THIS SOFTWARE IS PROVIDED BY THE COPYRIGHT HOLDER "AS IS".  IN NO EVENT SHALL THE COPYRIGHT HOLDER BE LIABLE FOR ANY DIRECT, INDIRECT, INCIDENTAL, SPECIAL, EXEMPLARY, OR CONSEQUENTIAL DAMAGES (INCLUDING, BUT NOT LIMITED TO, PROCUREMENT OF SUBSTITUTE GOODS OR SERVICES; LOSS OF USE, DATA, OR PROFITS; OR BUSINESS INTERRUPTION) HOWEVER CAUSED AND ON ANY THEORY OF LIABILITY, WHETHER IN CONTRACT, STRICT LIABILITY, OR TORT (INCLUDING NEGLIGENCE OR OTHERWISE) ARISING IN ANY WAY OUT OF THE USE OF THIS SOFTWARE, EVEN IF ADVISED OF THE POSSIBILITY OF SUCH DAMAGE.
fprintf('Linear Welding Density Estimator - v6.0');
k=1; % k is the cycle control parameter (program always cycle runs, unless terminated by user)
```

```
        while (k>0)
        clear; % clear variables
        e=-1; % -1 is signal value for Otus method
        % Comment out next line in order to use Otsu method for Black/White thresholding.  Otherwise the value specified here is used as threshold
(Otsu's method overdrive)
        % e=153; % Binary (Black=0 & white=255) image [specify a cutoff value above which gray tones are turned white (=1), whereas the rest
is turned black (=0)].  Default Value is 153.
        % clc; % Uncomment this line to clear matlab command window on each run
        file=input('\n\n*Specify filename (case sensitive), e.g.  sample.tif, or press Ctrl+C to abort:  ','s'); % specifies image file (case
sensitive)
        close all; % closes all windows except current one
        S=imread(file); % reads image file
        G=S; % G is a copy of the original image
        % creates a dimensional array (rows,columns) of origimal image (G)
        [m2 n2] = size(G);
        imshow(S); % shows current image
        image(S); axis image % Display image with true aspect ratio
        pause; % shows the image
        %%%%%%%%%%%%%%%%%%%%%%%%%%
        % 1.  IMAGE REGION SELECTION SECTION
        fprintf('\nDefine image region for analysis or press Ctrl+C to abort:\n');
        % Bring MATLAB's Command Window to the front
        drawnow;
        commandwindow;
        fprintf(' - Enter V to select a region using mouse clicks on the image (default).\n');
        fprintf(' - Enter M to select a region using image matrix"s rows and columns.\n');
        fprintf(' - Enter R to select a region using relative coordinates.\n');
        reply = input('','s');
        % Default Option for no imput
        if (isempty(reply)==1)
        reply='V';
        end
        % REGION: MATRIX COORDINATES - CODE SECTION
        if (reply=='m' || reply=='M')
        [m n] = size(S); % creates a dimensional array (rows,columns) of current image (S)
        matrix=imfinfo(file); % Gets image properties
        if (strcmp(matrix.ColorType,'truecolor')==1) % Column value convertion for analysis
        n=n/3;
        n2=n2/3;
        end
        fprintf ('\nPlease select rows and columns region (r1:r2, c1:c2) within the MxN image.\nDefault values are r1=c1=1, r2=M, c2=N (All
picture).\n\n');
        fprintf ('r1____\n | |\n |____|\nr2,c1 c2');
        % default values
        c=1; % c=c1;
        d=n; % d=c2;
        a=m; % a=r2;
        b=1; % b=r1;
        fprintf ('\n\nThe complete image matrix is %g x %g (rows x columns)', m, n);
        c=input('\nEnter the first row bound "r1":  '); % specifies one parameter for defining the image region
        if (isempty(c)==1) || (c<=1)
        c=1;
        end
        if (c>m)
        c=m;
```

```
end
c=abs(fix(c));
d=input('Enter the second row bound "r2":  '); % specifies one parameter for defining the image region
if (isempty(d)==1) || (d<=1)
d=1;
end
if (d>m)
d=m;
end
d=abs(fix(d));
a=input('\nEnter the first column bound "c1":  '); % specifies one parameter for defining the image region
if (isempty(a)==1) || (a<=1)
a=1;
end
if (a>n)
a=n;
end
a=abs(fix(a));
b=input('Enter the second column bound "c2":  '); % specifies one parameter for defining the image region
if (isempty(b)==1) || (b<=1)
b=1;
end
if (b>n)
b=n;
end
b=abs(fix(b));
% Warning section
if (b<=a)
fprintf ('\nWarning:  c1>=c2.  The region was adjusted based upon given inputs.\n');
end
if (d<=c)
fprintf ('\nWarning:  r1>=r2.  The region was adjusted based upon given inputs.\n');
end
sp(1)=min(a,b);
sp(2)=min(c,d);
sp(3)=max(a,b);
sp(4)=max(c,d);
A=[a c;b d];
A=sort(A);
c=A(1,2);
d=A(2,2);
a=A(1,1);
b=A(2,1);
S = G(c:d,a:b,:); % Trim out
figure
imshow(S);
pause; % pauses work until a key is pressed
end
% REGION: RELATIVE COORDINATES - CODE SECTION
if (reply=='r' || reply=='R')
[m n] = size(S); % creates a dimensional array (rows,columns) of current image (S)
matrix=imfinfo(file); % Gets image properties
if (strcmp(matrix.ColorType,'truecolor')==1) % Column value convertion for analysis
n=n/3;
n2=n2/3;
```

```
        end
        fprintf ('\nPlease select the image region bounds ([a,b] U [c,d]) in relative coordinates (1=total length).\nDefault values are a=c=0,
b=d=1 (All picture).\n\n');
        fprintf ('d____\n| |\n|____|\nc,a b');
        % default values
        a=0;
        b=1;
        c=0;
        d=1;
        a=input('\n\nEnter the left bound in the horizontal axis direction "a":  '); % specifies one parameter for defining the image region
        if (isempty(a)==1) || (a<0)
        a=0;
        end
        if (a>1)
        a=1;
        end
        a=abs(fix(a*n));
        if (a==0)
        a=1;
        end
        b=input('Enter the right bound in the horizontal axis direction "b":  '); % specifies one parameter for defining the image region
        if (isempty(b)==1) || (b>1)
        b=1;
        end
        if (b<0)
        b=0;
        end
        b=abs(fix(b*n));
        if (b==0)
        b=1;
        end
        c=input('\nEnter the lower bound in the vertical axis direction "c":  '); % specifies one parameter for defining the image region
        if (isempty(c)==1) || (c<0)
        c=0;
        end
        if (c>1)
        c=1;
        end
        c=abs(fix(c*m));
        if (c==0)
        c=1;
        end
        d=input('Enter the upper bound in the vertical axis direction "d":  '); % specifies one parameter for defining the image region
        if (isempty(d)==1) || (d>1)
        d=1;
        end
        if (d<0)
        d=0;
        end
        d=abs(fix(d*m));
        if (d==0)
        d=1;
        end
        % Warning section
        if (b<=a)
```

```
fprintf ('\nWarning:  a>b.  The region was adjusted based upon given inputs.\n');
end
if (d<=c)
fprintf ('\nWarning:  c>d.  The region was adjusted based upon given inputs.\n');
end
A=[a c;b d];
A=sort(A);
c=A(1,2);
d=A(2,2);
a=A(1,1);
b=A(2,1);
S = G(c:d,a:b,:); % Trim out
sp(1)=a;
sp(2)=c;
sp(3)=b;
sp(4)=d;
% Display the image subset with appropriate axis ratio
figure;
imshow(S);
pause; % pauses work until a key is pressed
end
% REGION: MOUSE CLICKS- CODE SECTION
if (reply~='m' && reply~='M' && reply~='r' && reply~='R')
% Use ginput to select corner points of a rectangular region by pointing and clicking the mouse twice
h=2;
p = ginput(h);
% Get the x and y corner coordinates as real positive integers.
% Cordinates are row number and column number from the upper left corner of image matrix.
[m n] = size(S); % creates an dimensional array (rows,columns) of current image.
matrix=imfinfo(file);
if (strcmp(matrix.ColorType,'truecolor')==1)
for i=1:2*h;
if p(i)<=1
p(i)=1;
end
% x max range
if i<=h && p(i)>n/3
p(i)=n/3;
end
% y max range
if i>h && p(i)>m
p(i)=m;
end
end
n=n/3;
n2=n2/3;
else
for i=1:2*h;
if p(i)<=1
p(i)=1;
end
% x max range
if i<=h && p(i)>n
p(i)=n;
end
```

```
        % y max range
        if i>h && p(i)>m
        p(i)=m;
        end
        end
        end
        sp(1) = min(floor(p(1)), floor(p(2))); %xmin
        sp(2) = min(floor(p(3)), floor(p(4))); %ymin
        sp(3) = max(ceil(p(1)), ceil(p(2))); %xmax
        sp(4) = max(ceil(p(3)), ceil(p(4))); %ymax
        % Index into the original image to create the new image
        MM = S(sp(2):sp(4), sp(1):  sp(3),:);
        % Display the subsetted image with appropriate axis ratio
        figure;
        imshow(S);
        image(MM);
        axis image % Display image with true aspect ratio
        pause; % pauses work until a key is pressed
        % [Write image to graphics file.]  % Uncomment the following 2 lines if you want to save a copy of the cropped picture (a TIFF file
with 'file_c' as the name)
        %imwrite(MM,'file_c.tif', 'TIFF');
        %S=imread('file_c.tif');
        S=MM;
        end
        %%%%%%%%%%%%%%%%%%%%%%%%%
        % 2.  IMAGE ANALYSIS
        % image type identification and convertion to grayscale
        G=S;
        matrix=imfinfo(file);
        if (strcmp(matrix.ColorType,'indexed')==1)
        image(S),colormap(map)
        G=ind2gray(S,colormap(gray(length(map)))); % Turns image to grayscale (8bits)
        figure, imshow(G); % shows current image
        image(G);
        axis image % Display image with true aspect ratio
        pause; % pauses work until a key is pressed
        end
        if (strcmp(matrix.ColorType,'truecolor')==1)
        G=rgb2gray(S); % Turns image to grayscale (8bits)
        figure, imshow(G); % shows current image
        image(G);
        axis image % Display image with true aspect ratio
        pause; % pauses work until a key is pressed
        end
        % Contrast Adjustment of Grayscale image
        % G=imadjust(G);
        % black & white image convertion
        if e==-1
        e = graythresh(G); % calculates threshold using the Otsu method
        X=im2bw(G, e);
        e=e*255;
        else
        X = G > e; % e is the cutoff value for grayscale image analysis.  Its value is specified at the begining of this file.
        end
        figure;
```

```
        imshow(X); % shows current image
        pause; % pauses work until a key is pressed
        Z=X;
        [m n] = size(Z); % creates an array of the dimension (rows,columns) of current image
        Z2 = imerode(Z,strel('line',2*m,90)); % Extends the black sections vertically all the way through the picture, so as to create 'bands'
of white and black independent of vertical (y-axis direction) position
        figure, imshow(Z2); % shows current image
        pause; % pauses work until a key is pressed
        s = size(Z2); % creates an array of the dimension (rows,columns) of current image
        t = s(2); % total length [assigns t the horizontal (x-axis direction) length of current image]
        w = sum(Z2(1,1:n)); % white length [binary sum (white=1, black=0) of the first horizontal line of current image]
        b = t - w; % black length ["in a black & white image, what is not white, is black"]
        LWD=w/t; % linear percentage of white pixels [This is an estimator of Linear Welding Density]
        % FILE INFORMATION
        fprintf('------------\n');
        file2=strcat('file=',file,' [',num2str(m2),'x',num2str(n2),' (Rows x Columns in image matrix)]');
        fprintf(file2);
        fprintf('\n8-bit grayscale threshold value for black/white (Black=0 <=t-> white=255):  %g',e);
        %Spaces
        bar_s=max(floor(log10(sp(1)+1)),floor(log10(sp(3)+1)));
        d=1;
        fprintf('\nSelected image rectangular region:\nPi:  r');
        for i=1:bar_s+d;
        fprintf(' ');
        end
        fprintf('c\n %g',sp(2));
        for i=1:bar_s-floor(log10(sp(1)+1))+d;
        fprintf(' ');
        end
        fprintf('%g\n %g',sp(1),sp(4));
        for i=1:bar_s-floor(log10(sp(3)+1))+d;
        fprintf(' ');
        end
        fprintf('%g',sp(3));
        fprintf(' \n');
        fprintf('LWD = \n');
        fprintf(num2str(LWD)); % prints linear welding density (LWD)
        fprintf('\n------------'); % Credits:  Rael Gonzalez, Pedro Tejada.  Nov 2008.
        % Brings MATLAB's Command Window to the front
        drawnow;
        commandwindow;
        k=1;
        end
```

A.2 Publication Permissions Supplement

This section includes all required permissions for publication of the papers presented as chapters of this dissertation.

Date: Thursday, April 22, 2010

Name: Raelvim Gonzalez
Address: 1359 E 1000 N APT 203
Logan, UT, 84321
Phone: (435)-213-7191
Email: rael.gonzalez@aggiemail.usu.edu

Dear Dr. Brent Stucker:

I am preparing my dissertation in the Department of Mechanical and Aerospace Engineering at Utah State University. I hope to complete my degree in spring of 2010.

I am preparing a multiple paper dissertation, which will include the papers listed below. Because you are co-author on these papers I am requesting your permission to include the material just as it appeared in the paper. Please advise me of any changes you require.

Please indicate your approval of this request by signing in the space provided and attaching any other form or instruction necessary to confirm permission. If you have any questions, please feel free to contact me. Thank you for your assistance.

Regards,

Raelvim Gonzalez

I hereby give permission to RAELVIM GONZALEZ to reprint the following articles in his dissertation.

1. R. Gonzalez & Stucker, B., "An automatic routine for Linear Welding Density estimation through image processing", Journal *of Manufacturing Science and Engineering*, submitted for publication (2010).

2. R. Gonzalez & Stucker, B., "Experimental determination of optimum parameters for stainless steel 316L annealed ultrasonic consolidation", *Rapid Prototyping Journal*, submitted for publication (2010).

Signed:  Date: 4/22/10